FoxM1 and Mammary Gland Biology:
From Drug Resistance to Differentiation

By

Janai RyanMarie Carr
B.S., University of California, San Diego, 2002

THESIS

Submitted as partial fulfillment of the requirements for the degree of
Doctor of Philosophy in Biochemistry and Molecular Genetics
In the Graduate College of the
University of Illinois at Chicago, 2013

DEFENSE COMMITTEE:

Pradip Raychaudhuri, Chair and Advisor
Karen Colley, Biochemistry and Molecular Genetics
Jonna Frasor, Physiology
Nissim Hay, Biochemistry and Molecular Genetics
Bradley Merrill, Biochemistry and Molecular Genetics
Angela Tyner, Biochemistry and Molecular Genetics

To my parents for giving me the gifts of unconditional love and education

ACKNOWLEDGEMENTS

I would first like to thank Pradip Raychaudhuri for his invaluable mentorship and friendship. When I started in the lab I was young, ambitious, and scattered. He helped to shape my ideas and form them into coherent science and I will be forever grateful for it. For having confidence in me while questioning me, I thank you.

I would like to acknowledge all of the members of my committee, Karen Colley, Jonna Frasor, Nissim Hay, Brad Merrill, and Angela Tyner for always demanding more.

Thank you to all of the people in the UIC core facilities for their help. Namely, Jewell Graves in the flow cytometry core and Aaron and Lee in the animal facility.

To Hyun Jung Park and Zebin Wang, thank you for always being the front line for my ideas. You have helped to complete, shape, and refine all of my experiments. Thank you for your support and your friendship.

To all of the members of the Raychaudhuri lab, thank you for the discussions and suggestions and for creating an environment that people want to work in. A special thanks to Megan Kiefer and Jing Li for helping to make the transition back to medical possible.

Thank you to Larry Tobacman and the entire UIC MSTP for taking a chance.

I would like to thank Joanna Jen for teaching me to love science. The time in her lab was invaluable and created the foundation upon which I have been able to build all of my later work. In addition, I thank her

for introducing me to the world of physician-scientists and helping a young woman realize what she wanted to do with her future.

Thank you to Jose Criado, Manuel Sanchez-Alavez, Salvador Huitrón-Reséndiz, Steven Henriksen and everyone at Scripps Research for their patience. Each day, I rely on the techniques you taught me.

To Robyn, Tanis, Erica, Laura, Kai, Matt, Dee Dee, Senta, and Allison thank you for your friendship and all of the great distractions. Your support and love are irreplaceable.

To my Uncle Donald, thank you for always being there.

Thank you to all of my friends and family, there are too many of you to name but I appreciate you all.

To my parents Marshall and Yolanda and my brothers Marshall and Sean, I'm sorry I don't have the words to express how truly grateful I am to all of you. Thank you for your support and love. I would have never been able to make this journey without you. Thank you for being not only my family, but my friends.

TABLE of CONTENTS

LIST of FIGURES and TABLES

1. Introduction **Page**

2. FoxM1 Inhibits Mammary Luminal Differentiation Through Transcriptional Repression of GATA-3

3. FoxM1 Mediates Resistance to Herceptin and Paclitaxel

LIST of ABBREVIATIONS

FoxM1	Forkhead box transcription factor M1
PTHrP	Parathyroid hormone related protein
PTHR1	Parathyroid hormone receptor 1
PRLR	Prolactin Receptor
JAK	Janus kinase or “just another kinase”
STAT	Signal transducer and activator of transcription
WAP	Whey acidic promoter
MAPK	Mitogen activated protein kinase
PARP	Poly ADP ribose polymerase
C/EBP	CCAAT-enhancer binding proteins
BAK	Bcl-2 homologous antagonist killer
Bfl-1	BCL-2 related protein
MMP	Matrix metalloproteinase
RANK	Receptor activator of nuclear factor kappa-B (NF-κB)
RANKL	Receptor activator of NF-κB ligand
ERα	Estrogen receptor alpha
PR	Progesterone receptor
HER2	Human epidermal growth factor receptor 2
MUC1	Mucin 1
ESA	Epithelial specific antigen
GATA-3	G-A-T-A binding transcription factor 3
MDR1	Multi-drug resistant protein 1
MMTV-PyMT	Mouse Mammary Tumor Virus – Polyoma Middle T Antigen

SUMMARY

The goal of this work is to better understand the mechanisms by which FoxM1 promotes tumor development and progression. FoxM1 is overexpressed in nearly every tumor type examined. While it was believed that the functions of FoxM1 were limited to promoting proliferation, this view is incomplete. Comparing early grade tumors to late aggressive metastatic tumors shows no difference in rate of proliferation (Hanahan and Weinberg, 2011). Therefore, it seems unlikely that the levels of FoxM1 would be need to be elevated in tumors as they progress. While it is possible that the FoxM1 expression increases indirectly, in response to upstream signaling, we believed this increase is specific and necessary for tumor progression. In breast cancers, FoxM1 is correlated with an undifferentiated tumor type and poor patient prognosis. I worked to identify a mechanism by which FoxM1 promotes the growth and development of high-grade tumors. In this process, we identified FoxM1 as a regulator of GATA-3, a factor highly correlated with estrogen expression. Previous studies showed that GATA-3 is silenced by methylation as tumors advance. We demonstrate that FoxM1 can promote the methylation of the GATA-3 promoter by an Rb dependent mechanism. In addition, this work assigned a novel function to FoxM1, the ability to function as a transcriptional repressor. I was also interested in the ability of FoxM1 to promote resistance to breast cancer treatments, specifically the HER2 targeting antibody Herceptin and the microtubule stabilizer Paclitaxel. From this work we identified FoxM1 as a target in resistant tumors. In addition, we demonstrated that targeting FoxM1 functioned to sensitize cells to treatments. This study indicates that perhaps through targeting FoxM1 it would be possible to administer lower doses of chemotherapeutic agents resulting in less toxicity. The lab has worked to develop a small peptide inhibitor of FoxM1. Using this peptide, we were able to demonstrate that targeting FoxM1 does in fact lead to sensitization of both parental and resistant cell lines to treatment. This work assigns novel functions to FoxM1 and provides rationale for establishing it as a target in aggressive breast tumors.

1. Introduction

The work presented here focuses on the role of FoxM1 in regulating two different aspects of mammary tumor biology. The first being the ability of FoxM1 to promote a drug resistant phenotype and the second, to negatively regulate mammary luminal differentiation. These two seemingly unrelated processes share a common ground, the breast cancer stem cell. Both drug response and differentiation are intricately related to stem cell biology. Therefore, an introduction of mammary gland biology followed by a detailed discussion of breast cancer and the breast cancer stem cell will follow. In addition to FoxM1, proteins that were discovered to be key coactivators or targets, GATA-3, DNMT3, and Rb will be discussed in detail below.

A. Mammary Gland Differentiation

A.1. Developmental Regulation

The mammary gland is derived from ecotodermal tissue. Organogenesis begins at embryonic day 10 in the mouse with the formation of a thickened region of surface epithelium termed the mammary line. *Lef-1*, a transcription factor in the WNT/β-Catenin pathway is the earliest marker of mammary epithelium and appears at embryonic day 11-12. At this time, the primordial mammary strucutures, or mammary placodes appear (Mailleux et al., 2002). Epithelial cells migrate into the region and undergo early differentiation to produce a mammary bud. Late in embryogenesis, in response to parathyroid hormone related protein (PTHrP) signaling through parathyroid hormone receptor (PTHR1), mammary buds become the primary branched epithelial structure present in the postnatal mouse (Wysolmerski et al., 1998; Dunbar et al., 1999).

During puberty (5-6 weeks of age), the rudimentary mammary gland forms terminal end bud structures and begins to invade the surrounding fat pad. The terminal end bud structure is of particular significance because cap cells, or those found in the invading front make up the stem cell population.

Progeny of these cells expand and differentiate as they move down the structure to form the mature cell types of the duct. Cells in the center undergo apoptosis to generate a functional lumen (Williams and Daniel, 1983; Smalley and Ashworth, 2003). This period of extensive growth and ductal expansion is dependent on estrogen receptor α signaling in both the epithelium and stroma (Bocchinfuso et al., 2000; Mueller et al., 2002; Mallepell et al., 2006). Ductal expansion is in part mediated by estrogen regulation of progesterone and prolactin expression. Hormone receptors are generally expressed in non-proliferating epithelial cells and signal through paracrine mechanisms. Through paracrine pathways involving growth factor signaling, these cells promote the proliferation of receptor negative cells resulting in a mature branched mammary structure (LaMarca and Rosen, 2008).

While estrogen receptor α is crucial to ductal expansion during puberty, it is not required for epithelial growth and branching during pregnancy (Hennighausen and Robinson, 2005). Prolactin and progesterone are the key hormones mediating alveolar differentiation. Prolactin is the key upstream initiator. Prolactin signals through prolactin receptor (PRLR) to induce pathways involved in epithelial proliferation, differentiation, and survival. Upon binding to prolactin, PRLR dimerizes and Janus Kinase 2 (JAK2) phosphorylates the receptors, which results in activation of the transcription factor STAT5 (signal transducer and activator of transcription 5). STAT5 is the key transcriptional activator of the pregnancy differentiation program. Targets include the milk proteins whey acidic protein (WAP) and β-Casein. Additionally, PRLR activates MAPK, Akt, and progesterone signaling to promote cellular proliferation independent of STAT5 activation (Hennighausen and Robinson, 2005; Wagner and Rui, 2008). This combination of proliferation and differentiation leads to the gland undergoing further growth and tertiary branching to create alveoli or bud-like structures to support milk production.

After weaning, the process of involution begins to return the gland to the pre-pregnancy state. Involution involves two phases that are characterized by their reversibility. The first phase is reversible and involves widespread caspase-3 and PARP mediated apoptosis of the secretory epithelium (Baxter et al., 2007). This is marked by a decrease in the expression of pro-survival genes STAT5 and Akt that are

crucial to maintaining the epithelium during pregnancy and an increase in p-STAT3 (Sutherland et al., 2007). Activated STAT3 functions in several ways to mediate apoptosis. STAT3 targets C/EBPδ which activates pro-apoptotic genes including BAK and p53 while repressing the pro-survival gene Bfl1 and the cell cycle regulator Cyclin D1 (Baxter et al., 2007). Additionally, STAT3 activates the NFκB subunits, p50α and p55α, that function to decrease pro-survival signaling through the Akt pathway. STAT3 functions to mediate the switch to the second phase of involution, the irreversible macrophage and protease mediated remodeling process. Through activation of Oncostatin M, a member of the IL-6 family, STAT3 helps to promote macrophage activity and in effect, the removal of apoptotic cells. This second phase relies heavily of the matrixmetalloproteinase (MMP) family of proteins. Specifically, MMP2 and MMP3, which function to remodel the extracellular matrix and stroma (Sutherland et al., 2007).

A.2. Stem and Progenitor Compartment

The cellular plasticity of the mammary gland that is evident throughout development can be attributed to a stem cell population (Kordon and Smith, 1998). The three mature cell types of the mammary gland can be produced from a single progenitor (Stingl et al., 2006; Shackleton et al., 2006). A pool of pluripotent stem cells in the mammary gland gives rise to lineage restricted progenitor cells that can be further differentiated into mature luminal (alveolar or ductal) or myoepithelial cells (Visvader et al., 2009).

While it was hypothesized that a mammary stem cell must exist, it was not proven until 1959. DeOme and colleagues showed that if you clear the endogenous epithelium from a prepubescent mouse and place a fragment of a mammary gland from a mature mouse in the cleared fat pad, an entire mammary structure would form (DeOme et al., 1959). It was decades later when the mammary stem cell was conclusively identified. Kordon and Smith used retroviral tagging to show that the entire mammary gland was likely generated from one cell and not a pool of cells (Kordon and Smith, 1998). Small numbers of cells were infected, implanted into the cleared fat pad, allowed to regenerate, and the mice were analyzed after the first pregnancy. It was observed by southern blot that approximately 88% of the

cells harbored the same viral insertion, indicating that they were likely the progeny of one cell. Additionally, they noted that this cell resided in the basal compartment (Kordon and Smith, 1998). Several years after this, flow cytometry markers that could be used to enrich stem cells were identified (Stingl et al., 2006). Using these markers, it was shown that a single "stem cell" was capable of regenerating the entire mammary gland (Shackleton et al., 2006).

After the identification of the mammary stem cell population numerous studies aimed at understanding the regulation of this compartment have been performed. As a result, several common pathways have been implicated in stem progenitor regulation such as Wnt, Notch, and p53. Wnt signaling is required for the embryonic development of the mammary gland. Transplantation studies demonstrated that Wnt signaling is required for the maintenance of the stem cell population in the gland. Epithelial cells from Lrp5 (Wnt coreceptor) knockout mice were not able to regenerate the ductal structure in recipient mice (Lindvall et al., 2006). Several studies had demonstrated that Notch signaling was needed for stem cell maintenance but the cell type targeted by Notch was unclear (Dontu et al., 2004; Buono et al., 2006). The Visvader group showed that Notch functions in the luminal progenitor (CD61+) population to increase progenitor cell self-renewal (Bouras et al., 2008).

One key feature of stem cells is asymmetric cell division. Each time a stem cell divides it should generate an identical stem cell as well as a cell committed to differentiate. In mammary stem cells it was unclear what regulates asymmetric division. In an elegant study by Cicalese and colleagues it was shown that p53 is a key regulator of stem cell of this process (Cicalese et al., 2009). In the absence of p53, cells divide symmetrically and one stem cell gives rise to two identical stem cells, which leads to an expansion of the stem cell pool at the expense of differentiation (Cicalese et al., 2009).

Recently, it was shown that steroid hormones are responsible for regulating the stem cell population. While the number of stem cells in the gland was not altered by ovectomy in mice, the ability of the stem cells to repopulate in recipient mice was impaired indicating that hormones are important in maintaining the "stemness" of these cells. Specifically progesterone and prolactin were responsible for

expanding the stem cell pool during pregnancy. This finding is interesting because stem cells are progesterone and estrogen receptor negative. Two groups simultaneously showed that hormones signal through the RANK pathway in differentiated cells to signal to stem cell pools that express RANK ligand (RANKL). This pathway is needed to keep stem cells from becoming quiescent and keeping them in a replication competent state (Joshi et al., 2010, Asselin-Labat et al., 2010). These studies demonstrate a role for hormones in regulating the stem cell compartment and suggest a mechanism for maintaining a balance between stem and differentiated populations.

B. Breast Cancer

B.1. Tumor Grade and Differentiation

Breast cancer is the mostly commonly diagnosed tumor type in women of the western hemisphere. In the United States alone, breast cancer accounts for 40,000 deaths each year, second only to lung cancer (Jemal et al., 2010). In breast cancer, there is a clear correlation between tumor grade and patient survival, making analysis and understanding of grade particularly important (Elston and Ellis, 1991). Mammary tumor grade is a measure of the level of differentiation. Assigning tumor grade depends on several factors according to the Nottingham Grading System (NGS): (1) gland histology or degree of tubule formation, (2) nuclear pleomorphism, and (3) mitotic index. There are three grades. Grade 1 tumors are well differentiated and more than 75% of the gland has recognizable tubule formation. Grade 2 tumors are moderately differentiated while grade 3 tumors are poorly differentiated, contain less than 10% tubules and have a high mitotic index (Elston and Ellis, 1991; Rakha et al., 2010). This scale is commonly used and recommended by several professional agencies because it has prognostic significance. Patients with low-grade tumors have high survival rates that have been attributed to a high rate of response to endrocrine and chemotherapy regimens and low rates of metastasis. The inverse is true as well. Grade three tumors have high rates of relapse and metastasis and poor patient survival. While this system has clear clinical and prognostic value, additional markers are needed. In particular, grade 2 tumors create a prognostic “gray area.” Over the past several years, molecular classification of tumors is

moving to the forefront of breast cancer research. This shift is slower clinically because of cost and time constraints and the prognostic value of molecular classification is not as clear as that of tumor grade (Rakha et al., 2010).

Molecular breast cancer classification includes five main subtypes; luminal A, luminal B, triple negative or basal type, HER2 positive, and more recently, claudin-low (Perou et al., 2000; Sorlie et al., 2001; Creighton et al., 2009). Luminal A and B are estrogen receptor (ER) and progesterone receptor (PR) positive and HER2/ErbB2 negative. These tumors are well differentiated in comparison to the other subtypes. They differ in the amount of steroid hormone receptors, luminal B tumors are "less positive" for ER and PR receptors and therefore carry a slightly lower prognosis than type A. HER2 positive tumors can be ER or PR positive as well but are classified by amplification of the oncogene HER2/ErbB2, a member of the growth factor signaling pathway. Triple negative tumors are as the name indicates, ER, PR, and HER2 negative. These tumors have a molecular signature similar to the myoepithelial or basal cells of the mammary gland. Given that mammary stem cells are found in the myoepithelial compartment it is not surprising that triple negative tumors have a "stem-like" signature. These tumors are generally highly aggressive and poorly differentiated. More recently, the claudin-low subtype was characterized. These tumors have a "stem-like" signature and in addition have high levels of genes associated with epithelial to mesenchymal transition (Ginestier et al., 2007; Creighton et al., 2009). Analysis of patient prognosis by tumor grade or molecular subtype leads to the same conclusion, tumors that histologically appear more differentiated or display markers of differentiation have a better patient outcome.

B.2. Breast Cancer Stem Cell

Over the past several years, there has been a surge in the amount of work that has focused on understanding the regulation and development of mammary stem and progenitor cells. This is in part due to the identification of the breast cancer stem cell. Within a solid breast tumor, only a small portion of cells are capable of forming a tumor upon secondary passage, indicating that only a small number of cells have tumorigenic abilities (Al-Hajj et al., 2003). Therefore, an operational definition of a cancer stem cell

is a cell that is able to give rise to a heterogenous tumor upon implantation or arrival at a metastatic site. Additionally, these cells have surface markers and molecular profiles similar to stem cells. The cell of origin for breast cancer is not known, yet increasing evidence points to a progenitor or stem cell as the culprit. Given that breast cancer may originate from an undifferentiated cell, recurrence is associated with a cancer stem cell, and that there is a clear relationship between differentiation and patient outcome, an understanding of mammary stem and progenitor cells is key to understanding breast cancer.

B.2A. Identification. The concept of a cancer stem cell comes from studies in neoplasms of hematopoietic origin. It was first shown that among tumor cells isolated from mouse models of leukemia or multiple myeloma only 1 in approximately 10,000 were able to form colonies *in vitro* (Park et al., 1971). Additionally, only 1-4% of tumor cells were able to grow in the spleen of recipient mice (Reya et al., 2001). Evidence for stem cells in solid tumors came later. Small numbers of cells would grow in soft agar assay after isolation from lung tumors. This was also true in solid tumors of the reproductive and neurological systems (Fidler et al., 1977; Fidler et al., 1982; Heppner, et al., 1984). Conclusive evidence for human breast cancer stem cells came from the Clarke group in 2003. By using the cell surface markers, CD44 and CD24, this group identified the CD44+,CD24lo population as a tumor stem cell. They showed that as few as 100 of these cells were able to regenerate a tumor in NOD/SCID mice as compared to 50,000 bulk tumor cells. Tumors regenerated from this subpopulation were able to give rise to the phenotypical heterogeneity visible in the primary tumor (Al-Hajj et al., 2003).

B.2B. *In Vitro* Culture of Mammary Stem Cells. While, the importance of rigorously analyzing the breast cancer stem cell population was evident, early attempts to grow mammary stem/progenitor cells on a solid substrate *in vitro* failed because cells would go on to terminally differentiate (Reynolds and Weiss, 1996; Romanov et al., 2001). In 2003 Dontu and colleagues developed an in vitro system of growing mammary stem and progenitor cells as “mammospheres.” The mammosphere model was based

on previous work that demonstrated that a population of neural cells could be grown in suspension and 5-20% of these cells were undifferentiated (Dontu et al., 2003; Reynolds and Weiss, 2006).

The authors took tissue from human reduction mammoplasty, digested it using a series of enzymes, and grew the cells in serum free media supplemented with stem cell and growth factors. It was determined that these cells lacked markers of luminal differentiation, including Mucin 1 (MUC1) and cytokeratin 18 while expressing markers of bipotential cells including epithelial-specific antigen (ESA), and α6 integrin. In addition, once plated on collagen or matrigel, sphere derived cells differentiated into both luminal and basal cells indicating the presence of bipotential stem cells. The mammosphere system provides a system for culturing stem and progenitor cells and measuring their ability to differentiate. In addition, the mammosphere assay allows for quantification of stem cell renewal activity. By serial passaging of equal numbers of cells and counting, the percentage of cells with "self-renewal" capabilites can be determined (Dontu et al., 2003). Later, it was demonstrated that mammospheres could be generated using breast cancer cell lines or mammary tumors and used as a measure of relative stem cell number. In addition, it allows for manipulation of the cells by retrovirus expressing shRNA or expressing a gene thereby allowing for careful examination of signaling pathways (Grimshaw et al., 2008; Korkaya et al., 2008). This system has been used as a screen for drugs that target the stem cell population and as a model to understand the mechanisms of resistance of the stem cell pool (O'Brien et al., 2008; Kakarala et al., 2008).

B.2C. Regulation. While the relationship between the normal mammary stem cell and the breast cancer stem cell is not known, there is a clear overlap in the regulatory mechanisms. Specifically, Wnt, Notch and HER2 signaling have been implicated in breast cancer stem cell self-renewal (Visvader et al., 2009). As previously mentioned, Wnt signaling regulates self-renewal of the bipotential stem cell (Reya and Clevers, 2005). Expression of Wnt from the mammary specific MMTV (mouse mammary tumor virus) promoter leads to tumor formation and Wnt signaling is able to promote dysregulated stem cell self-renewal in the mammary gland. In MMTV-Wnt tumors, there is an increase in the number of

progenitor cells and in the ability of these cells to regenerate in vivo (Li et al., 2003; Shackleton et al., 2006; Vaillant et al., 2008).

Notch signaling helps to limit the bipotential stem cell pool and promote progenitor cell expansion in the normal mammary environment. In the context of tumor formation dysregulated Notch expression can have detrimental effects. Addition of Notch family members leads to an expansion of cancer stem cells while reduction of Notch signaling using an inhibitor or antibody leads to a reduction of cancer stem cells (Farnie et al., 2007).

HER2 is a member of the EGF family of growth factor receptors. Amplification or overexpression of HER2 occurs in 25-30% of human breast cancers. Korkaya and colleagues demonstrated that addition of HER2 leads to an expansion of the progenitor colonies in culture and showed that when these progenitor colonies were grown in matrigel they formed ducts with hyperplastic features (Korkaya et al., 2008).

B.3. Drug Resistance and Metastasis

In the treatment of breast cancer, there are two closely related major clinical challenges, that of drug resistance and metastasis. The mammary gland is not an essential organ to the maintenance of life therefore, patients rarely succumb to primary tumors. Patients die of metastasis to essential organs, namely bone, lung, and brain. Generally, primary tumors are resected and chemotherapy and/or endocrine therapies are given. While this therapy is curative for some patients, others go on to develop metastasis or have tumors that recur and are resistant to therapies. The known mechanisms of drug resistance and metastasis are numerable and beyond the scope of this work. For this reason, the focus will be on resistance to a commonly used chemotherapeutic, Paclitaxel and the targeted monoclonal antibody Herceptin (or Trastuzumab). Additionally, a brief overview of metastasis will be discussed in the context of the relationship to breast cancer stem cells.

B.3A. Mechanisms of Drug Resistance. The receptor typrosine kinase ErbB2/HER2 is a member of the epidermal growth factor (EGF) family of receptors. HER2 has no known ligand, but functions by forming heterodimers with other family members to promote intracellular signaling (Le et al., 2005). Pathways downstream of HER2 include phosphatidylinositol 3-kinase (PI3K), RasGAP, and signal transducer and activator of transcription 5 (STAT5) (Yarden et al., 2001). Amplification of HER2 is a sign of a highly aggressive tumor type with few treatment options. Several therapies aimed at inhibiting HER2 signaling are in use, including the monoclonal antibody Herceptin (Trastuzumab) that functions to disrupt the interaction between HER2 and its preferred binding partner HER3 (Junttila et al., 2009). Treatment with Herceptin results in accumulation of the Cdk inhibitor p27 and subsequent G1/S cell cycle arrest. Unfortunately, the efficacy of Herceptin as a monotherapy is thought to be less than 30% and in combination with microtubule stabilizing drugs approximately 60% (Burris et al., 2000). Resistance to Herceptin develops quickly and is thought to stem from compensated signaling by other EGF family members or dysregulation of downstream pathways such as PI3K/Akt (Nagata et al., 2004; Nahta et al., 2004; Pohlmann et al., 2009).

Herceptin is commonly used in conjunction with other therapies, including Paclitaxel. The primary mechanism of action of Paclitaxel is to bind β-tubulin and prevent dissociation of α/β tubulin dimers, resulting in mitotic failure and consequent apoptosis (Xiao et al., 2006). Paclitaxel is used in the treatment of multiple tumor types and has shown particular success in treatment of metastatic breast cancer. Yet, resistance does occur. Insensitivity to Taxol has been shown in cells that overexpress HER2. On average, cells with HER2 amplification require a 100-fold higher dose of Taxol to produce the same effect (Azambuja et al., 2008). Resistance to Taxol has been attributed to additional mechanisms including increased expression of multi-drug resistant 1 (MDR1), a protein that can pump toxins out of cells. Other commonly documented mechanisms of resistance include changes in microtubule stability or mutations in the tubulin proteins (Orr et al., 2003). In studies of human samples, Stathmin, a regulator of microtuble dynamics, has been shown to promote Taxol resistance (Balachandran et al., 2003).

B.3B. Metastatic Cascade. The process of metastasis is complex and requires multiple steps. First, a cell must intravasate into the bloodstream, survive the harsh environment, extravasate out of the blood and into the distant tissue, survive and grow there. Focusing on breast cancers of epithelial origin, in order for a cell to enter the bloodstream, it generally undergoes epithelial to mesenchymal transition (EMT). This step is important because mesenchymal cells have increased motility due to decreased attachment to surrounding cells (Hanahan and Weinberg, 2011). Additionally, the surrounding stroma has to be remodeled in order for the cell to reach the blood supply. In order for this to happen, tumor cells secrete proteins capable of breaking down stroma factors such as matrixmetalloproteinases (Nguyen et al., 2009).

Once a cell detaches from the basement membrane and enters the bloodstream, it generally undergoes a specialized form of cell death termed anoikis (Nguyen et al., 2009). In order for a cell to metastasize it must be resistant to anoikis and be able to survive the harsh environment of the bloodstream. Once a cell arrives at a distant site, it must leave the bloodstream and begin to proliferate in the new tissue. Breast cancers preferentially metastasize to lung, brain, and bone while other tumor types show preferences for other organs (Nguyen et al., 2009). This provides evidence that the process of metastasis is not completely random and that there are qualities inherent to the tumor and tumor cells that dictate the metastatic process. One such process is the formation of a metastatic niche. The location of metastases in the distant organ are not random, they are localized to specific areas. Within these areas there are bone marrow derived cells such as myeloid VEGF+ cells that generate a "niche" that mimics the bone marrow stem cell niche and supports growth of tumor cells in distant organs (Psaila and Lyden, 2009).

B.3C. Breast Cancer Stem Cells, Metastasis, and Drug Resistance. Over the past decade, a strong case has been built towards stem cells being at the root of tumor recurrence after therapy. Given that stem cells must persist through the life of the organism, they are inherently resistance to apoptosis. One generic assay of stem cell identification includes Hoescht staining. Stem cells contain high numbers of non-specific pumps (MDR family) that function to exclude environmental toxins (Dean et al., 2005). Also,

stem cells are resistant to apoptotic stimuli including the pathways induced by radiation therapy and chemotherapy (Dave et al., 2009). It is thought that this resistance is mediated by developmental pathway signaling including Wnt, Hedgehog, and Notch (Woodward et al., 2007; Li et al., 2008). Perhaps the clearest evidence for stem cell involvement in resistance comes from studies showing that after treatment, the amount of CD44 positive stem cells was increased significantly, implying that treatment leads to an enrichment of breast cancer stem cells (Li et al., 2008; Creighton et al., 2009).

Additionally, stem cells have been implicated in every step of the metastatic cascade. The Weinberg lab and now many others have shown that once a cell undergoes EMT it takes on markers of stem cells. Also, that tumor stem cells have mesenchymal markers (Mani et al., 2008). Given the inherent resistance to apoptosis and that stem cells can grow independent of a basement membrane it is not surprising that stem cells are resistant to anoikis and therefore more likely to survive in the bloodstream (Dontu et al., 2003). The metastatic niche recapitulates the bone marrow niche and is designed to support the growth of undifferentiated cells (Nguyen et al., 2009). Taken together, studies indicate that stem cells are better equipped to metastasize as compared to more differentiated tumor cell counterparts.

B.4. DNA Methylation and Breast Cancer

The addition of methylation marks to DNA occurs at CpG dinucleotides. In the human genome there approximately 28 million CpG sites and 10% of these are located in CpG islands, or high density regions, that are typically in the promoter region of genes (Jones and Baylin, 2007). DNA methylation generally results in the recruitment of additional epigenetic modifiers including histone deacetylases and the result is long term silencing of gene expression (Huang and Esteller, 2010).

DNA hypermethylation has been correlated with several critical events in breast cancer development and progression including tumorigenesis, invasion, metastasis, and drug resistance. In breast tumors, more than 150 genes have been shown to be hypermethylated including hormone receptors (estrogen receptor α and estrogen receptor β), cell cycle proteins (p16Ink4a and p14ARF), classic tumor supressors (BRCA1 and GATA-3), and genes important in epithelial maintenance such as E-Cadherin (Yan et al., 2000; Lujambio et al., 2007; Huang and Esteller, 2010). The understanding that tumor

suppressor genes are regulated epigenetically adds another layer of complexity to the understanding of breast cancer. While it was traditionally believed that certain genes would be mutated and therefore non functional in breast cancer, the understanding of epigenetics helped to explain why intact genes did not result in protein expression. Hypermethylation of many of these genes is thought to be correlated with a more malignant phenotype. For example DNA methylation of p16Ink4a is thought to contribute to the cell cycle dysregulation present in breast cancer (Herman et al., 1995).

DNA methylation is regulated by the DNA methyltransferase family of proteins. While there are many DNA methyltransferases, generally, three are considered to make up the core set of proteins. DNMT1 is a replication-associated protein responsible for placing methyl marks on newly synthesized DNA (Jones and Baylin, 2002). DNMT3a and DNMT3b are responsible for the majority of non-replication related methylation. Specifically, overexpression or dysregulation of DNMT3b is thought to contribute to the hypermethylated phenotype in breast cancer (Girault et al., 2003; Roll et al., 2008).

C. GATA-3, Regulator of Mammary Luminal Differentiation

C.1. Identification

GATA-3 belongs to the GATA family of zinc finger transcription factors. This family is involved in differentiation of various tissue types, specifically, GATA-1 is important in lymphocyte differentiation and GATA-3 is important in neuronal differentiation as well as T-cell maturation (Weiss and Orkin, 1995). A role for GATA-3 in the mammary gland was originally identified in a screen comparing estrogen receptor positive (MCF-7 and T47D) and negative cell lines (MDA-MB-231 and HBL-100). By cDNA array it was the most differentially expressed gene (Hoch et al., 1999). Based on this, several groups sought to understand the relationship of GATA-3 to mammary tumor biology.

C.2. GATA-3 and Differentiation

Two groups have shown that the GATA-3 transcription factor is expressed specifically in luminal cells and is required for differentiation (Asselin-Labat et al., 2007; Kouros-Mehr et al., 2006). Using the cre-lox system, it was shown that mice with mammary specific loss of GATA-3 showed gross defects.

When GATA-3 was deleted early in development using Keratin14-cre, mice failed to form mammary glands. Using MMTV-cre mammary glands showed decreased number of ductal trees and a decrease in markers of luminal differentiation such as estrogen receptor alpha and Keratin 18. These studies showed that GATA-3 is important for specifying cell fate in the mammary gland and for the branching and elongation stage that occurs during puberty. During pregnancy, there is extensive proliferation and outgrowth of mammary structures as well as the production of milk. Using the pregnancy specific WAP-cre it was shown that loss of GATA-3 led to a severe defect in milk production and less development of lobular alveolar units. Essentially, as shown in Figure 1.1, GATA-3 is necessary for the differentiation of luminal progenitors into CD61- ductal and alveolar cells and loss of GATA-3 led to an increase in CD61+ mammary progenitor cells. Additionally, it was shown that the forkhead box family member FoxA1 is a downstream target of GATA-3 (Asselin-Labat et al., 2007, Kouros-Mehr et al., 2006).

C.3. GATA-3 and Breast Cancer

Interestingly, one group went on to examine GATA-3 expression in a mouse model of adenocarcinomas. The MMTV-PyMT mouse (polyoma middle T-antigen under control of a mammary specific promoter) develops tumors that show a stepwise progression from hyperplasia to a highly metastatic undifferentiated adenocarcinoma (Lin et al., 2003). These mice develop hundreds of tumors making it difficult to follow the progression of a single tumor. Kouros-Mehr et al mated these mice to mice expressing GFP and then transplanted tumors to recipient mice, which allowed them to follow a single tumor over time. They showed that at 5 weeks when tumors were hyperplastic, GATA-3 expression was high. At 8 weeks tumors were at early carcinoma stage and showed a partial loss of GATA-3 while at 18 weeks tumors were GATA-3 negative. Also, cells that had metastasized to the lung were all GATA-3 negative showing that GATA-3 is a marker of tumor development in this model (Kouros-Mehr et al., 2008). Infecting transplanted tumors with a retrovirus containing GATA-3 led to an increase in tumor size but an increase in markers of differentiation and a 27 fold reduction in numbers of metastatic cells. Importantly, all metastatic cells were again GATA-3 negative indicating that GATA-3

Figure 1.1

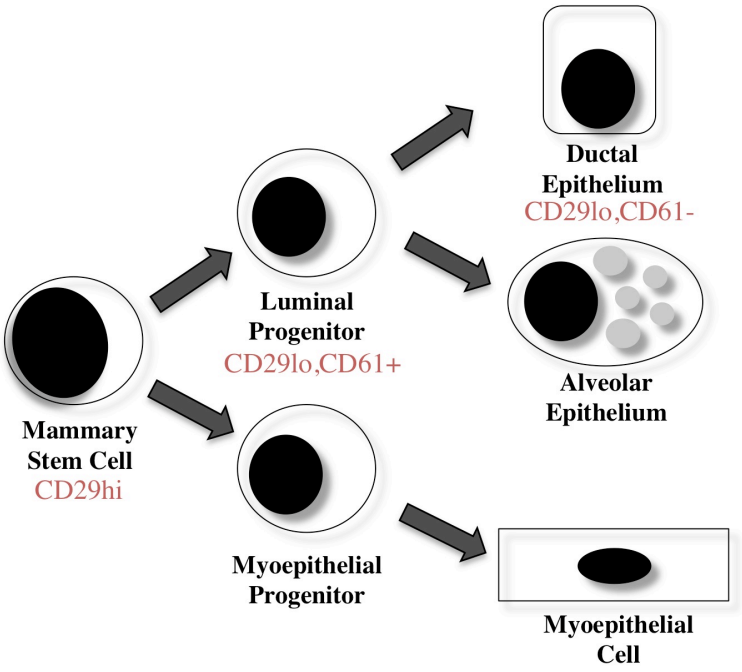
Ductal
Epithelium
CD29lo,CD61-
Luminal
Progenitor
CD29lo,CD61+
Alveolar
Epithelium
Mammary
Stem Cell
CD29hi
Myoepithelial
Progenitor
Myoepithelial
Cell

must be lost for cells to metastasize (Kouros-Mehr et al, 2008). Yan and colleagues attributed the ability of GATA-3 to inhibit metastasis to a key tumor suppressor function, the inhibition of EMT. Knockdown of GATA-3 in MCF-7 cells led to the cells becoming more mesenchymal as shown by the expression of vimentin and N-cadherin at the expense of E-cadherin (Yan et al., 2010).

In studies of human mammary tumors, it was observed that as tumors progressed and became more metastatic, GATA-3 expression was extinguished. One group showed that GATA-3 is often the target of DNA methylation in high-grade tumors (Yoon et al., 2000). This loss of GATA-3 has been associated with poor patient survival and a failure to respond to endocrine therapies (Albergaria et al., 2009; Yan et al., 2010; Yoon et al., 2010).

D. Retinoblastoma 1 (Rb) and Mammary Biology

The Rb1 protein was the first tumor suppressor identified. Loss of Rb leads to formation of the pediatric tumor retinoblastoma. Osteosarcoma, small cell lung carcinoma, and other tumor types have mutations or functional inactivation of Rb expression as well. Rb is a key regulator of the cell cycle. The E2F family of transcription factors are required for entry into S-phase. Rb binds to E2F, keeping the protein inactive and unable to transcriptionally upregulate genes required for S-phase entry. At the G1-S transition, Rb is phosphorylated by cyclin dependent kinases (CDK), which disrupts the Rb/E2F interaction and allows cell cycle progression (Classon and Harlow, 2002).

In a 2001 study by Robinson and colleagues, Rb null primordial mammary glands were removed from embryos and transplanted into recipient mice. This transplantation was necessary because Rb null mice die during embyrogenesis. Using this model, huge deficits in mammary development were not observed. Of note, this study did not examine pregnancy. The gland formed normally and major signaling pathways were not altered (Robinson et al., 2001).

A later study by Jiang et al sought to investigate the functional consequences of an inactivatable version of Rb in vivo. These mice had a delay in terminal end bud formation and a concomitant reduction in PCNA expression indicating a proliferation defect. These mice displayed another unique phenotype. Adult mice had signs of precocious pregnancy differentiation, the glands looked similar to mice that were

in the early stages of pregnancy. Perhaps most interesting, these mice developed hyperplasia and some mice when on to develop adenocarcinomas. This is a surprising phenotype for a tumor suppressor gene. The authors attributed this to the ability of Rb to promote cell survival. Mammary cells with unphosphorylatable Rb were resistant to apoptosis (Jiang et al., 2010).

E. The Transcription Factor FoxM1

FoxM1 was first identified using an antibody, MPM2, that specifically targets proteins that are phosphorylated during the cell cycle. Originally, FoxM1 was named MPP2 (MPM2 reactive phosphoprotein 2) later, Trident/WIN (winged helix identified in INS-1 cells), and HNF-3/HFH-11 (hepatocyte nuclear factor-3/forkhead homolog-11). The gene was cloned later using degenerate primers for the forkhead box DNA binding domain (Westendorf et al., 1994; Korver et al., 1997a, 1997b; Yao et al., 1997; Ye et al., 1997; Costa et al., 2003). While FoxM1 is expressed ubiquitously in the developing embryo, expression in adult mice is restricted to proliferating cells including those of the small intestine, colon, thymus, and testis (Korver et al., 1997; Ye et al., 1997).

Studies in yeast and mice have shown that FoxM1 is not essential for the early stages of embryogenesis but is required for organogenesis (Korver et al., 1998). Approximately half of FoxM1 knockout mice die between pregnancy day 19 and birth, late in embryonic development. The knockout animals that are born tend to gasp for air and suffocate shortly after birth. Careful examination of these mice led to the observation that FoxM1 knockout animals have a defect in their cardiomyocytes. The heart is hypertrophic and cardiomyocyte nuclei are enlarged, indicative of polyploidy. Polyploidy in both heart and lung tissue of knockout animals was confirmed. This phenotype of nuclear polyploidy mirrored that of p21 deficient mice providing the first hint that FoxM1 is a critical regulator of S-phase and a potential regulator of p21 (Korver et al., 1998).

Later studies demonstrated that FoxM1 knockout mice showed defects in liver as well as lung development. Mice show defects in liver organization. They do not develop bile ducts and have a reduction in the number of hepatocytes and large hepatic veins (Krupczak-Hollis et al., 2004). The lungs of embryonic FoxM1 knockout mice have significant vascular defects including a reduction in the number

of vessels and a hypertrophy of the vascular smooth muscle (Kim et al., 2005). From the early studies showing that FoxM1 was phosphorylated by the cell cycle and that cardiomyoctes displayed a polyploidy phenotype, it was hypothesized that FoxM1 played a role in regulating the cell cycle. Several groups later proved this when transcriptional targets of FoxM1 were identified. It was also demonstrated that FoxM1 has roles outside of cell cycle regulation and functions as a potent oncogene, pushing FoxM1 to the forefront of cancer research and identifying it as a potential therapeutic target.

E.1. FoxM1 Domains and Splice Variants

FoxM1 is part of the forkhead box family of transcription factors that contains more than 50 members that play a role in a wide spectrum of biological processes including proliferation, differentiation, and apoptosis. Members of this family all contain a homologous forkhead box DNA binding domain while the additional motifs bear little homology (Myatt and Lam, 2007). FoxM1 contains a centrally located DNA binding domain and a C-terminal transcriptional activation domain. Additionally, FoxM1 contains an N-terminal autorepressive domain and a central inhibitory domain that will be discussed in greater depth later (Wierstra and Alves, 2007).

There are three FoxM1 isoforms, FoxM1a, FoxM1b, and FoxM1c that have been cloned from human cells. The proteins are a result of alternative splicing from the same gene transcript present on chromosome 12p. FoxM1a contains two additional in frame exons while FoxM1c contains only one of these and FoxM1b does not contain any additional exons. While all of the proteins bind to the same DNA sequence, FoxM1a is not capable of transcriptional activation. Only FoxM1b and FoxM1c are evolutionarily conserved and transcriptionally active therefore, they will be collectively referred to as FoxM1 (Ye et al., 1997).

E.2. Cell Cycle Regulation

FoxM1 expression, activation, and degradation are all controlled by the cell cycle. In response to proliferative signaling, FoxM1 expression and phosphorylation is induced during G1/S and levels peak at

G2/M (Major 2004). In order for FoxM1 to transactivate target genes, it must be phosphorylated. While all of the regulative phosphorylation sites are not known and characterized, it has been demonstrated that FoxM1 is targeted for phosphorylation by several cell cycle regulated kinases. These include, Cyclin-Cdk complexes and Polo-like kinase 1 (PLK1) (Fu et al., 2008; Chen et al., 2009). These phosphorylation events are required for FoxM1 to recruit additional transcriptional activators such as p300/CREB-binding protein (CBP) histone acetyltransferase proteins (Major et al., 2004).

During the G1/S transition, FoxM1 transcriptionally upregulates Cks1 and Skp2, part of the SCF (Skp1-Cullin1-F-box) ubiquitin ligase complex that targets the cyclin-cdk inhibitors p27 and p21 for degradation (Wang et al, 2005; Petrovic et al., 2008). Additional G1/S phase targets include the direct target, Cyclin D1 and potentially Cyclin D2, Cyclin E, and Cdc25A indirectly through a transcriptional activation of c-myc (Wierstra and Alves, 2007).

FoxM1 is required for the successful entry and completion of mitosis. FoxM1 deficient cells fail to properly exit mitosis and undergo mitotic catastrophe, a specific type of cell death (Wonsey and Follettie, 2005). Mitotic transcriptional targets include genes important in spindle integrity such as Aurora B Kinase, Survivin, CENP-A, KIF20A, Nek-2, and PLK1 (Laoukili et al., 2005; Wang et al., 2005; Wierstra and Alves, 2007). At the end of mitosis, FoxM1 is degraded in a proteasome dependent manner. FoxM1 is targeted by the APC/Cdh1 ubiquitin ligase complex for degradation (Park et al., 2008; Laoukili et al., 2008). Additional negative regulators of FoxM1 include the tumor supressors p19ARF and p53 (Costa 2005a; Gusarova et al., 2007; Barsotti et al., 2009; Pandit et al., 2009).

E.3. FoxM1 as an Oncogene

Given the role of FoxM1 in regulation cell cycle, it is perhaps unsurprising that FoxM1 is overexpressed in every tumor type examined including those of reproductive, neurological, and hematological origin (Pilarsky et al., 2004; Myatt and Lam, 2007). FoxM1 deletion has significant effects on tumor growth. Mice with a liver specific deletion of FoxM1 are resistant to carcinogen induced tumor formation (Kalinichenko et al., 2004). In a later study, liver tumors were allowed to form and then FoxM1 was deleted using conditionally expressed cre and analyzed 10 weeks later. Livers lacking FoxM1 had

fewer numbers of tumors and these tumors were smaller in size further confirming the role of FoxM1 as an oncogene (Gusarova et al., 2007). As previously mentioned, FoxM1 is negative regulated by p19 ARF. This protein sequesters FoxM1 in the nucleolus where it is kept inactive. Interestingly, a short ARF peptide that contains amino acids 26-44 are sufficient to sequester FoxM1 and inhibit growth of tumor cells in vitro. Additionally, ARF peptide treatment in vivo led to an inhibition of liver tumor growth (Gusarova et al., 2007). Of note, overexpression of FoxM1 and deletion of ARF in a mouse model of liver cancer led to cells metastasizing to the lung further emphasizing the relationship between FoxM1 and ARF (Park et al., 2010).

Deletion of FoxM1 in pancreatic cancer cell lines led to an inhibition of cell invasion presumably due to a reduction in matrix metalloproteases, MMP-2 and MMP-9, transcriptional targets of FoxM1 and stromal remodeling proteins. Additionally, loss of FoxM1 led to a reduction in the regulators of angiogenic factors including VEGF (Wang et al., 2007). In lung cancer this effect could also be observed. Deletion of FoxM1 led to a failure of the mice to form carcinogen-induced tumors and interestingly, conditional deletion of FoxM1 in established tumors led to a drastic reduction in tumor size and animal survival (Wang et al., 2009).

Studies in tumor models including the prostate (LADY and TRAMP mice), glioblastoma, and lung cancers demonstrate that FoxM1 expression leads to accelerated proliferation and as a result, increased tumor growth. Additionally, FoxM1 protects from apoptosis, which leads to an increase in tumorgenecity (Kalin et al., 2006; Kim et al., 2006; Liu et al., 2006).

Elevated FoxM1 has continuously emerged as a marker of poor patient outcome further emphasizing the role of FoxM1 as an onocogene. In a study of colorectal cancer patients, FoxM1 was significantly upregulated and correlated with a lack of tumor differentiation and high rates of proliferation (Uddin et al., 2011). In malignant peripheral nerve sheath tumors (MPNST's), FoxM1 was shown to be the target of gene amplification. This alteration in the copy number of FoxM1 served as a predictor of poor patient outcome (Yu et al., 2011). This trend is continued in squamous cell lung tumors where FoxM1 was associated with high tumor grade and lower survival (Yang et al., 2009).

In a recent study, FoxM1 was identified as an early marker of breast cell transformation. In microarray data comparing ductal carcinoma in situ (DCIS) samples to normal tissue in mice, FoxM1 emerged as one of the seven markers of transformation in mammary epithelial cells (Kretschmer et al., 2011). Another study of human tumors provided additional insight into the pattern of FoxM1 expression. Bektas and colleagues demonstrated that FoxM1 is correlated with expression of HER2/ErbB2, a marker of an aggressive tumor type. Additionally, high FoxM1 expression was predictive of poor patient survival and metastatic relapse (Bektas et al., 2008; Yau et al., 2011).

E.3A. FoxM1 and ROS. Given the widespread expression of FoxM1 across various tumor types it was generally thought that this was directly related to the ability of FoxM1 to regulate the cell cycle. Yet, it is becoming increasing apparent that FoxM1 can direct additional cellular processes important in tumor progression such as regulation of reactive oxygen species.

Reactive oxygen species are generated as products of intracellular metabolic processes and are thought to be generally harmful to cells. While it has been shown that another forkhead box transcription factor, FoxO can function to protect cells from oxidative stress, this pathway is inactivated by Akt signaling in proliferating cells. In tumor cells, where FoxO is commonly inactive, high amounts of ROS are produced and a balance between production and breakdown must still be maintained. It was demonstrated that FoxM1 can active the transcription of key ROS scavenger genes including manganese superoxide dismutase (MnSOD) and catalase, thereby protecting tumor cells from harmful ROS. Additionally, in this study, it was shown that tumor cells that have activated Akt signaling are “addicated” to FoxM1 for survival, which establishes FoxM1 as a therapeutic target in various tumor types (Park et al., 2009).

E.3B. FoxM1 and Metastasis. In a recent study by Park and colleagues it was shown that FoxM1 is able to regulate processes important in metastasis. As previously mentioned, FoxM1 overexpressing, ARF deleted HCC cells were metastatic when compared to control cell lines. Interestingly, it was

observed that hepatocellular carcinoma cells expressing FoxM1 in the absence of ARF had a mesenchymal appearance compared to ARF knockout. Additionally, these cells lacked expression of E-Cadherin, an epithelial marker and had increased expression of vimentin and α-SMA, markers of mesenchymal cell types. This phenotype was attributed to an increase in Akt signaling observed in these cells (Park et al., 2011). Additionally, this study showed that these cells expressed high amounts of lysyl oxidase (LOX) genes that are involved in the formation of a metastatic niche. Cells that metastasize are generally restricted to certain organs and regions according to the initial tumor type. Primary tumors establish the "soil" for metastasis by releasing factors that regulate distant sites and LOX genes fall into this category. This study showed that FoxM1 promotes the formation of the pre-metastatic niche, which can account for the ability of FoxM1 to increase metastatic growth (Park et al., 2011).

2. FoxM1 Inhibits Mammary Luminal Differentiation Through Transcriptional Repression of GATA-3

A. Overview

Elevated expression of FoxM1 in breast cancer correlates with an undifferentiated tumor phenotype and a poor clinical outcome. A role of FoxM1 in regulating mammary differentiation, however, was unknown. Here, we show that regeneration of mouse mammary glands with elevated levels of FoxM1 leads to aberrant ductal morphology and expansion of the luminal progenitor pool. Conversely, in vivo knockdown of FoxM1 results in a shift towards the differentiated state. FoxM1 inhibits luminal differentiation via a novel mechanism, transcriptional repression of GATA-3. FoxM1 associates with DNMT3 and promotes DNA methylation of the GATA-3 promoter in an Rb-dependent manner, revealing a new role of the FoxM1/Rb interaction. This study identifies FoxM1 as a critical regulator of GATA-3 expression and mammary luminal differentiation.

B. Characterization of FoxM1 Expression in Breast Cancer and Mammary Development

Tumor grade is inversely correlated with patient outcome. Well-differentiated or low-grade tumors maintain the structure of the gland of origin, have a low mitotic index, and are highly responsive to therapy. High-grade or poorly differentiated tumors show the converse pattern. Tumors display irregular nuclei, atypical tubular structure, and are associated with high rates of metastasis and poor patient survival (Elston and Ellis, 1991). Analysis of publicly available microarray data (Oncomine) demonstrates that the expression of *FoxM1* increases with tumor grade in human breast cancers (Figure 2.1).

From human tumor analysis we hypothesize that FoxM1 may negatively regulate mammary differentiation. To investigate this, we examined the normal pattern of expression throughout the key stages of postnatal mammary development. Pregnancy, a period of ductal growth and expansion, showed high levels that steadily decreased through days 1, 5 and 10 of lactation; while involution, characterized by apoptosis and remodeling, exhibited the lowest expression. This pattern was also reflected at the

Figure 2.1

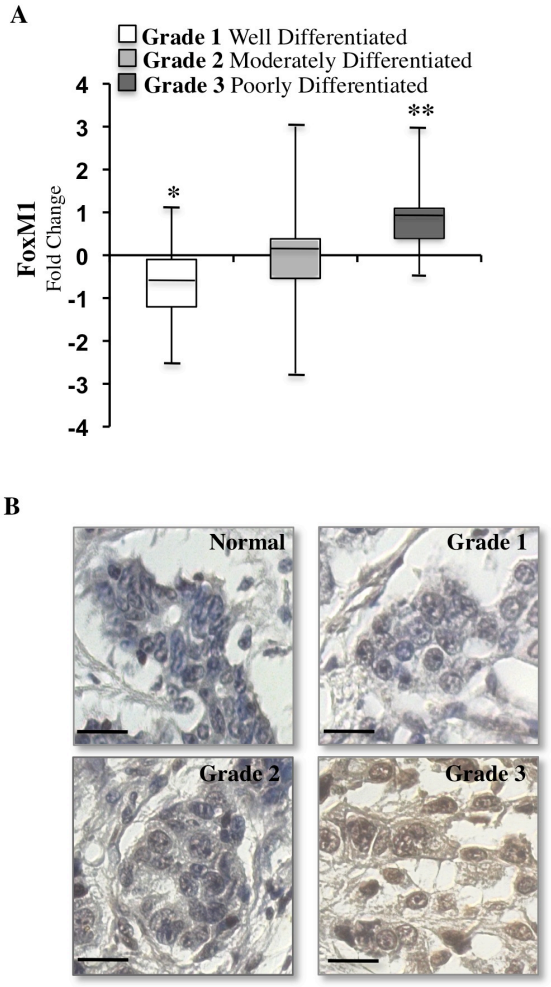

Figure 2.1. FoxM1 is inversely correlated with breast cancer tumor grade. (A) Oncomine, a publicly available microarray database was used to analyze FoxM1 expression in 200 samples of invasive ductal carcinoma. Samples were organized by grade and fold-change of FoxM1 RNA from normal was graphed using a box plot *$p<10^{-6}$. (B) Representative immunohistochemistry of FoxM1 in normal mammary tissue as well as grade 1, grade2, and grade 3 breast carcinomas are shown. Scale bar represents 10μm.

protein level by immunohistochemistry (Figure 2.2). Mammary terminal end buds, present during puberty are of particular significance because the cap cells or those found in the invading front compose the progenitor cell population. Strong nuclear staining for FoxM1 was observed in the cap and progenitor cells (Figure 2.2, top left). At all stages of development, FoxM1 expression was primarily found in cells of luminal lineage. To confirm this observation, we used in situ hybridization to identify *FoxM1* mRNA followed by immunostaining for luminal and myoepithelial cell types. There was a clear overlap of antisense probe hybridization and cytokeratin 18 staining indicating FoxM1 is expressed mainly in luminal cells (Figure 2.3).

The timing and pattern of expression suggests that *FoxM1* levels are higher in cells that are less differentiated. Previously defined flow cytometry markers were used to separate mammary stem cells (CD29hi), luminal progenitors (CD29lo, CD61+), and differentiated luminal cells (CD29lo, CD61-) (Stingl et al., 2006; Shackleton et al., 2006; Asselin-Labat et al., 2007). Sorted RNA from C57BL/6 mice was analyzed for *FoxM1* expression using quantitative RT-PCR. The level of *FoxM1* in stem cells was ten-fold higher than differentiated cells, while luminal progenitors showed a nearly 50-fold increase. Expression of cytokeratin 18, c-kit, and smooth muscle actin were used to determine the purity of luminal, luminal progenitors and myoepithelial populations respectively (Figure 2.4; Lim et al., 2009). Taken together, these results demonstrate that *FoxM1* expression is highest in luminal progenitor cells and decreases upon differentiation.

C. Loss of FoxM1 Leads to a Delay in Lobuloalveolar Development During Pregnancy

In order to examine the role of FoxM1 at key stages of mammary development, we utilized the previously established WAP-Cre system (Wagner et al., 1997). Mice expressing WAP-Cre were crossed with mice harboring the *FoxM1* gene flanked by LoxP sites (*FoxM1* FL/FL). This system allows deletion of *FoxM1* in epithelial cells as they differentiate during pregnancy. During the second pregnancy, we examined mammary glands at the following time points: 8 weeks (virgin), pregnancy day 6 (early

Figure 2.2

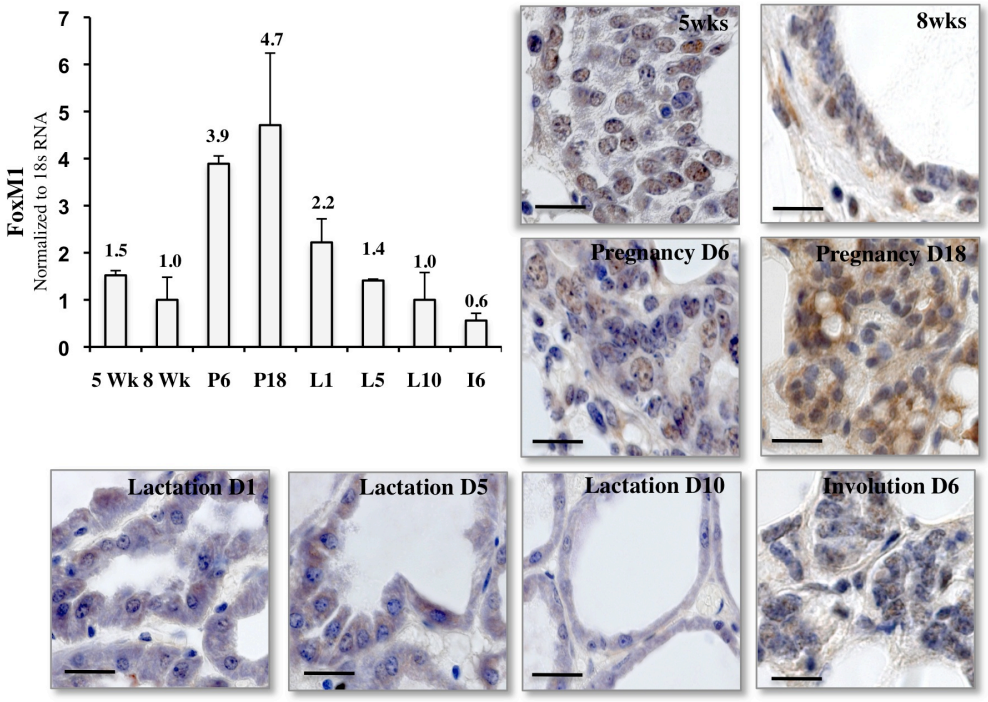

Figure 2.2. Characterization of FoxM1 expression during postnatal development. Levels of FoxM1 RNA were determined by semi-quantitative RT-PCR and protein was analyzed using western blotting. All samples were collected from inguinal mammary glands at various developmental stages: 5 weeks (puberty), 8 weeks (virgin adult), P6, P18 (early and late pregnancy), L1, L5, L10 (lactation), and I6 (involution). 4-7 mice were used for each stage. Glands from each stage were sectioned and stained for FoxM1 expression using DAB and hemetoxylin counterstain.

Figure 2.3

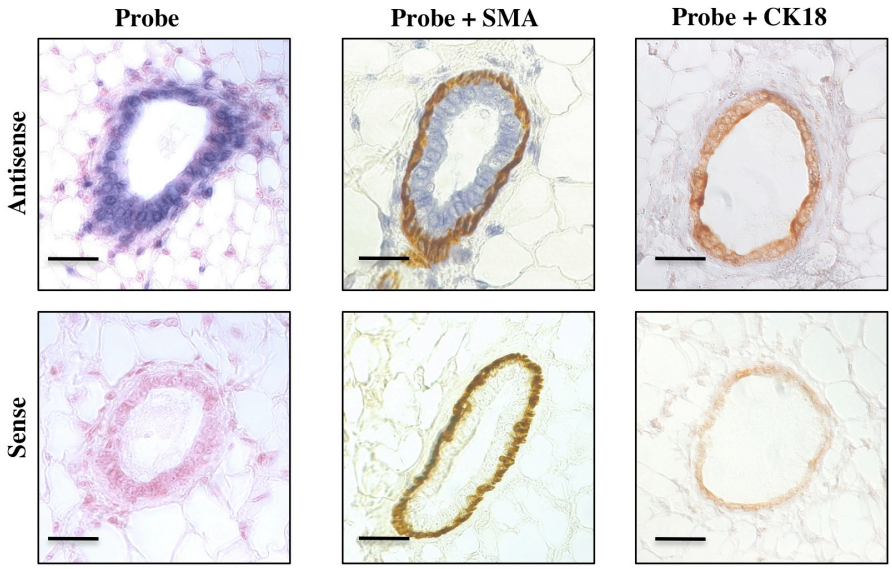

Figure 2.3. FoxM1 expression is limited to luminal cells. In situ hybridization using a FoxM1 sense or antisense probe was used to stain wildtype tissue. After, samples were immunostained with smooth muscle actin or cytokeratin 18 antibody as indicated. Scale bar represents 50μM.

Figure 2.4

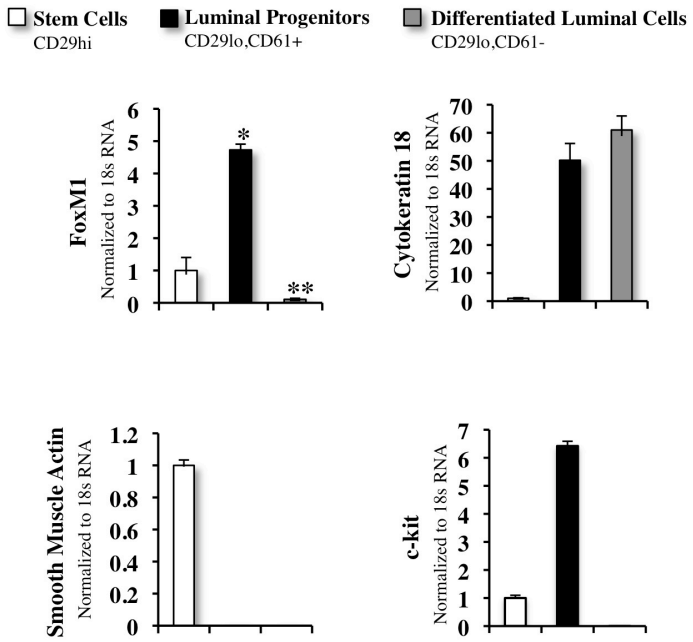

Figure 2.4. FoxM1 is expressed in undifferentiated luminal cells. Mammary glands from 8-week-old C57BL/6 mice were digested and stained for CD24, CD29, and CD61. Stem cells, luminal progenitors, and luminal cells were sorted. Cytokeratin 18, smooth muscle actin, and c-kit were used to assess the purity of the populations. RT-PCR shows relative expression of CK18, SMA, and FoxM1. Data is normalized to the stem cell population *p<10-4 **p<0.05.

pregnancy), pregnancy day 18 (late pregnancy), lactation days 1,5, 10, and involution day 6 (Figure 2.5). During early stages of pregnancy, the mammary epithelium expands and begins to form lobuloalveolar units (Hennighausen and Robinson, 2005). These structures were clearly seen in wild-type mice at pregnancy day 6 but, none of the *FoxM1* FL/FL mice developed lobuloalveolar structures. The pregnancy day 6 glands in the *FoxM1* FL/FL mice appeared similar to those of 8-week virgin controls (Figure 2.5).These glands failed to form appreciable alveoli as evidenced in whole mount analysis (Figures 2.5). At pregnancy day 18 however, alveoli were clearly visible, albeit in reduced number, indicating a delay in aleveolar differentiation in the *FoxM1* FL/FL mice.

Lactating glands in *FoxM1* FL/FL mice were histologically different from those of wild-type mice. *FoxM1* FL/FL glands appeared flattened and the number of milk globules in the alveoli was reduced compared to those of wildtype (Figure 2.6). Pups from the *FoxM1* FL/FL mice survived and did not differ in weight in comparison to pups born to control mice indicating FL/FL mice were able to produce sufficient milk to support their litters (data not shown). Western blot of key milk proteins showed a delay in accumulation of both α and β-casein in FL/FL mice during pregnancy. Yet, on lactation day 1, *FoxM1* FL/FL mice and WT mice showed equivalent expression of milk proteins (Figure 2.7). This observation was supported by immunohistochemical staining for the milk proteins (Figure 2.7). Taken together, these data suggest that the loss of *FoxM1* leads to a delay in lobuloalveolar differentiation.

D. Acute Loss of FoxM1 Results in an Increase in Differentiated Luminal Cells

To determine whether FoxM1 acts as a regulator of luminal cell differentiation in virgin mice, we analyzed the consequences of *FoxM1* deletion in mammary tissue using the WAP-rtTA-Cre deletion system. Unlike the WAP-Cre system, the WAP-rtTA system allows for deletion in non-pregnant mice (Kouros-Mehr et al., 2006). *FoxM1* FL/+ and FL/FL littermates, expressing the inducible Cre, were given doxycycline in their drinking water for 5 or 15 days. After 5 days of treatment, we observed an 80% reduction of *FoxM1* in luminal progenitors and 90% in differentiated luminal cells while stem cells did not show a significant reduction (Figure 2.8).

Figure 2.5

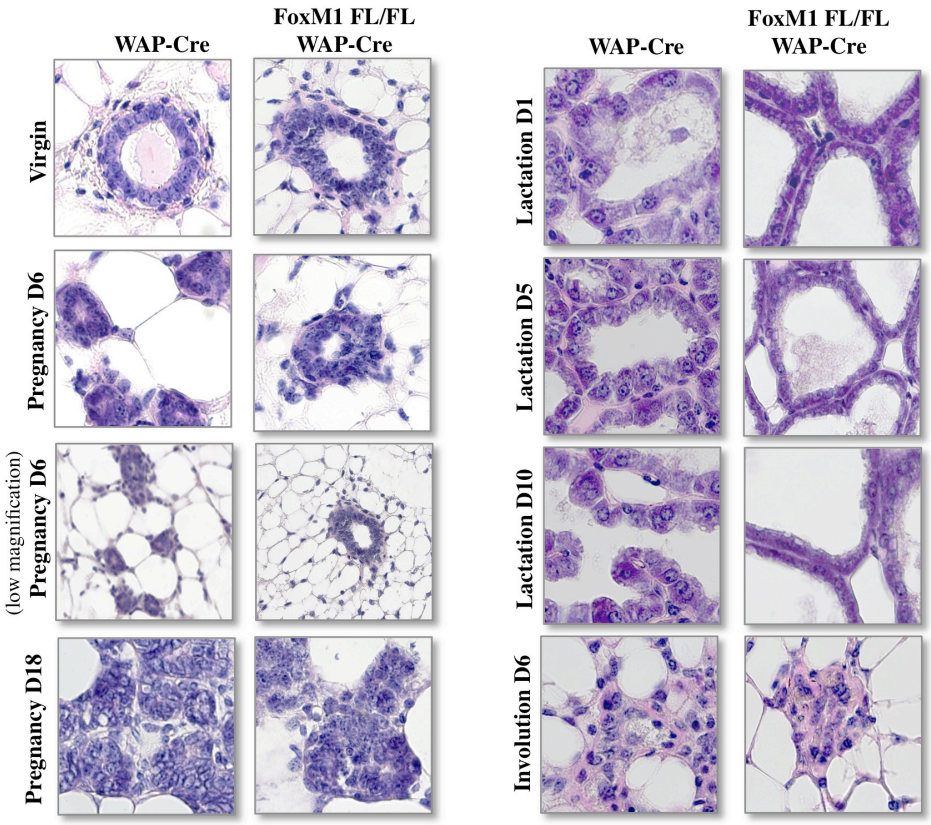

Figure 2.5. FoxM1 loss results in defects in mammary development during pregnancy. H&E staining of mammary gland sections from each time-point is shown. Control glands expressing only WAP-Cre are shown on right and glands lacking FoxM1 are shown in adjacent panels. A lower magnification of pregnancy day 6 glands is shown to better demonstrate details. Scale bar represents 10μM. .

Figure 2.6

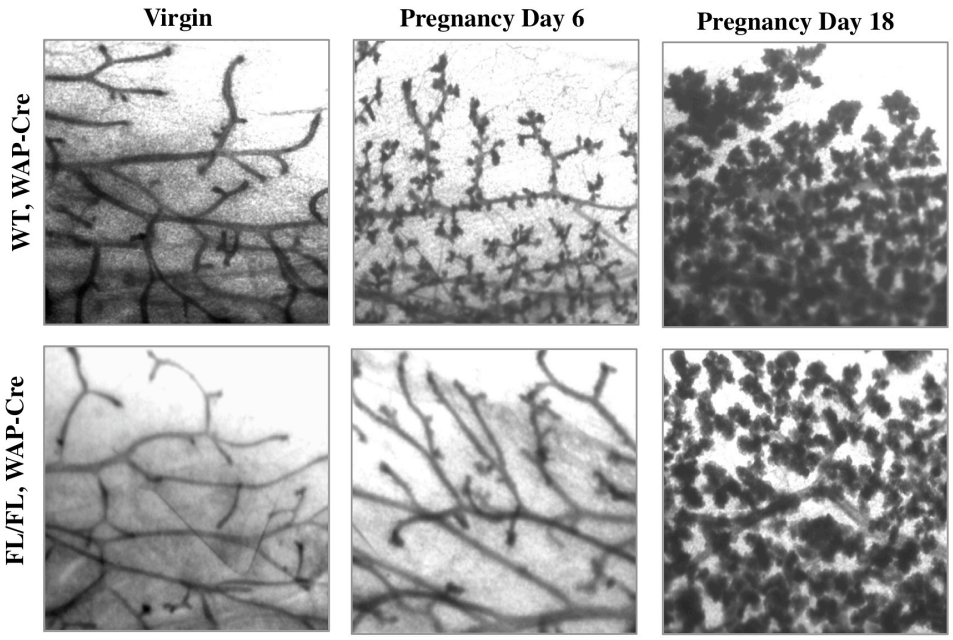

Figure 2.6. FoxM1 loss effects alveolar structure development in early pregnancy. Representative carmine alum whole mount analysis of mice expressing WAP-Cre and either wildtype *FoxM1* or *FoxM1* FL/FL. Pictures taken at 3x magnification are shown in black and white to increase the clarity. 4-8 mice from both genotypes were analyzed at every stage.

Figure 2.7

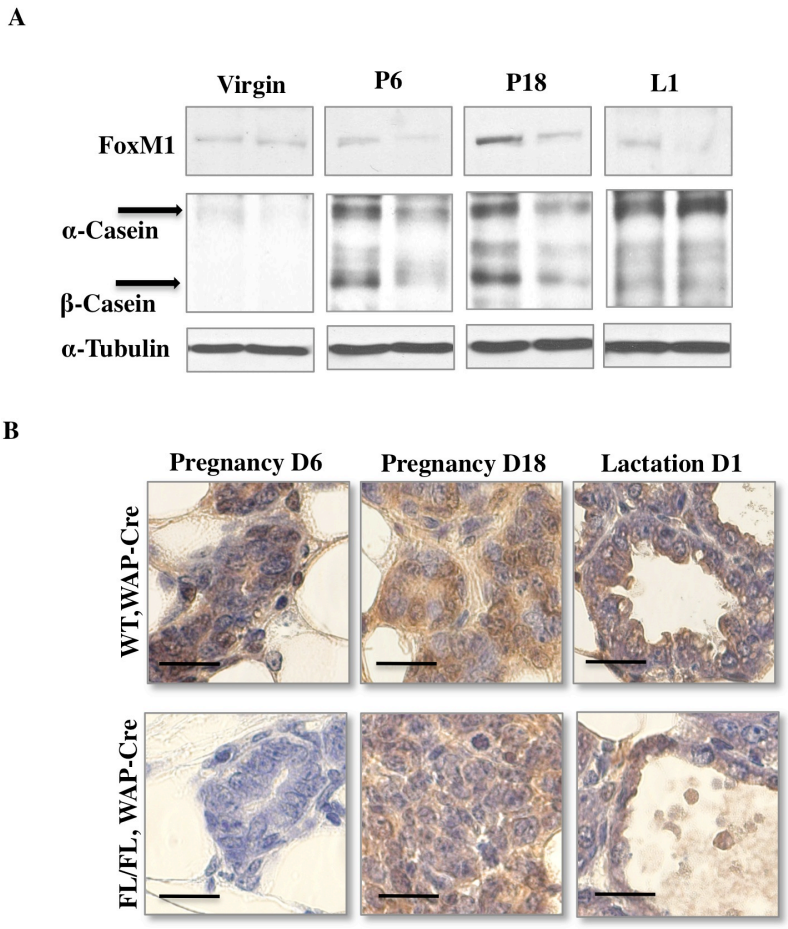

Figure 2.7 FoxM1 loss leads to decreased expression of milk proteins. (A) Western blot of FoxM1, α-Casein, and β-Casein are shown. α-tubulin is provided as a loading control. (B) Immunohistochemistry using an antibody against mouse milk is shown in the lower panel. Staining is done using DAB with a hematoxylin counterstain.

Figure 2.8

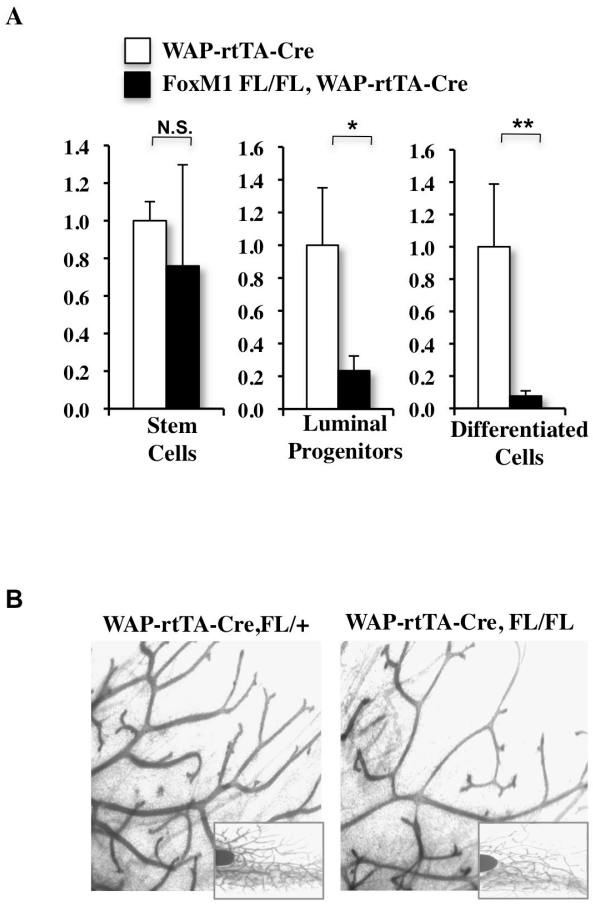

Figure 2.8. Histology of Acute FoxM1 Deletion. (A) Four 8- week-old WAP-rtTA-Cre and FoxM1 FL/FL, WAP-rTA-Cre mice were treated with doxycycline (2mg/ml) in their drinking water for five days. Stem, luminal progenitor, and luminal cells were sorted and FoxM1 expression was analyzed by RT-PCR *p<0.01 **p<10-3. (B) Whole mount of inguinal mammary glands 15 days after doxycycline treatment were visualized with carmine alum stain. Higher magnification (3X) is shown with lower magnification in the inset (1X). Images are shown in black and white in order to increase the clarity.

After 15 days of doxycycline, FoxM1 protein was undetectable by immunostaining. Whole mount staining using carmine alum showed that *FoxM1* FL/FL, WAP-rtTA-Cre mice had narrow ductal branching, whereas the *FoxM1* FL/+ mice appeared identical to wildtype mice (Figure 2.8). Quantification of the number of branches showed no difference between FL/+ and FL/FL glands (Figure 2.9). On closer examination of the recombinant glands by sectioning, *FoxM1* FL/FL mice exhibited abnormal histological staining by H&E. Glands were not composed of a single layer of epithelial cells and lumens were filled with cells that expanded beyond the myoepithelial layer (Figure 2.10). The rates of proliferation and apoptosis were similar between both genotypes (Figure 2.9). Staining of cytokeratin 18 and estrogen receptor alpha indicated that the cells were mature luminal epithelium, suggesting an expansion of the differentiated pool (Figure 2.10).

Stem, progenitor, and differentiated pools were analyzed after 15 days of treatment to examine the effects of *FoxM1* deletion on mammary cell subtypes. There was an approximate 20% increase in differentiated luminal cells with a concomitant loss in stem and progenitor populations demonstrating that loss of *FoxM1* in the mammary gland resulted in a shift towards the differentiated state (Figure 2.11). Interestingly, the stem cell population was affected by the loss of *FoxM1*, yet *FoxM1* was not deleted in this population. The effect on the stem cell pool was likely secondary to changes in the differentiated cell population as it has been shown that the stem cell pool is regulated through hormonally mediated paracrine signaling by differentiated luminal cells (Asselin-Labat et al., 2010; Joshi et al., 2010). Consistent with the observation that *FoxM1* loss leads to a shift towards the differentiated state, deletion resulted in an increase in markers of luminal differentiation, including *estrogen receptor alpha, amphiregulin, cytokeratin 18,* and *cadherin 11* (Figure 2.12). Taken together, these data demonstrate that loss of *FoxM1* in the adult gland leads to an increase in differentiated cells and a loss of progenitor pools.

E. Increased Expression of FoxM1 Inhibits Luminal Differentiation

In order to explore the consequences of high levels of *FoxM1* on mammary differentiation, we regenerated the mouse mammary gland with elevated expression of *FoxM1*. We took advantage of previous work involving mammospheres, an ex-vivo system of culturing mammary stem and progenitor

Figure 2.9

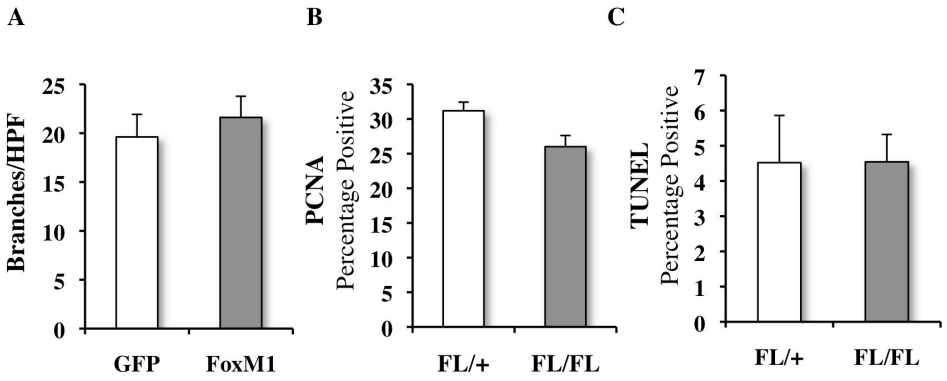

Figure 2.9. Additional Analysis of *In Vivo* Models. (A) Quantification of whole mount branching is shown. The number of branches in ten high power fields (HPF) from four glands were counted. (B) PCNA staining of both control and FL/FL glands was performed. Ten high power fields from four mice of each genotype were used for quantification. The number of positive cells over the total cell number was determined and the percentage was graphed. (C) TUNEL assay of paraffin sections was performed. DAPI was used to determine total cell number. Quantification from 10 high power fields in four mice of each genotype is shown.

Figure 2.10

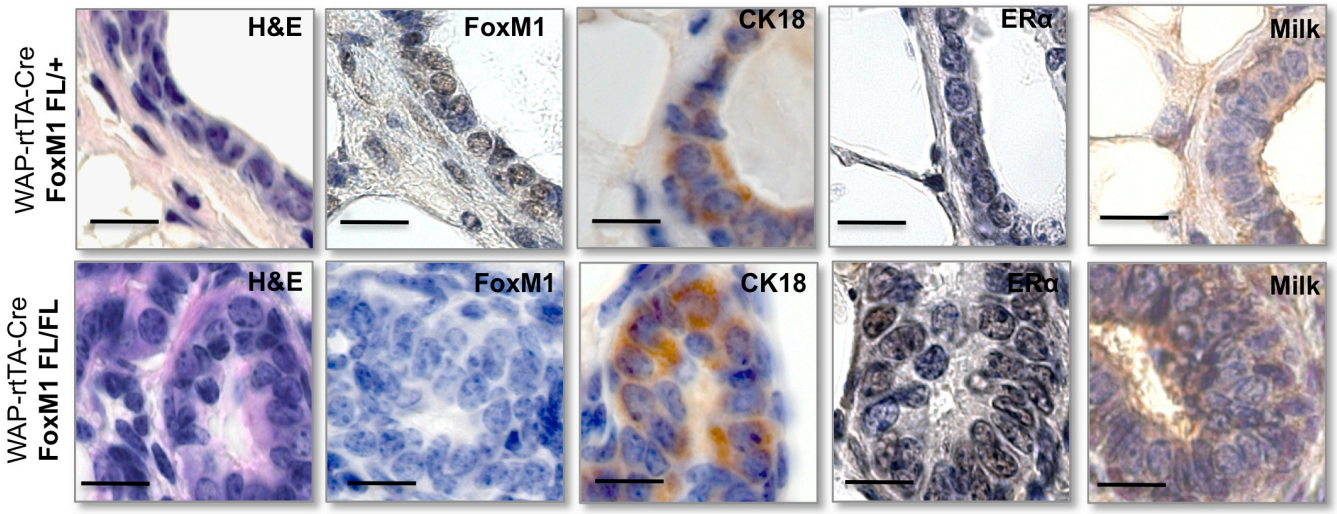

Figure 2.10. Markers of Differentiation in Acute FoxM1 Deletion. Hematoxylin and eosin staining as well as immunohistochemistry of FoxM1, cytokeratin 18, estrogen receptor alpha, and milk are shown after 15 days of treatment. Scale bar represents 10μm.

Figure 2.11

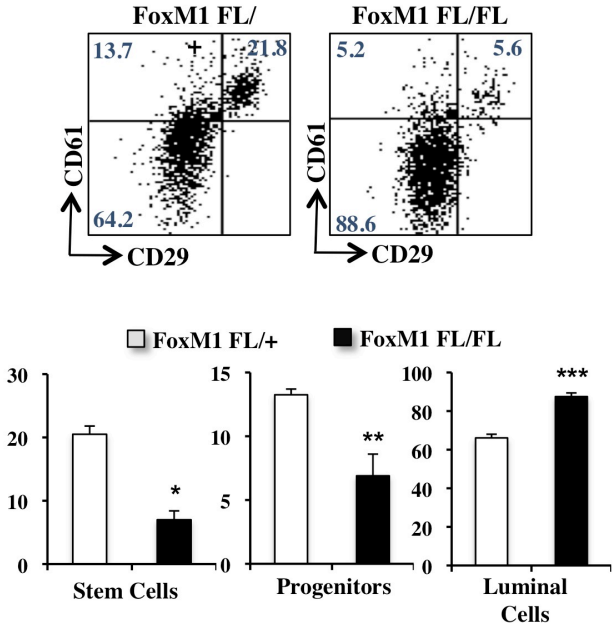

Figure 2.11. FoxM1 deletion leads to an expansion of differentiated luminal cells. Flow cytometry analysis of stem cells, luminal progenitors, and differentiated luminal cells. The plots show CD29 and CD61 expression of cells that stained positive for CD24. Percentage of each cell type for both genotypes is shown below *p<0.04 **p<0.05 ***p<0.03.

Figure 2.12

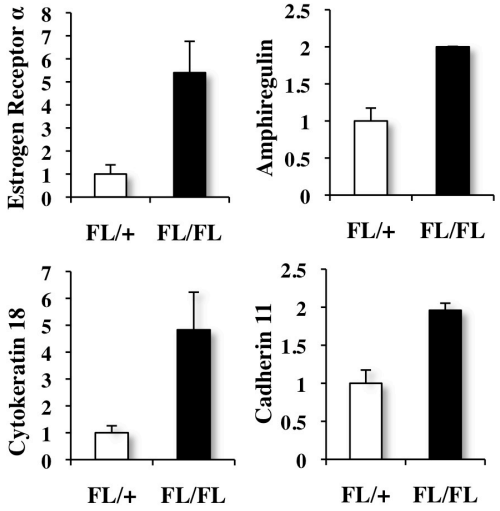

Figure 2.12. FoxM1 deletion leads to an increase of differentiated luminal cell markers. RT-PCR of *estrogen receptor alpha, amphiregulin, cytokeratin 18, and cadherin 11* are shown normalized to 18s RNA *$p<10^{-3}$, **$p<0.05$, ***$p<0.01$.

cells (Dontu et al., 2003). These mammospheres can be genetically manipulated by viruses and subsequently implanted into the cleared fat pad of 3-4 week old prepubescent mice. After 7-8 weeks, manipulated cells repopulate the entire gland (Deome et al., 1959; Liao et al., 2007).

Mammary epithelial cells were obtained from 6-8 week old mice, infected with retrovirus expressing either *GFP* or *GFP-FoxM1*, then allowed to form spheres. *GFP* positive mammosphere cells were identified by sorting and injected into the cleared fat pads of 3-4 week old mice. *GFP* and *GFP-FoxM1* positive cells were placed on contralateral sides of the same animal, allowing each animal to function as their own control (Figure 2.13). On whole mount analysis, *GFP-FoxM1* glands showed narrowing in comparison to their *GFP* counterparts (Figure 2.13). Regenerated glands were sectioned and stained to analyze the architecture of individual ducts. *GFP* glands showed the expected staining pattern while *FoxM1* expressing glands showed distinct hyperplastic regions of excessive cell infiltration, epithelial cells were filling the lumen or spreading beyond the basal layer (Figure 2.14).

To further investigate the altered architecture of *FoxM1* expressing glands, sections were analyzed using immunohistochemistry. Staining with the basal marker, smooth muscle actin (SMA) revealed a startling phenotype. As expected, *GFP* glands contained a layer of SMA positive cells surrounding luminal cells while *FoxM1* expressing glands contained the expected pattern as well as SMA positive cells surrounded by luminal cells (Figure 2.14). This phenotype was previously observed in glands expressing shRNA to Cbf-1, a notch cofactor and was correlated with an expansion of undifferentiated mammary cells (Bouras et al., 2008). Of note, these cells did not stain positive with the basal marker p63, indicating that they were not misplaced myoepithelial cells (Figure 2.15). Additionally, these changes could not be attributed to the ability of FoxM1 to regulate proliferation or apoptosis as there were no differences in markers for either (Figure 2.15).

Cytokeratin 18 staining shows a uniform luminal restricted staining pattern (Henninghausen and Robinson 2005). The *GFP* glands exhibited this typical staining pattern, while the *FoxM1* glands showed a punctate pattern distinct from differentiated luminal cells. The expanded cells did not stain positive for

Figure 2.13

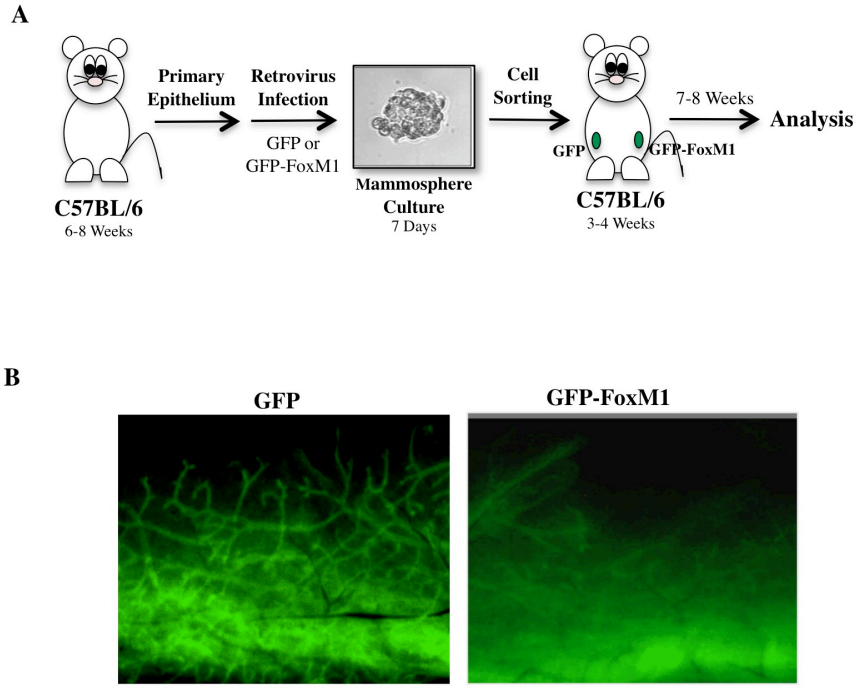

Figure 2.13. Regeneration of mouse mammary glands with FoxM1. (A) Schematic representation of experimental design. (B) GFP whole mount imaging of mammary glands. Boxed areas are shown in the inset at lower magnification.

Figure 2.14

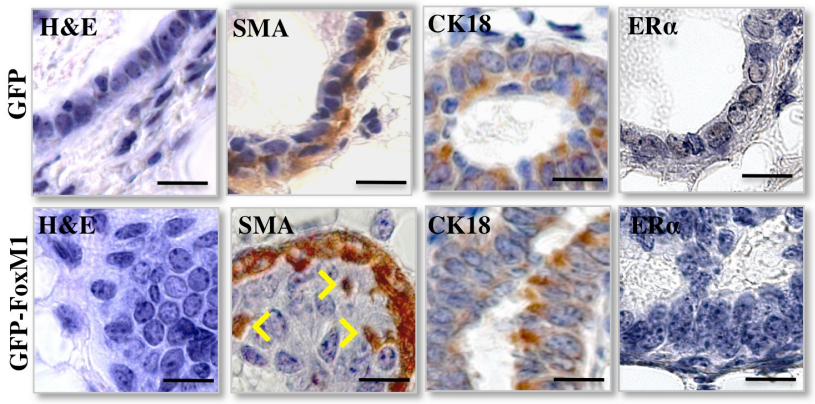

Figure 2.14. Histology of regenerated glands. Hematoxylin and eosin and immunohistochemistry of GFP and FoxM1-GFP glands. Smooth muscle actin, cytokeratin 18, and estrogen receptor alpha immunostaining is shown. Arrows in SMA section are showing displaced SMA+ cells surrounded by luminal cells. Representative sections from six mice are shown. Scale bar represents 10μm.

Figure 2.15

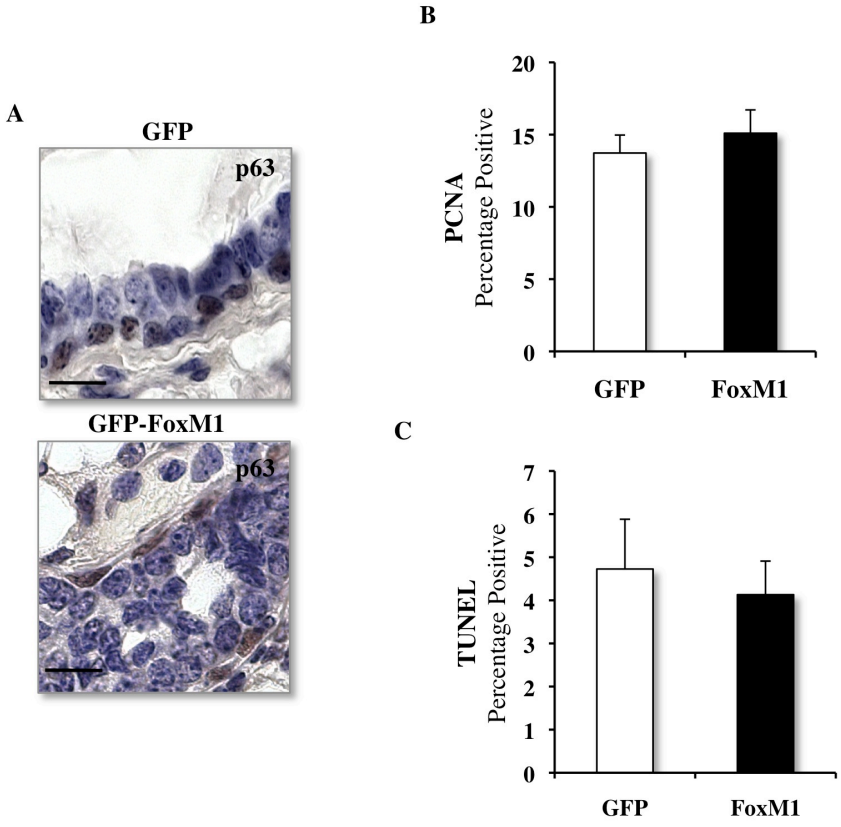

Figure 2.15. Additional Analysis of Regeneration Model. (A) Immunohistochemistry of p63 was performed using DAB and hematoxylin counterstain. Scale bar represents 10μM. (B) PCNA quantification was performed as described in panel B. (C) TUNEL assay of GFP and FoxM1 expressing glands quantification is shown.

Figure 2.16

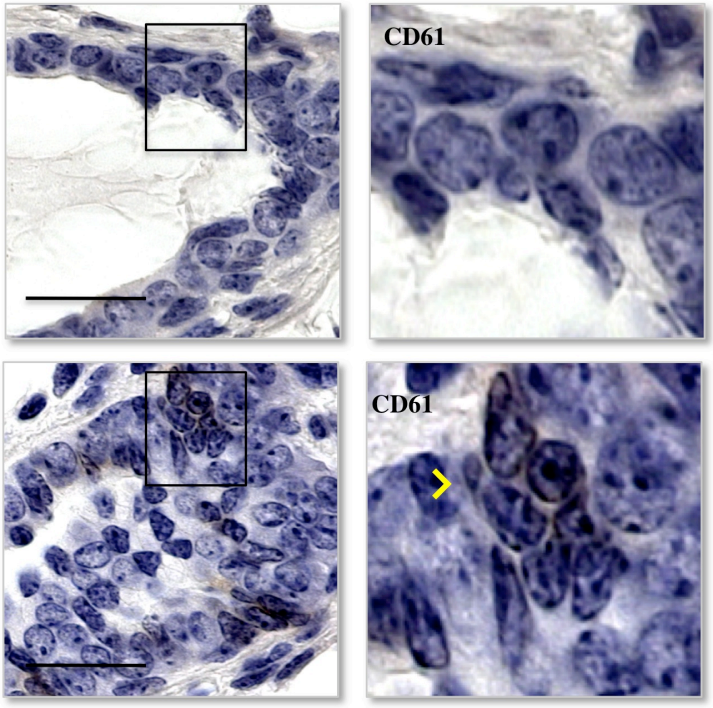

Figure 2.16. Expansion of luminal progenitor population in FoxM1 overexpressing glands. CD61 immunohistochemistry is shown. Enlarged images of GFP and GFP-FoxM1 mice are displayed in the right panel. Arrowhead shows a cluster of CD61+ cells. .

estrogen receptor alpha, indicating the expansion of an undifferentiated cell of luminal origin. This notion is further supported by staining for CD61, a marker of luminal progenitors. Glands expressing *FoxM1* exhibited an increased number and intensity of CD61 positive cells as compared to control glands (Figure 2.16).

To confirm the expansion of an undifferentiated cell type in *FoxM1* expressing glands, we analyzed cell populations using flow cytometry. Comparing *FoxM1* to paired *GFP* controls showed a distinct shift away from the differentiated state. The luminal progenitor pool expanded considerably, approximately 20%, with a similar reduction in the percentage of differentiated cells, suggesting that addition of *FoxM1* resulted in a failure of cells to properly exit the luminal progenitor pool and differentiate fully (Figure 2.17). Consistent with this notion, RT-PCR data showed a reduction in *estrogen receptor alpha, amphiregulin, cytokeratin 18*, and *cadherin 11*, markers of luminal differentiation (Figure 2.18).

F. FoxM1 is a Negative Regulator of GATA-3 *In Vivo*

The hyperplastic phenotype has been previously observed after acute loss of *GATA-3* in the mammary gland (Kouros-Mehr 2006). GATA-3 has been shown to be a key regulator of luminal differentiation and a tumor suppressor (Asselin-Labat 2007, Dydensborg 2009, Yoon 2010). We hypothesize that FoxM1 functions as a negative regulator of GATA-3. Glands in which *FoxM1* was deleted showed a considerable increase in GATA-3 RNA and protein levels by western blot and RT-PCR respectively. Conversely, the RNA and protein level of GATA-3 was significantly decreased in *GFP-FoxM1* expressing glands compared to *GFP* counterparts (Figure 2.19). Sorted luminal progenitors from both overexpression and knockdown mice also exhibited evidence that FoxM1 regulates GATA-3 in the progenitor population (Figure 2.20). GATA-3 immunostaining generally shows a pattern of strong nuclear staining in luminal cells that was evident in control glands. *FoxM1* deletion resulted in an increased staining intensity while overexpression resulted in a decreased and diffuse staining pattern for GATA-3 (Figure 2.21).

Figure 2.17

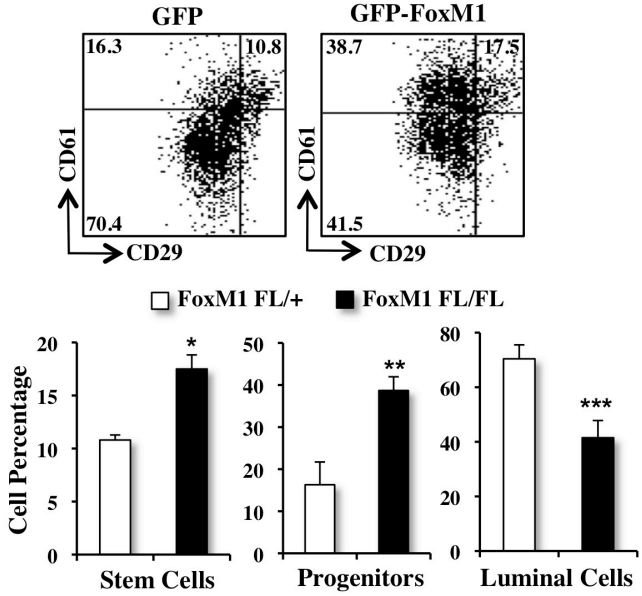

Figure 2.17. FoxM1 overexpression results in an expansion of undifferentiated mammary cells. Analysis of mammary stem cells, luminal progenitor, and luminal cell pools was performed in GFP or FoxM1-GFP expressing mice. Glands were digested to generate single cell suspensions, stained, and examined by flow cytometry. Representative dot plots of CD24+ cells are shown with percentages listed in each box. The bottom panel provides quantification from four mice. The percentage of each population is shown relative to the GFP control in the same animal *p<0.03 **p<0.01 ***p<0.001

Figure 2.18

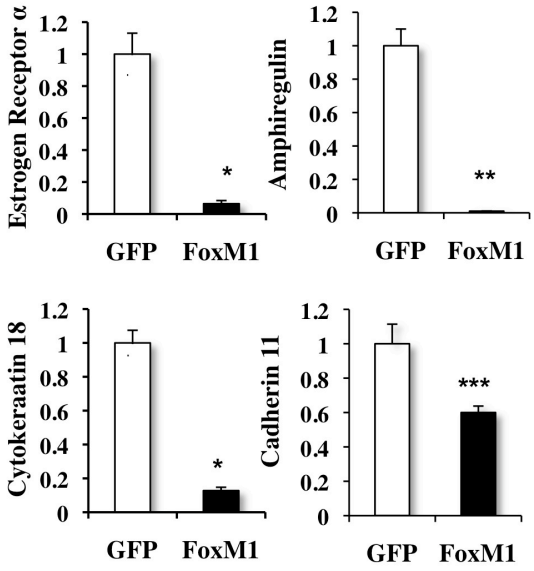

Figure 2.18. FoM1 overexpression in vivo results in a loss of differentiation markers. RT-PCR analysis of GFP and GFP-FoxM1 glands for expression of *estrogen receptor alpha, cytokeratin 18, amphiregulin, and cadherin 11* *$p<10^{-4}$ **$p<0.001$ ***$p<0.05$.

Figure 2.19

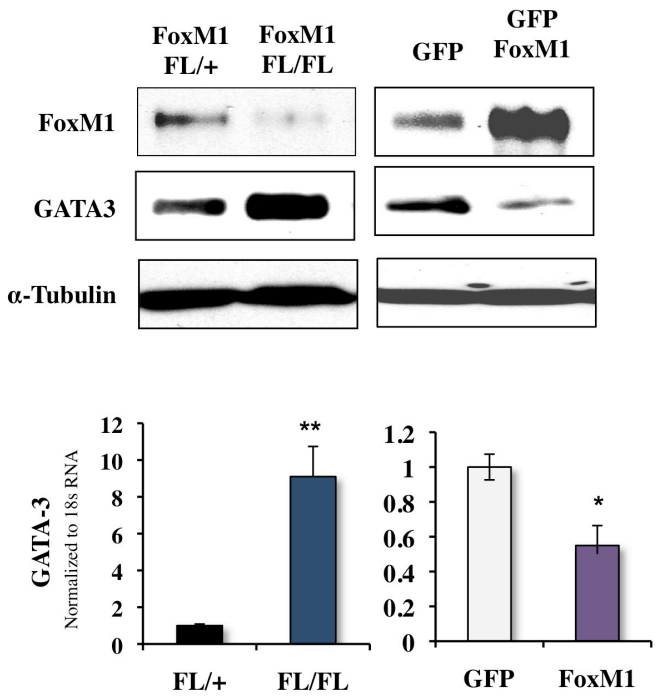

Figure 2.19. FoxM1 is a negative regulator of GATA-3 in vivo. Western blot analysis of FoxM1 and GATA-3 protein levels in WAP-rtTA-Cre, FoxM1 FL/+ (control) and WAP-rtTA-Cre, FoxM1 FL/FL as well as GFP (control) and GFP-FoxM1 expressing animals are shown in the top panel. Alpha tubulin is shown as a loading control. RT-PCR expression of glands is shown below, GATA-3 expression is normalized to 18S RNA. *$p<0.05$, **$p<10^{-6}$

Figure 2.20

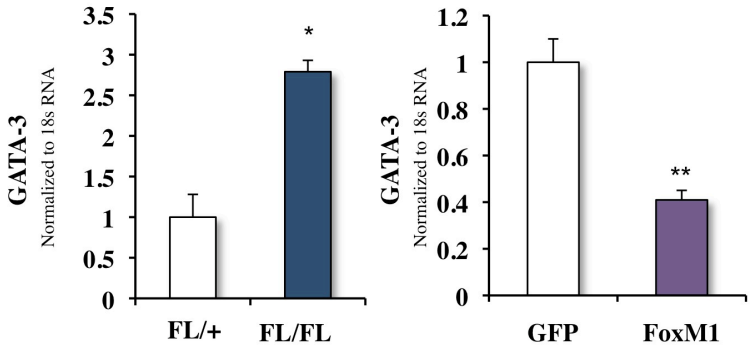

Figure 2.20. FoxM1 and GATA-3 expression are inversely correlated in luminal progenitors. Luminal progenitors (CD24+,CD61+) cells were sorted from control, FoxM1 knockdown and FoxM1 overexpressing glands. RNA was extracted from sorted cells and GATA-3 expression was determined by RT-PCR. Samples are normalized to 18S RNA. *p<0.001, **p<0.05

Figure 2.21

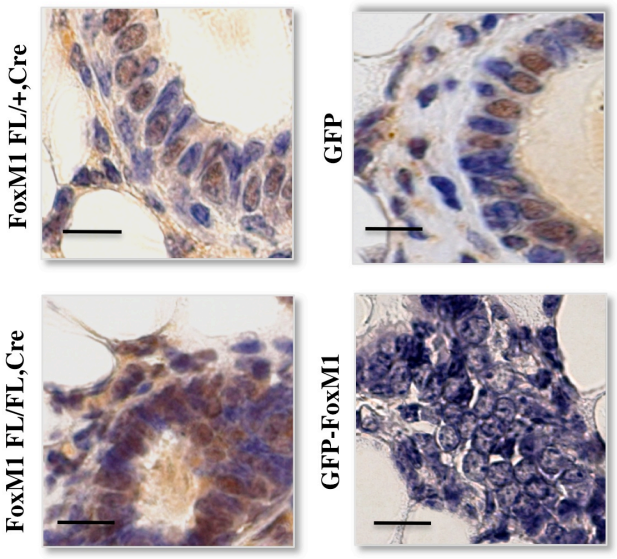

Figure 2.21. Expression of GATA-3 in FoxM1 *in vivo* models. Immunohistochemical staining of GATA-3 expression using DAB and hematoxylin counterstain

Figure 2.22

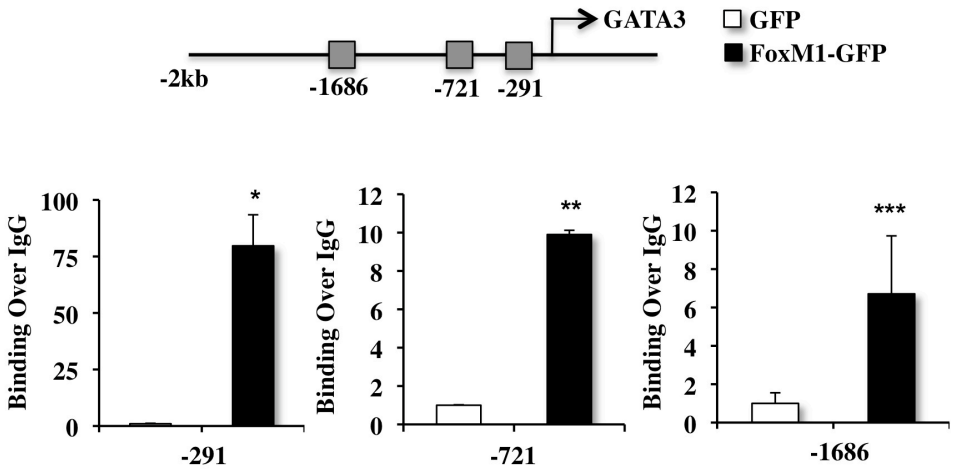

Figure 2.22. FoxM1 effects are mediated by direct regulation of GATA-3. Binding of FoxM1 to the promoter of GATA-3 was analyzed using an in vivo ChIP experiment. FoxM1 antibody was used to immunoprecipitate FoxM1 in glands of C57BL/6 mice. RT-PCR was used for three different regions of the GATA-3 promoter that have putative FoxM1 binding sites. Graph displays relative binding over an IgG control *$p<10^{-5}$ **$p<0.003$ ***$p<0.001$.

The mouse promoter of GATA-3 contains three FoxM1 consensus sequences within 2kb of the transcriptional start site. In vivo chromatin immunoprecipitation (ChIP) assay showed that endogenous FoxM1 was bound to all of these sites in the mammary gland (Figure 2.22). Taken together, the data indicates that FoxM1 is able to bind and repress transcription of *GATA-3* in vivo.

We then sought to determine whether the inhibition of mammary luminal differentiation by FoxM1 was linked to the repression of GATA-3. To investigate this, we coexpressed *GATA-3* along with *FoxM1* in mammary stem cells using retroviruses. The reconstituted glands were harvested and the cell populations were analyzed by sorting. Coexpression of *GATA-3* reversed the defects observed in *FoxM1* expressing mammary glands (Figure 2.23). Immunohistochemistry showed that glands expressing both *FoxM1* and *GATA-3* had visible lumens and no extensive cellular hyperplasia. In addition, expression of markers of differentiated cells was also corrected (Figure 2.24). While *GATA-3* expression reversed the effects of *FoxM1* on luminal differentiation, it alone had no detectable effect on increasing the luminal differentiation, suggesting that the level of *GATA-3* overexpression, in our experiments was insufficient to drive luminal differentiation. *GATA-3* expression had little effect on the stem cell population. We suspect that *FoxM1* increases stem cells independently of GATA-3 because, in other systems, FoxM1 has been shown to stimulate expression of the "stemness genes" (Wang 2011).

In order to confirm the role of GATA-3-regulation in FoxM1-mediated inhibition of luminal differentiation, we analyzed the effect of *GATA-3* depletion in *FoxM1*-depleted glands. Infection of mammospheres formed from *FoxM1* FL/FL and WT WAP-rtTA-Cre mice with either control or *GATA-3* targeting shRNA allowed for regeneration of glands that lacked both *FoxM1* and *GATA-3*. Analysis of these glands by flow cytometry demonstrated that knockdown of *GATA-3* was sufficient to reverse the loss of luminal progenitors and expansion of differentiated cells observed in mice after loss of *FoxM1* (Figure 2.25). Histologically, the *FoxM1* knockdown phenotype was reversed by knockdown of *GATA-3* (Figure 2.26). These observations suggest that repression of *GATA-3* is the dominant mechanism by which FoxM1 inhibits differentiation of mammary progenitors.

Figure 2.23

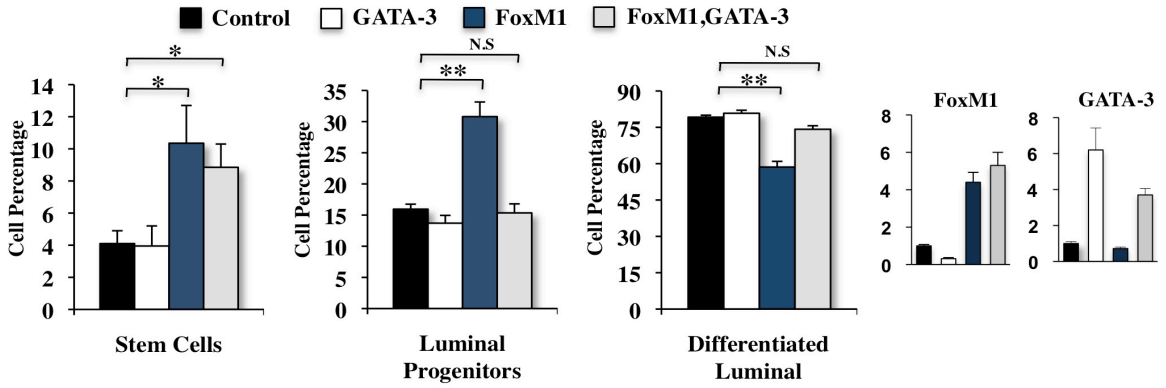

Figure 2.23. Overexpression of GATA-3 Rescues the FoxM1 Overexpression Phenotype. Graph summarizing flow cytometry data from control, GATA-3, FoxM1, and FoxM1-GATA-3 expressing mice. Each group contains four mice and percentage of each cell type is graphed. p-values are calculated as compared to control animals *p<0.05, **p<0.01. Semi-quantitative RT-PCR of GATA-3 and FoxM1 expression is shown in graphs to the right.

Figure 2.24

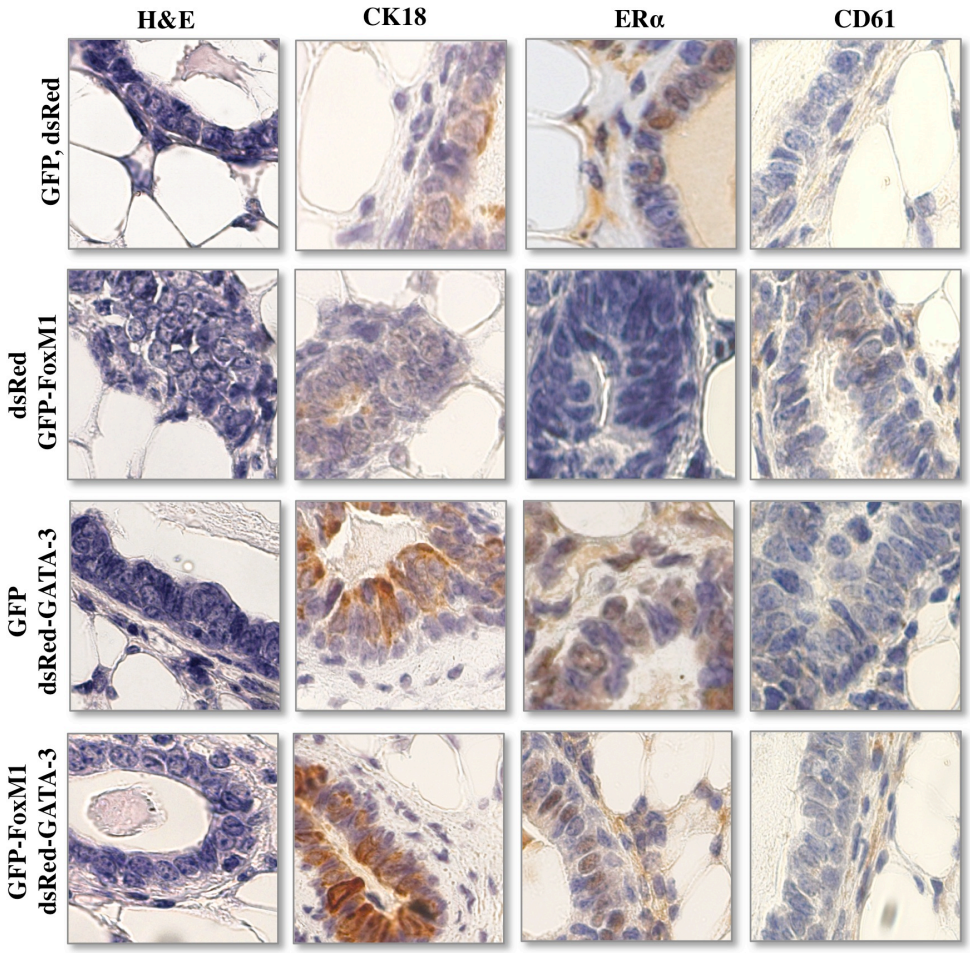

Figure 2.24. Immunostaining of glands coexpressing FoxM1 and GATA-3 in vivo. Glands regenerated with retroviruses expressing GFP, dsRed, GFP-FoxM1, and dsRed-GATA-3 were fixed, paraffin embedded, and sectioned. Sections were stained with H&E, cytokeratin 18 (CK18), estrogen receptor alpha (ERα), and CD61. Immunostaining was performed with DAB and hematoxylin counterstain.

Figure 2.25

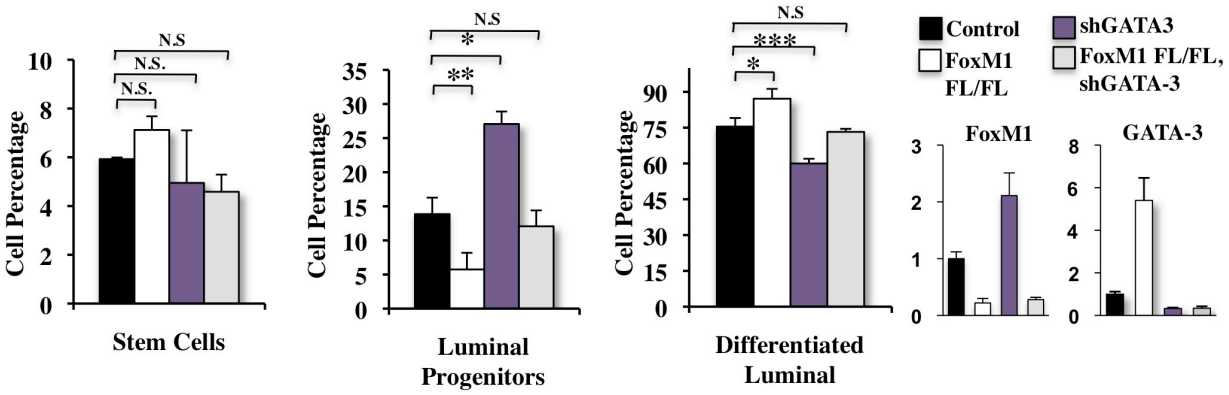

Figure 2.25. Silencing of GATA-3 rescues the phenotype of FoxM1 depleted glands. Flow cytometry analysis of glands regenerated with either WT or FoxM1 FL/FL, WAP-tTA-Cre and either shRNA control or GATA-3 targeting shRNA. All mice were fed doxycyline for 14 days following the surgery. Glands were analyzed after 8 weeks. Data collected from five mice is shown in the graph. N.S. (not significant), *p<0.05, **p<0.001, ***p<0.01. Semi-quantitative RT-PCR of FoxM1 and GATA-3 expression is shown in graphs to the right.

Figure 2.26

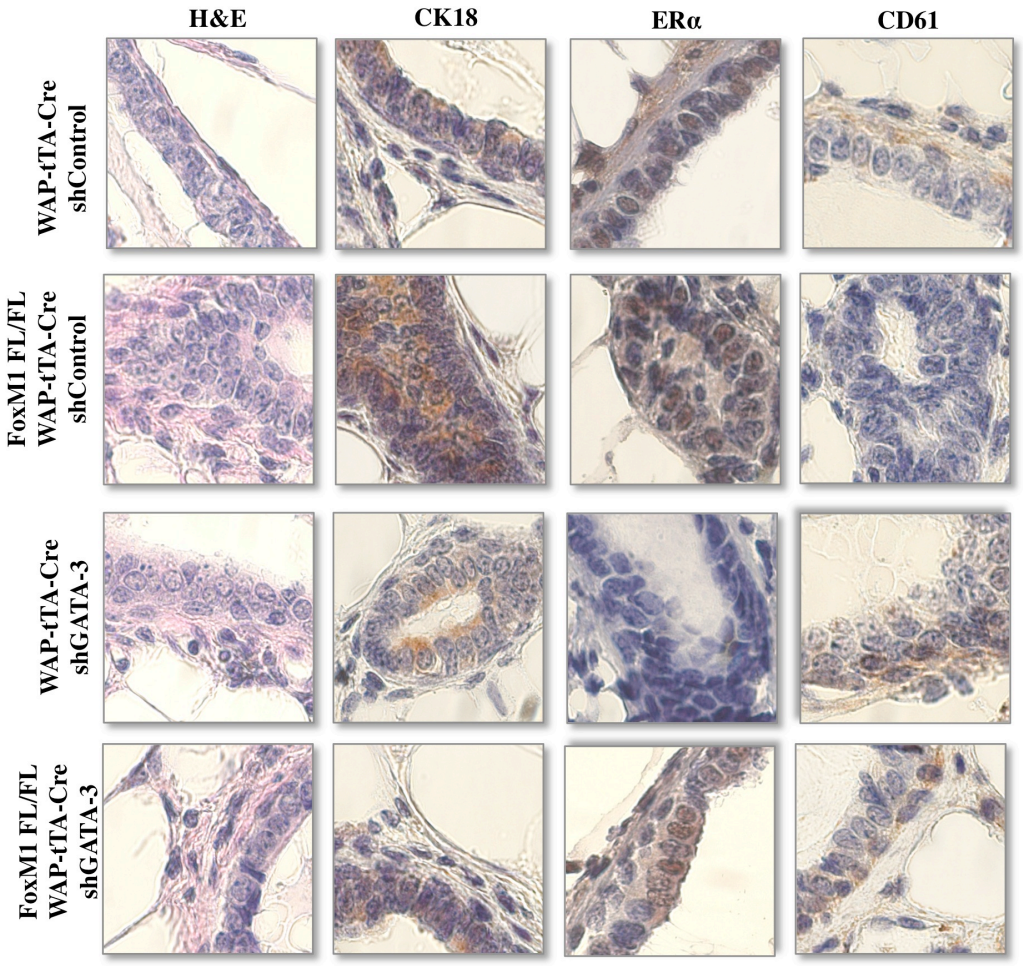

Figure 2.26. Analysis of glands lacking both FoxM1 and GATA-3. Glands regenerated with retroviruses expressing WT or *FoxM1* FL/FL WAP along with control or GATA-3 targeting shRNA were fixed, paraffin embedded, and sectioned. A total of four mice were analyzed for each genotype. All sections were stained with H&E, cytokeratin 18 (CK18), estrogen receptor alpha (ERα), and CD61. Immunostaining was performed with DAB and hematoxylin counterstain.

G. FoxM1 Promotes GATA-3 Methylation in an Rb-Dependent Manner

Given the observations in mouse studies that FoxM1 inhibits GATA-3, we expect to see an inverse correlation between GATA-3 and FoxM1 expression in human breast tumor samples. Consistent with that, analyses of publicly available database reveals an opposite expression pattern of FoxM1 and GATA-3 (Figure 2.27). FoxM1 binding sites are conserved across the mammalian genome (Figure 2.28). The mouse and human GATA-3 promoters contain three FoxM1 consensus sites within 2kb of the start site. We confirmed the direct binding of FoxM1 to the human GATA-3 promoter, indicating that FoxM1 can regulate *GATA-3* transcriptional levels in human breast cancer cells. Additionally, treatment of MDA-MB-453 cells with siRNA to *FoxM1* resulted in a reduction in binding, demonstrating the specificity of the assay (Figure 2.29). Previous studies showed that the promoter of *GATA-3* could be targeted for DNA methylation during tumor progression (Yan 2000). We hypothesized that the repression by FoxM1 may be methylation dependent therefore, we measured the ability of FoxM1 to inhibit *GATA-3* in the presence of the methyltransferase inhibitor, 5'azacytidine (5'AZA). Addition of 5'AZA ablated the repression of *GATA-3* after FoxM1 over-expression, demonstrating that repression is methylation dependent (Figure 2.29). DNMT3b has been specifically implicated in mammary tumor biology. It was shown to be responsible for the hypermethylated phenotype and subsequent decrease in expression of tumor suppressor genes in breast cancer (Roll 2008). We explored the possibility that FoxM1 could function in a complex with DNMT3b and target the *GATA-3* promoter for methylation. We observed that FoxM1 co-immunoprecipitated with DNMT3b (Figure 2.29). Moreover, in the presence of control siRNA, binding of DNMT3b was detected by ChIP in the regions of the *GATA-3* promoter that contained FoxM1 binding sites. The binding was significantly decreased when cells were treated with siRNA to FoxM1, indicating that DNMT3b binds to the *GATA-3* promoter in a FoxM1 dependent manner (Figure 2.29).

Previous studies have shown that the tumor suppressor Rb could bind FoxM1 (Major 2004, Wierstra and Alves 2006). We confirmed this binding in breast cancer cells. In addition, we demonstrate that DNMT3b and Rb are present in a complex (Figure 2.30). Therefore, we investigated whether FoxM1 requires Rb for inhibition of *GATA-3* transcription. We utilized a doxycycline inducible shRNA system to

Figure 2.27

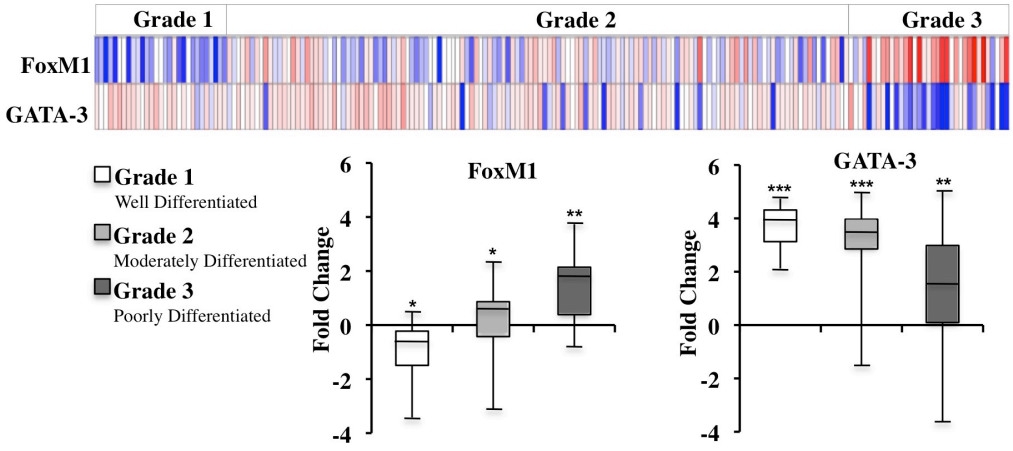

Figure 2.27. FoxM1 and GATA-3 are inversely correlated in breast cancer samples. FoxM1 and GATA-3 expression in human breast cancers. Fold change from normal is graphed. Heat map of individual samples is shown above the graphs *$p<10^{-3}$ **$p<10^{-5}$ ***$p<10^{-11}$

Figure 2.28

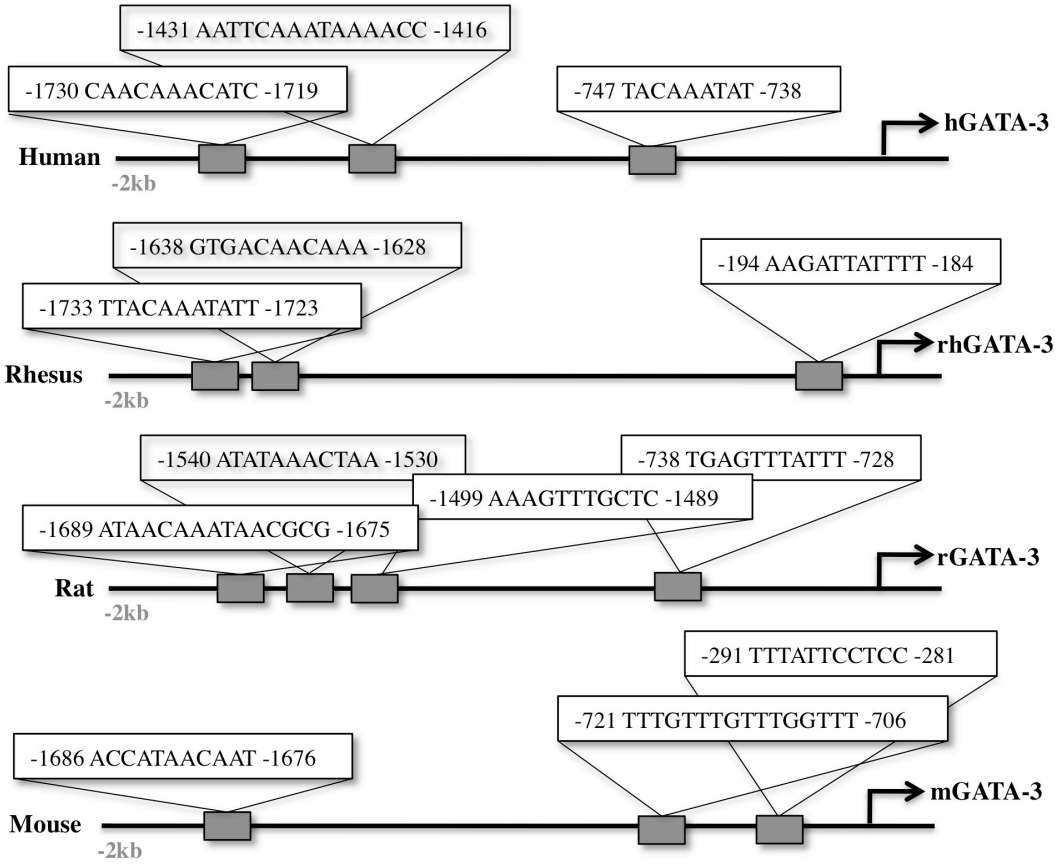

Figure 2.28 Consensus FoxM1 Binding Sites Across Species. FoxM1 consensus binding sites were determined using Macvector software in humans, rhesus monkey, rat, and mouse genomes. 2kb upstream of the transcriptional start was analyzed. The location of these sites in the genome are shown above.

Figure 2.29

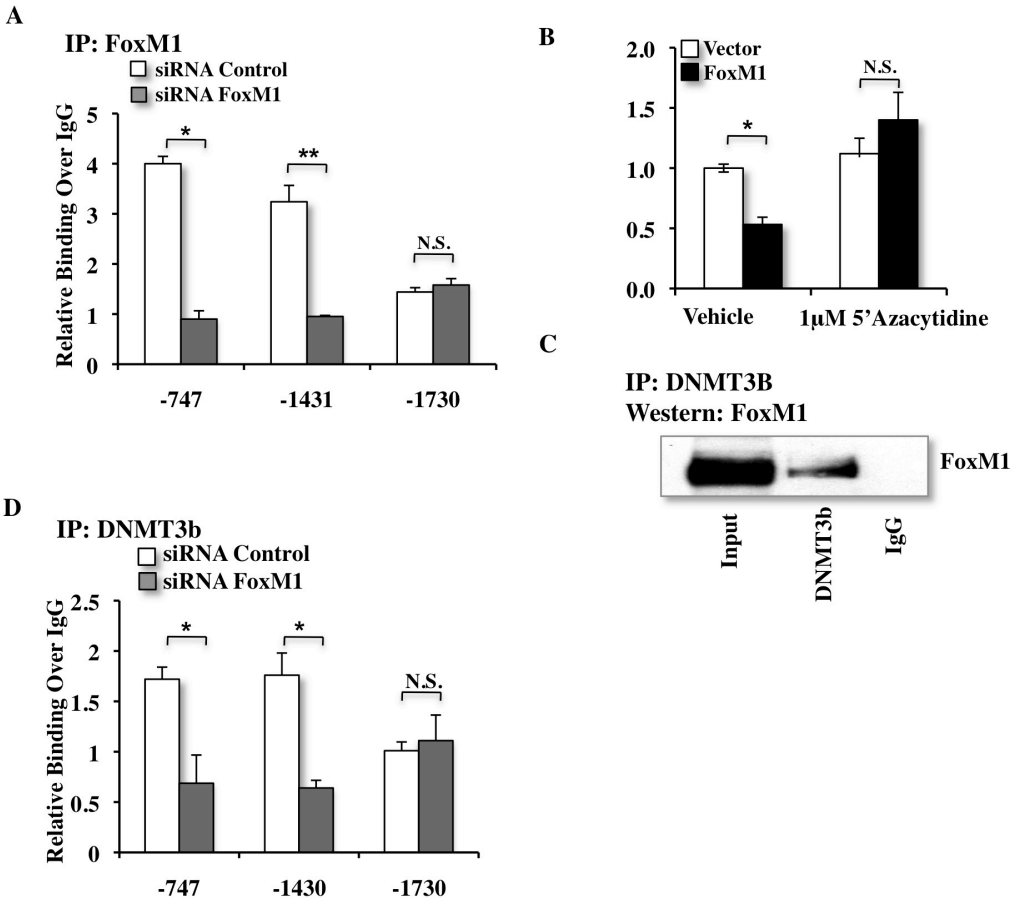

Figure 2.29. FoxM1 transcriptional repression of GATA-3 is methylation dependent. **(A)** MDA-MB-453 ells were treated with either control or FoxM1 targeting siRNA. Chromatin immunopreciptation assay of FoxM1 binding to the GATA-3 promoter was performed. Quantitative PCR results are shown *p<0.01. (B) FoxM1 was transfected into MDA-MB-453 cells and 4 hours later, either vehicle (PBS) or 1uM of 5'azacytidine was added to each plate. Samples were collected 48 hours later and RT-PCR of GATA-3 expression is shown as normalized to GAPDH *p<0.01. (C) Cells were collected and immunopreciption was performed using DNMT3b antibody, western blot of FoxM1 is shown. (D) 72 hours after transfection with control siRNA or FoxM1 targeting siRNA cells were fixed and chromatin immunoprecipitated (ChIP) with DNMT3b antibody or IgG was performed. Relative binding of DNMT3b to the GATA-3 promoter sites are graphed. Samples have been normalized to IgG and relative binding is shown *p<0.01, **p<0.05.

Figure 2.30

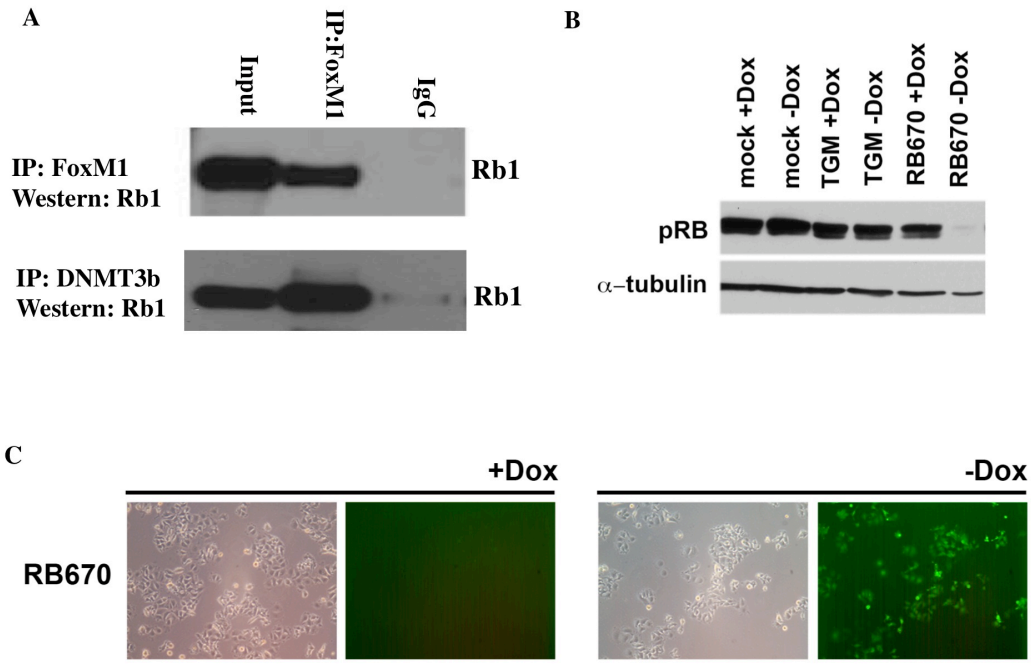

Figure 2.30. The Inducible Knockdown System and FoxM1/Rb/DNMT3b Complex. (A) Top panel: western blot demonstrating binding of endogenous FoxM1 to Rb1 in MDA-MB-453 cells. Bottom panel: western blot of endogenous binding of Rb to DNMT3b. Lysates were incubated with FoxM1 or IgG, complexes were collected by protein A/G beads and western blot was done for Rb1 protein. Input is 5% of total. (B) The level of pRB knockdown with RB670 was analyzed by immunoblot analysis of protein lysates from cells grown in media with (+Dox) and without the addition of doxycycline (-Dox). We observed at least 95% pRB knock down in –Dox condition. (C) The inducibility of GFP expression, indicative of the tight control of Rb shRNA production. Phase contrast and fluorescent microscopy of cells grown in the presence or absence of doxycycline is shown.

silence Rb (Figure 2.30). In the absence of Rb, expression of FoxM1 failed to repress GATA-3 and in fact led to a considerable increase (Figure 2.31). It is likely that FoxM1 binds the GATA-3 promoter and in the absence of Rb, the repressor complex cannot form and FoxM1 functions as an activator. ChIP experiments using control siRNA or siRNA specific to *FoxM1* showed that Rb could not bind to the *GATA-3* promoter in the absence of FoxM1 (Figure 2.31).

In order to functionally test this model, we analyzed the methylation status of the *GATA-3* promoter using methylation-specific PCR. Expression of *FoxM1* led to a considerable increase in methylation of *GATA-3* compared to control. Interestingly, the increase was ablated in the absence of Rb (Figures 2.32, 2.33, 2.34), demonstrating that the methylation and subsequent repression of *GATA-3* was Rb-dependent. We investigated whether knockdown of *Rb* in vivo could ablate the FoxM1 mediated inhibition of differentiation. Therefore, we regenerated mouse mammary glands expressing scrambled shRNA or shRNA targeting *Rb* in the presence and absence of *FoxM1*. Sorting experiments demonstrated that expression of *FoxM1* led to an inhibition of differentiation that was alleviated by the knockdown of *Rb* (Figure 2.35). Taken together, the data support a model in which FoxM1 functions in a complex with DNMT3b and Rb to inhibit *GATA-3* expression and in effect, mammary luminal differentiation.

H. FoxM1 Expression Leads to an Undifferentiated Tumor Phenotype

Our data indicates that FoxM1 inhibits GATA-3 and this repression leads to the expansion of an undifferentiated cell type. We hypothesize that this regulation also exists in tumors and that increased levels of FoxM1 in tumors will lead to a tumor of higher grade. In order to test this, we used the MMTV-PyMT tumor model. Mice expressing this transgnene develop mammary tumors at a young age that go on to metastasize in less than six months due to mammary specific expression of the polyoma middle T antigen (Kouros-Mehr 2008). We generated cell lines from mice expressing this oncogene and then infected cells with either a control vector or FoxM1 expressing vector. These cells were then implanted into the cleared fat pad of recipient mice. Eight weeks later, tumors were sectioned and analyzed. FoxM1 expression led to the formation of an aggressive, grade 3 tumor while the control vector led to grade 2

Figure 2.31

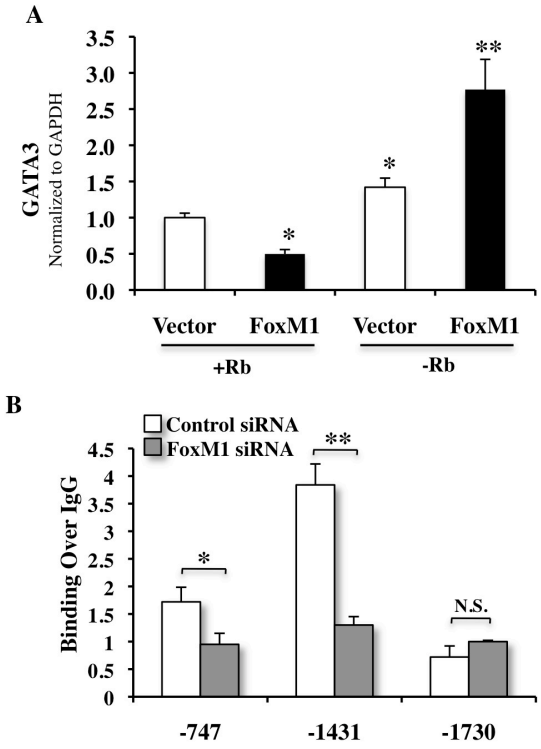

Figure 2.31. GATA-3 repression by FoxM1 is Rb-dependent. (A) Tet-off shRNA cell lines were either treated with doxycycline or vehicle for 14 days. Control or FoxM1 constructs were transfected into lines expressing Rb or where Rb was silenced by shRNA. RT-PCR of GATA-3 expression is shown normalized to GAPDH *p<0.05 **p<0.001. (B) Cells were transfected with control or FoxM1 targeting siRNA. After 72 hours, cells were collected and fixed for ChIP assay. IgG or Rb antibody was used for immunoprecipitation. RT-PCR of Rb binding to the GATA-3 promoter is shown *p<0.05 **p<10^{-4}.

Figure 2.32

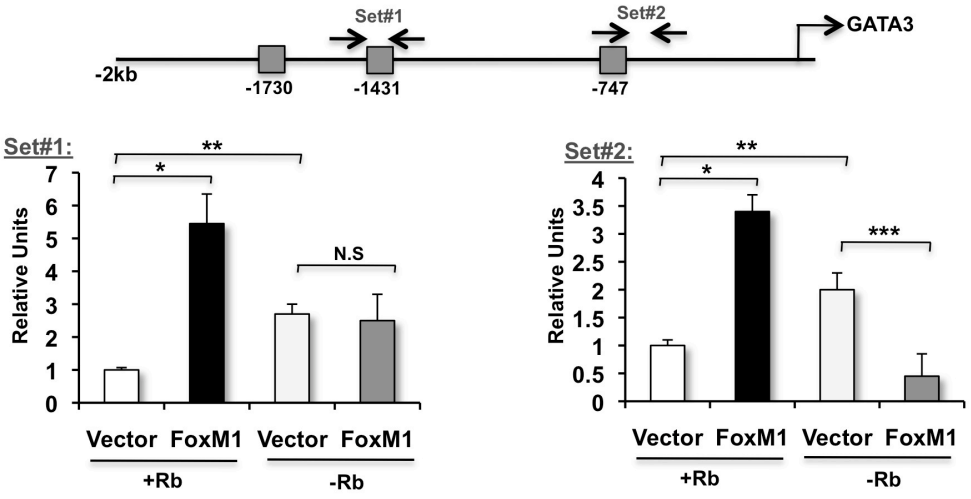

Figure 2.32. Methylation of GATA-3 promoter requires Rb. Tet-off shRNA cell lines were used for methylation specific PCR analysis of the GATA-3 promoter in the presence and absence of FoxM1 expression.

Figure 2.33

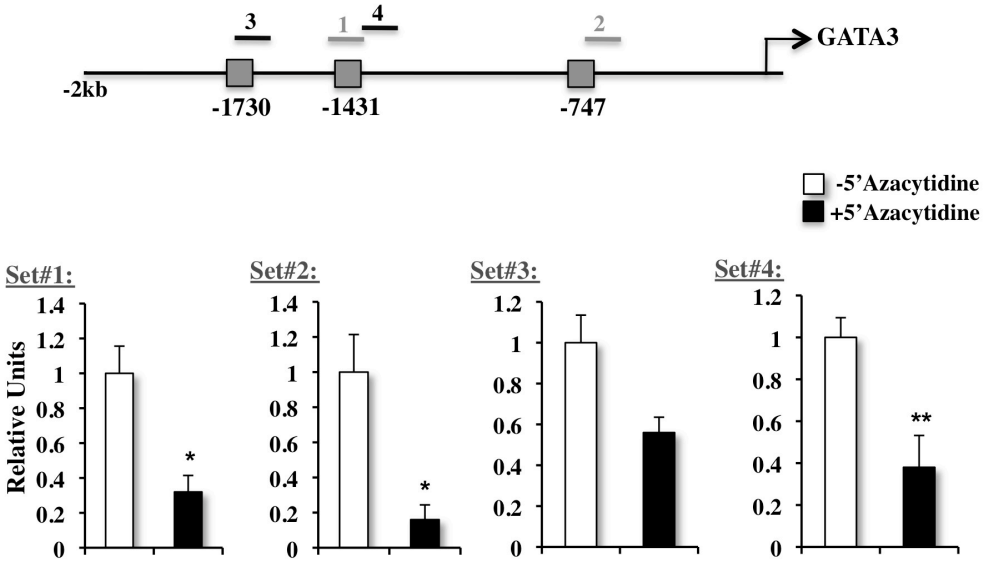

Figure 2.33. Validation of in vitro methylation assay. MCF-7 cells were treated with either vehicle or 1uM 5'azacytidine for 48 hours. Cells were collected and genomic DNA was purified and treated with bisulfite. Methylation specific PCR was performed. Data is normalized to β-Actin. *$p<0.01$, **$p<0.05$.

Figure 2.34

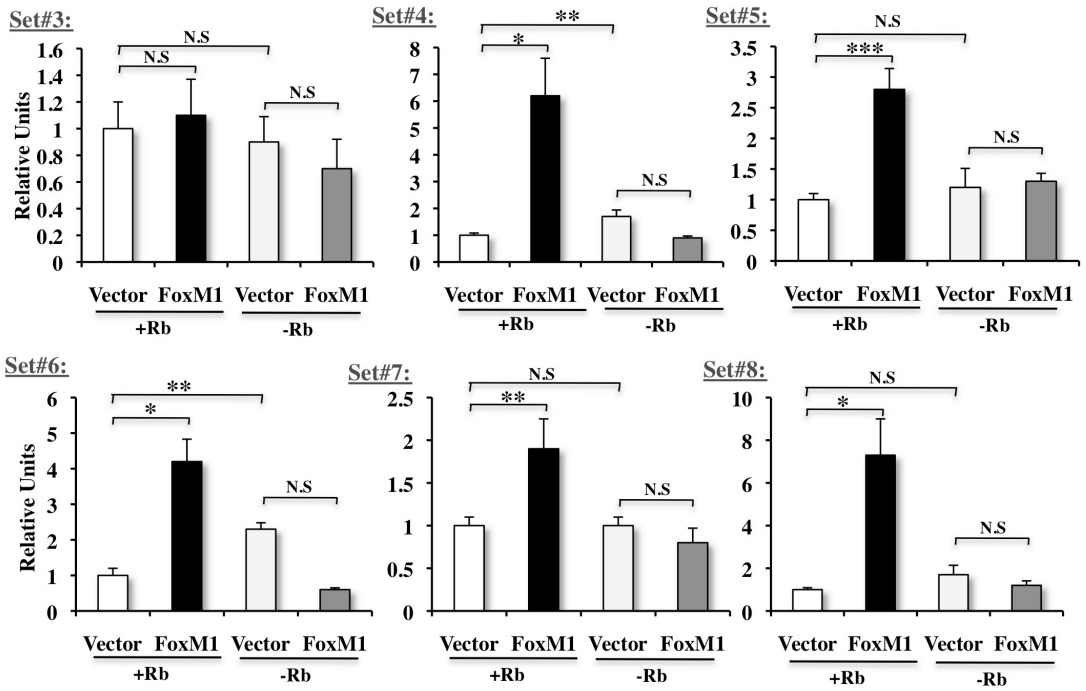

Figure 2.34. Additional methylation analysis. MCF-7 cells were treated with either doxycycline or vehicle for 14 days. Treatment with doxycycline led to reexpression of Rb due to silencing of shRNA targeting Rb. Cells were transfected with either vector or FoxM1 and collected 48 hours later. Genomic DNA was purified and bisulfite treated. RT-PCR results normalized to β-Actin are shown. N.S (not significant), *$p<10^{-4}$, **$p<.05$, ***$p<0.001$.

Figure 2.35

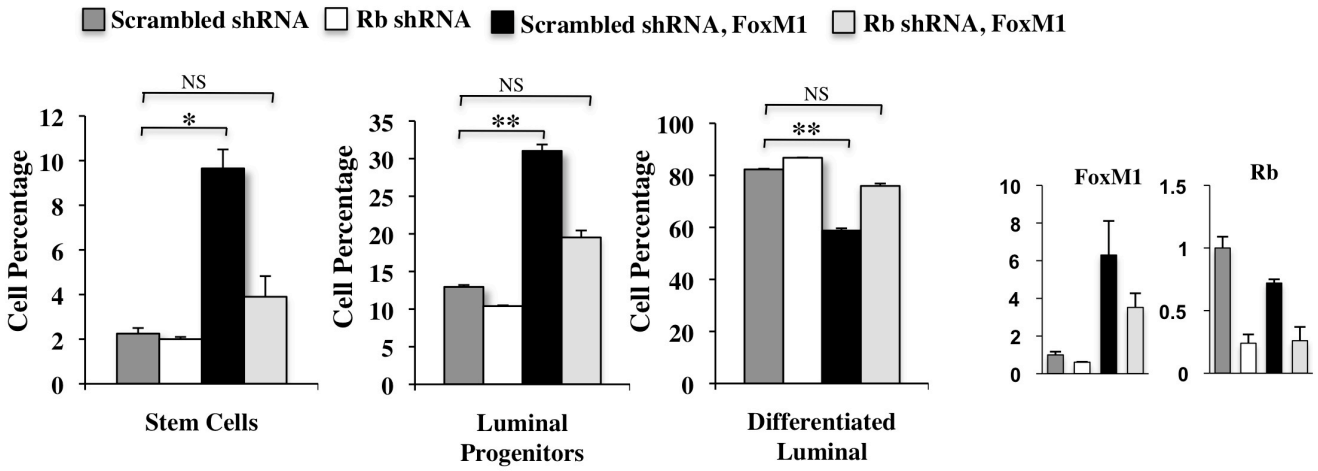

Figure 2.35. Knockdown of Rb can rescue the FoxM1 overexpression phnotype in vivo. Flow cytometry of stem cells, luminal progenitors, and differentiated cells from mice expressing scrambled shRNA, Rb-targeting shRNA, FoxM1, or both FoxM1 and Rb-targeting shRNA. Panel to the right shows semiquantitative RT-PCR of FoxM1, GATA-3 and Rb expression. Cyclophilin is shown as a loading control *$p<10^{-4}$ **$p<0.01$.

Figure 2.36

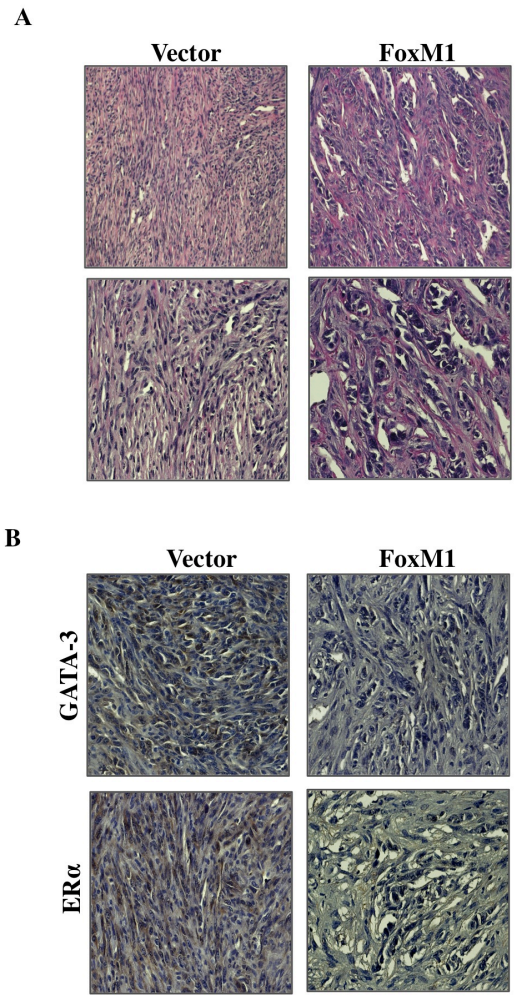

Figure 2.36 FoxM1 Induces Undifferentiated Tumors **(A)** MMTV-PyMT tumor cells were infected with wither empty vector or FoxM1 expressing vector. Infected cells were implanted into the cleared mammary fat pad of recipient mice. After 8 weeks, tumors were removed and stained using hematoxylin and eosin. Higher magnification images are shown in the bottom panel. **(B)** GATA-3 and ERα immunostaining of tumor samples are shown. Vector expression is shown in the left panel and FoxM1 expressing in the right. Samples are stained using DAB and a hematoxylin counterstain.

tumors. FoxM1 expressing tumors displayed no tubule formation, a high degree of nuclear pleomorphism and a high mitotic index (Figure 2.36) In line with the observation that FoxM1 tumors are less differentiated, these tumors had considerably lower levels of estrogen receptor alpha and GATA-3 expression (Figure 2.36).

3. FoxM1 Mediates Resistance to Herceptin and Paclitaxel

A. Overview

Inherent and acquired therapeutic resistance in breast cancer remains a major clinical challenge. In human breast cancer samples, overexpression of the oncogenic transcription factor FoxM1 has been suggested to be a marker of poor prognosis. One factor closely associated with poor prognosis is a failure to respond to therapy. We sought to determine if the elevated levels of FoxM1 in tumors could protect cells from drug therapies. In this study, we report that FoxM1 overexpression confers resistance to the HER2 monoclonal antibody Herceptin and microtubule-stabilizing drug paclitaxel, both as single agents and in combination. FoxM1 altered microtubule dynamics in order to protect tumor cells from paclitaxel-induced apoptosis. Mechanistic investigations revealed that the tubulin destabilizing protein Stathmin, whose expression also confers resistance to paclitaxel, is a direct transcriptional target of FoxM1. Significantly, attenuating FoxM1 expression by siRNA or an ARF-derived peptide inhibitor increased therapeutic sensitivity. Our findings indicate that targeting FoxM1 could relieve therapeutic resistance in breast cancer.

B. FoxM1 Overexpression Confers Herceptin Resistance

To investigate the hypothesis that increased FoxM1 is sufficient to induce resistance to Herceptin, we stably introduced FoxM1 expression cDNA in SKBR3, BT474, and MDA-MB-453. All cell lines have HER2 amplification and BT474 is estrogen receptor positive. Drug sensitivity was tested by colony formation assay. Cells were plated at low density and treated continuously with 10ug/ml of Herceptin for 14 days. As shown by quantification of the colony formation assay, FoxM1 overexpression resulted in a three to seven-fold increase in colony number as compared to pBabe expressing cells (Figure 3.1), providing evidence that FoxM1 confers resistance to Herceptin.

The magnitude of the G1/S arrest induced by Herceptin was measured by propidium iodide staining followed by flow cytometry (FACS) analysis. Cells were treated in 10ug/ml of Herceptin for 72 hours and cell cycle profiles were examined. The control pBabe lines showed a statistically significant

Figure 3.1

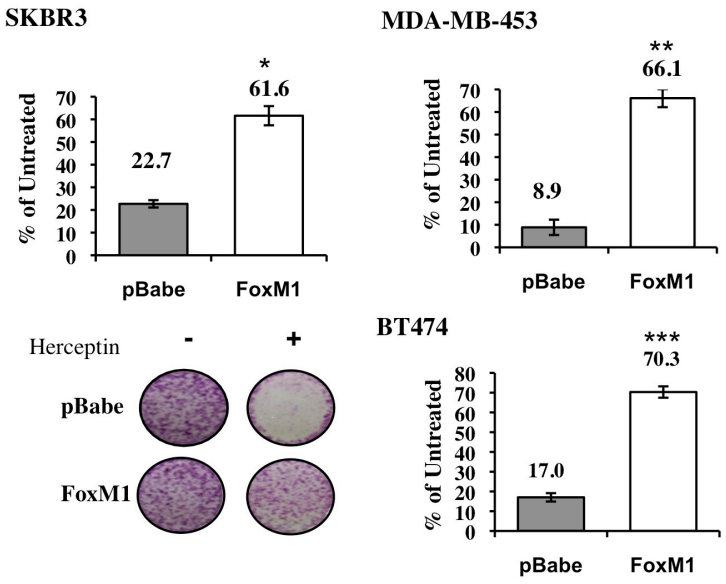

Figure 3.1. Multiple FoxM1 expressing lines are resistant to Herceptin. The response of SKBR3, MDA-MB-453, and BT474 stable cell lines to Herceptin was tested by colony forming assay. Cell lines were treated continuously with either 0 or 10ug/ml Herceptin for 14 days, media was changed every 3 days. Cells were plated in triplicate and the experiment was repeated three times. Representative wells for SKBR3 cells are shown. Graphs provide average quantification as a percentage of the untreated wells *$p<10^{-6}$, **$p<10^{-7}$, ***$p<10^{-8}$.

increase in the number of cells in G1, but the FoxM1 expressing cells did not exhibit any significant enrichment of the G1 population (Figure 3.2A). Herceptin alone does not induce apoptosis (Nahta et al., 2004). Consistent with that, none of the cell lines showed an increase in the sub-G1 population. To further investigate resistance in FoxM1-expressing cells, we measured the ability to incorporate BrdU (Figure 3.2B). Upon treatment, SKBR3-pBabe showed a substantial (35%) reduction in the number of BrdU-positive cells. FoxM1 expressing cells did not show any significant decrease in BrdU-incorporation. Taken together, these results indicate that FoxM1 overcomes the G1/S arrest and proliferation defect caused by Herceptin, allowing cells to continue to grow in the presence of the drug.

C. FoxM1 Prevents Herceptin Induced Accumulation of p27

While multiple mechanisms of resistance exist, previous reports indicated that low levels of p27 could contribute to Herceptin insensitivity (Nahta et al., 2004). FoxM1 functions as a negative regulator of p27 by increasing proteolysis. We hypothesized that the resistance observed in FoxM1 overexpressing cells could be due to a failure to accumulate p27. To test that possibility, SKBR3-pBabe or FoxM1 expressing lines were treated with 10ug/ml of Herceptin for 0, 24, 48, or 72 hours or with increasing doses. Western blot of FoxM1 and p27 levels showed that in control SKBR3 cells, the levels of FoxM1 decreased with treatment and the p27 levels accumulate as expected. Interestingly, in SKBR3-FoxM1 cell lines, the basal expression of p27 is lower and levels remained low even after a high-dose of Herceptin (Figure 3.3A and B). These results show that the likely mechanism by which FoxM1 confers resistance is by preventing the accumulation of p27 that is required for Herceptin induced G1/S arrest. Treatment with IgG did not cause changes in FoxM1 or p27, therefore these effects are specific to inhibition of the HER2 pathway and not a general antibody induced response (Figure 3.3B).

D. Targeting FoxM1 in Tumor Cells with Inherent Herceptin Resistance Increases Sensitivity

In order to generate cell lines that have inherent resistance to Herceptin, we cultured parental SKBR3, MDA-MB-453, and BT474 lines continuously in 5ug/ml of Herceptin. At the end of six months,

Figure 3.2

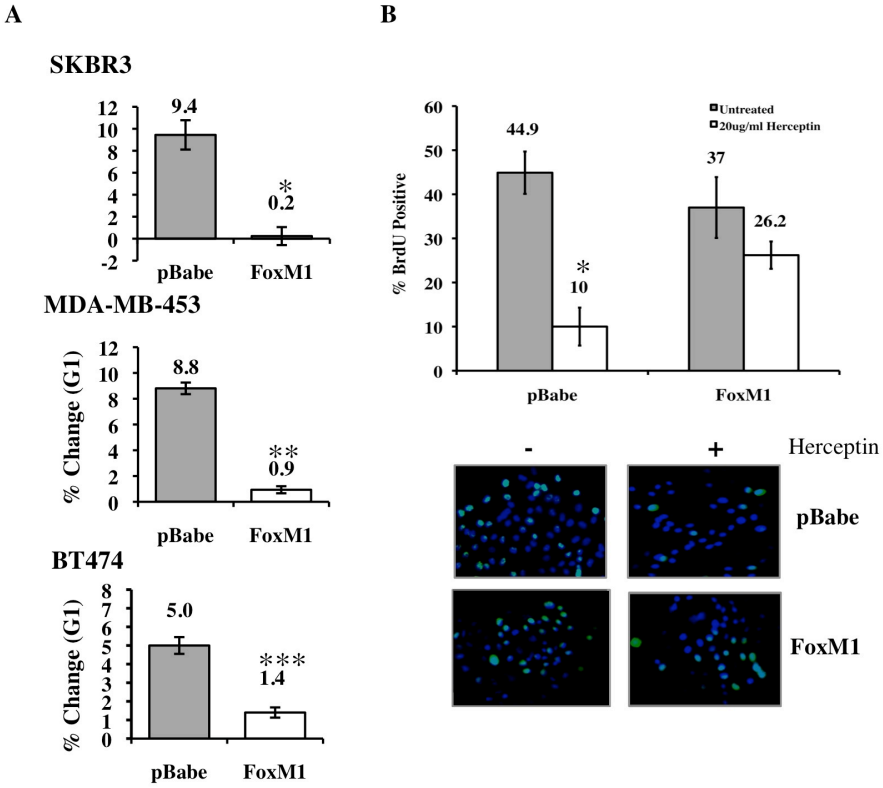

Figure 3.2. FoxM1 expressing lines do not undergo cell cycle arrest in response to Herceptin. (A) Stable cell lines expressing either pBabe or FoxM1 were treated with 10ug/ml of Herceptin for 48 hours, stained with propidium iodide, and subjected to FACS analysis. Percentage change in G1 phase is shown. Inset shows relative protein expression in FoxM1 versus pBabe stable cell lines *p<0.03, **p<0.001,***p<0.01. (B) SKBR3-pBabe and FoxM1 lines were either untreated or treated for 72 hours with Herceptin followed by a pulse of BrdU for 2 hours. Percentage of BrdU positive compared to DAPI positive cells are shown for each group, 500 cells in each experiment were counted *p<0.001. Average values are shown above error bars and representative pictures are shown below the graph.

Figure 3.3

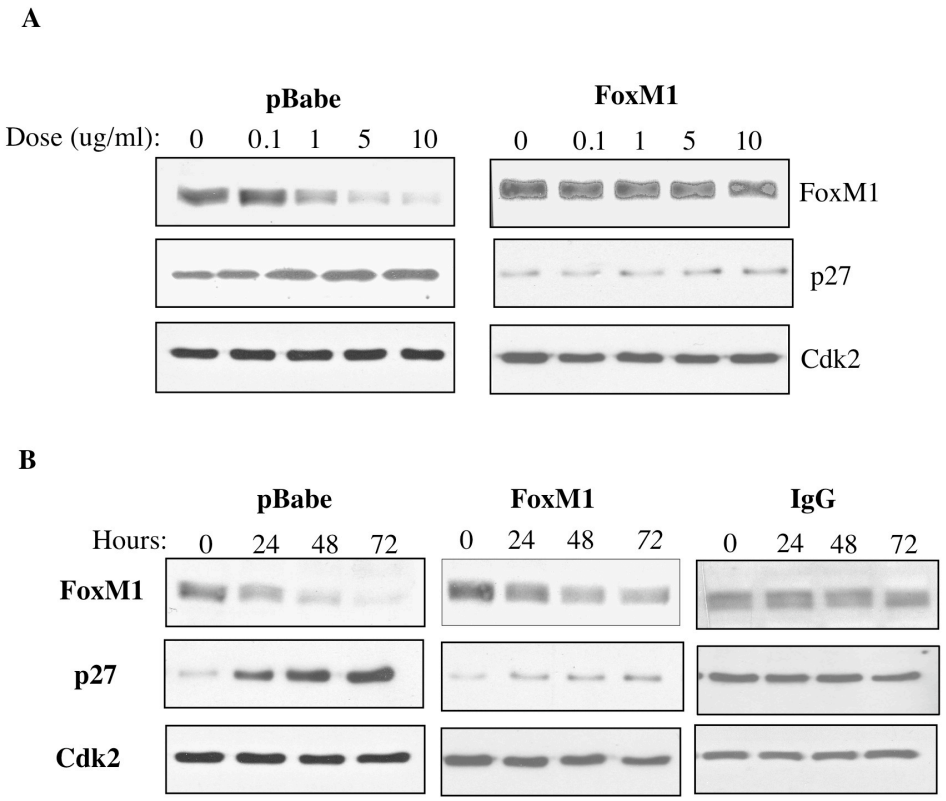

Figure III.3. SKBR3-FoxM1 cell lines fail to accumulate p27 after treatment with Herceptin. (A) SKBR3-pBabe and FoxM1 expressing cell lines were treated with increasing doses of Herceptin for 48 hours. Representative western blots of FoxM1 and p27 levels are shown. Cdk2 was used as a loading control. (B) SKBR3 stable cell lines were treated with 10ug/ml of Herceptin for 24, 48, and 72 hours. FoxM1 and p27 levels are shown by western blot. (Far Right Panel) SKBR3-pBabe cell lines were treated with 10ug/ml of IgG for indicated periods of time. FoxM1 and p27 were assayed by western blot and Cdk2 was used as a loading control.

the lines grew at the same rate in the presence or absence of Herceptin. The source of resistance in these ines is not uniform as we observed an increase in phosphorylated Akt in only SKBR3 (data not shown). FoxM1 levels in parental and resistant lines were assayed by western blot. Interestingly, levels of FoxM1 were higher in all resistant lines (Figure 3.4). This increase was reflected at the RNA level. To confirm a higher activity of FoxM1, we assayed the RNA levels of the known FoxM1 target genes. As shown in the SKBR3 resistant line, FoxM1 RNA levels were significantly increased (15-fold) as well as the levels of the p27 ubiquitin ligase components Skp2 (2.5-fold) and Cks1 (5.6-fold). Additionally, levels of the cell cycle regulators, Polo Like Kinase 1 (1.5-fold) and Cyclin B1 (16.6-fold) were amplified in the resistant line as compared to the parental control line (Figure 3.5).

FoxM1 levels are elevated in resistant lines and we observed that overexpression of FoxM1 could confer acquired resistance to Herceptin, we wanted to determine whether targeting FoxM1 could resensitize lines with inherent resistance. Knockdown of FoxM1 by siRNA in SKBR3 resistant cells led to a more than 75% percent reduction in cell number when used in conjunction with Herceptin. This effect was also observed in MDA-MB-453 cells (Figure 3.6). Collectively, these results indicate that FoxM1 is upregulated in resistant lines and that targeting FoxM1 provides a method of sensitizing resistant cells to Herceptin treatment.

E. FoxM1 Induces Expression of Stathmin to Confer Resistance to Paclitaxel

It has been previously reported that cells that overexpress HER2 display decreased sensitivity to apoptosis caused by Paclitaxel (Yu et al., 1998; Azambuja et al., 2008). While microtubule-stabilizing agents such as Taxol induce mitotic arrest and consequent apoptosis, some patients fail to respond to this drug. We were curious to determine whether FoxM1, which is downstream of HER2, could protect from Taxol induced apoptosis.

We noted that after seven days of treatment in a low dose of Taxol (0.1μM), only 25% of SKBR3-pBabe cells survived, while nearly 50% of SKBR3-FoxM1 cells were still viable (Figure 3.7A, upper panel). Moreover, knockdown of FoxM1 by siRNA in SKBR3 cells was able to sensitize to Taxol

Figure 3.4

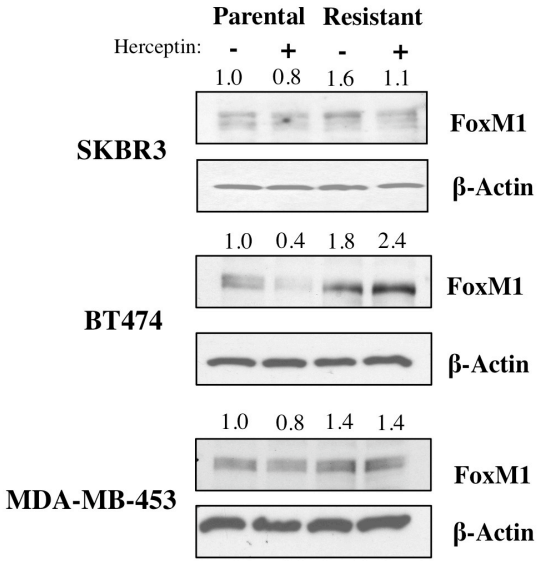

Figure 3.4. Herceptin resistant lines express higher levels of FoxM1 protein. Western blot showing FoxM1 protein levels in SKBR3, BT474, and MDA-MB-453 parental and resistant lines. Lines were continuously cultured in 5ug/ml of Herceptin for six months. Cells were placed in drug free media for 7 days prior to treatment and lysates were collected 72 hours after treatment with 10ug/ml of Herceptin. Quantification of FoxM1 bands by Image J is shown, using untreated parental lines for normalization.

Figure 3.5

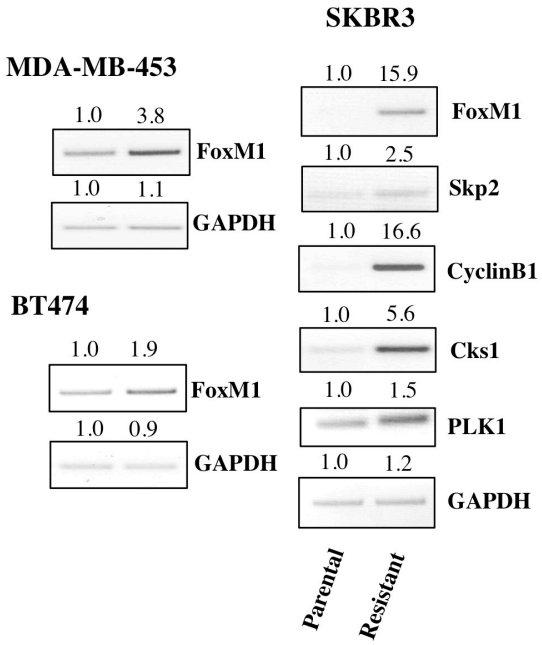

Figure 3.5. Herceptin resistant lines have higher FoxM1 activity. Semi-quantitative RT-PCR using cDNA from either parental or resistant SKBR3 cells was used to analyze target gene expression. Representative gel pictures are shown and quantification values normalized to GAPDH are shown above.

Figure 3.6

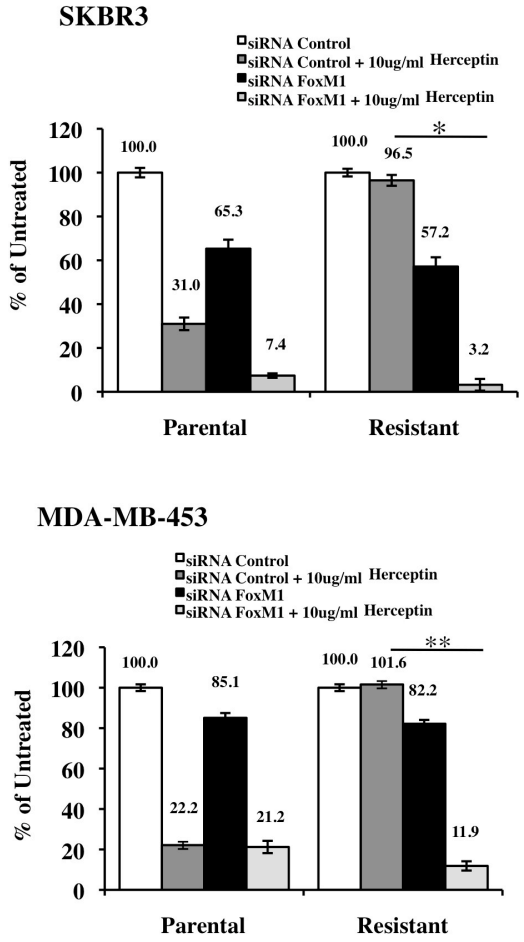

Figure 3.6. Resistant lines can be sensitized to Herceptin treatment by targeting FoxM1. Parental and resistant SKBR3 and MDA-MB-453 cells were transfected with control or FoxM1 specific siRNA. 48 hours later, 3 x 10^3 cells were plated in each well or a 24-well plate and left untreated or treated with 10ug/ml Herceptin. Media was changed every 3-4 days. After 14 days, colonies were stained with crystal violet and quantified by photoshop *$p<10^{-6}$, **$p<10^{-5}$.

as evidenced by a comparison of IC50 values between siRNA control and siRNA FoxM1 treated cells, 0.06uM vs. 0.01uM (Figure 3.7A, lower panel). This data indicates that FoxM1 can protect cells from Taxol induced cell death.

Several mechanisms to combat Taxol induced apoptosis have been reported. Namely, up-regulation of MDR1 (multi-drug resistant protein 1) a P-Glycoprotein family member that can shuttle toxins out of cells, up-regulation of the CIAP (inhibitors of apoptosis) family members including Survivin, and altered microtuble dynamics (Orr et al., 2003). We sought to investigate the mechanism by which FoxM1 could prevent Taxol induced apoptosis. We did not detect any effect of FoxM1 on the levels of MDR1 (data not shown). FoxM1 is known to positively regulate the CIAP family member Survivin and increased expression is known to protect cells from Taxol. However, in the mammary tumor cells, we did not observe increased expression of Survivin (data not shown). We went on to examine the possibility of altered microtubule dynamics induced by FoxM1. As Taxol is known to stabilize tubulin, we compared the ratio of polymerized to soluble microtubule fractions. We fractionated cell lysates to obtain polymerized and soluble tubulin fractions in SKBR3-pBabe and SKBR3-FoxM1 expressing lines that were left untreated or treated with Taxol. Without treatment, cells show similar tubulin ratios and nearly all detectable tublins were in the soluble form. Upon treatment with Taxol, SKBR3-pBabe cells show a dramatic shift towards the polymerized fraction. The FoxM1 expressing cells did show a shift towards the polymerized fraction but the ratio was considerably lower (0.56:1 FoxM1 vs. 3.76:1 pBabe (Figure 3.7B).

It has been previously established that increased expression and activity of the microtubule destabilizing protein Stathmin can confer resistance to Taxol induced apoptosis both in patient and cell culture samples (Alli et al., 2002; Balachandran et al., 2003). The hallmark of increased activity is a low ratio of polymerized to soluble tubulin as we observed in FoxM1 expressing cells (Giannakakou et al., 1997). Therefore, we compared Stathmin RNA expression in pBabe and FoxM1 expressing cell lines, and observed that FoxM1 cells express 2-fold more Stathmin compared to the pBabe control cells. This difference was also noted at the protein level (Figure 3.8A). In addition, chromatin immunoprecipitation

Figure 3.7

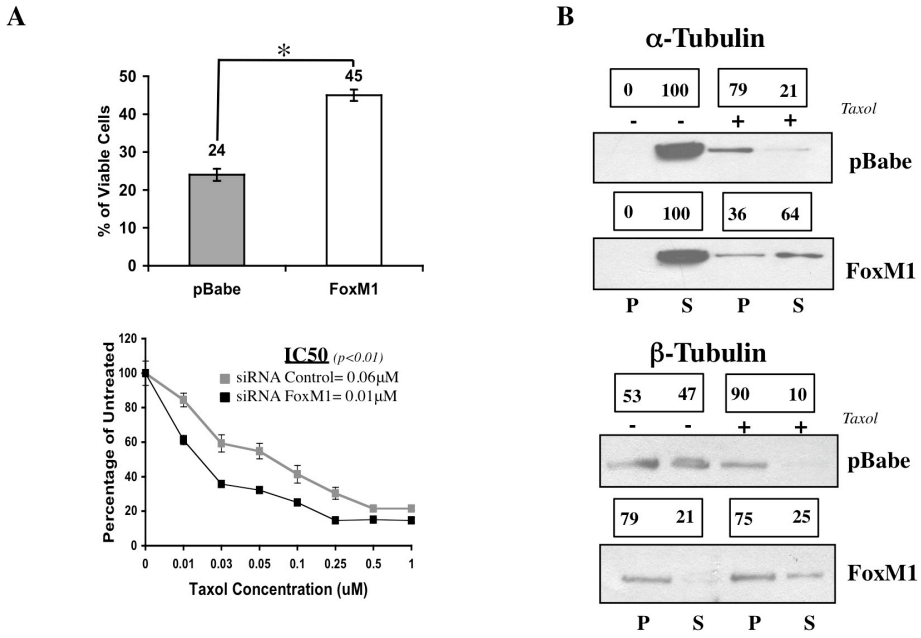

Figure 3.7. FoxM1 confers resistance to taxol by altering microtubule dynamics. (A) Top Panel: SKBR3-pBabe and FoxM1 expressing lines were treated continuously with 0.1 uM of Taxol for 7 days and viable cell numbers were determined by luminescent measurement of ATP. Bottom Panel: SKBR3 parental cells were treated with control siRNA or siRNA specific to FoxM1 for 72 hours then treated with indicated doses of Taxol for 24 hours. CellTiter Glo, a luminescence assay was used to measure cell viability *p<0.05. (B) Polymerized and soluble tubulin fractions from untreated and treated SKBR3-pBabe and FoxM1 cell lines were generated by centrifugation. Western blot was used to assay α-tubulin and β-tubulin ratios in polymerized and soluble fractions. Relative percentages are shown above western blot.

(ChIP) using SKBR3 cells with FoxM1 antibody showed enrichment of the Stathmin promoter region indicating that the RNA and subsequent protein increase in FoxM1 expressing lines is likely due to a direct interaction of FoxM1 with the Stathmin gene promoter (Figure 3.8B). Together, these studies demonstrate that SKBR3-FoxM1 cell lines are resistant to Taxol induced apoptosis by directly targeting and upregulating the microtubule destabilizing protein Stathmin.

F. FoxM1 Overexpression Protects From Herceptin and Paclitaxel in Combination

While the success of Herceptin as a single agent is significant, the best therapeutic response is seen when Herceptin is used in conjunction with other chemotherapeutic agents such as Taxol. We were interested in determining the role of FoxM1 in resistance towards combination therapy.

Pretreatment for 72 hours with Herceptin followed by Taxol treatment of both SKBR3- pBabe and FoxM1 cell lines revealed significant differences. The FoxM1-expressing cells exhibited resistance to killing. For example, seven days after Taxol treatment, only 10-12% of the pBabe cells survived, whereas the survival of the FoxM1-expressing cells was greater than 40% (Figure 3.9A). Knockdown of FoxM1 in SKBR3 sensitized the cells to combination treatment as evidenced by IC50 calculations, 0.097uM (siRNA Control) vs. 0.028uM (siRNA FoxM1) (Figure 3.9B).

Long-term combination treatment was also investigated by colony forming assay. Quantification of colony numbers show that approximately 55% of FoxM1-expressing cells survived after combination therapy, whereas only 26% of pBabe lines survived the treatment in SKBR3 cells (Figure 3.10). The ability of FoxM1 to mediate resistance to combination therapy was observed also in a comparison of pBabe vs. FoxM1 expressing MDA-MB-453 (4.5 vs. 39.6%) and BT474 (2.3 vs. 31%) cell lines (Figure 3.10). These data clearly indicate that FoxM1 can protect breast cancer cells from treatment with Herceptin and Paclitaxel in combination.

Figure 3.8

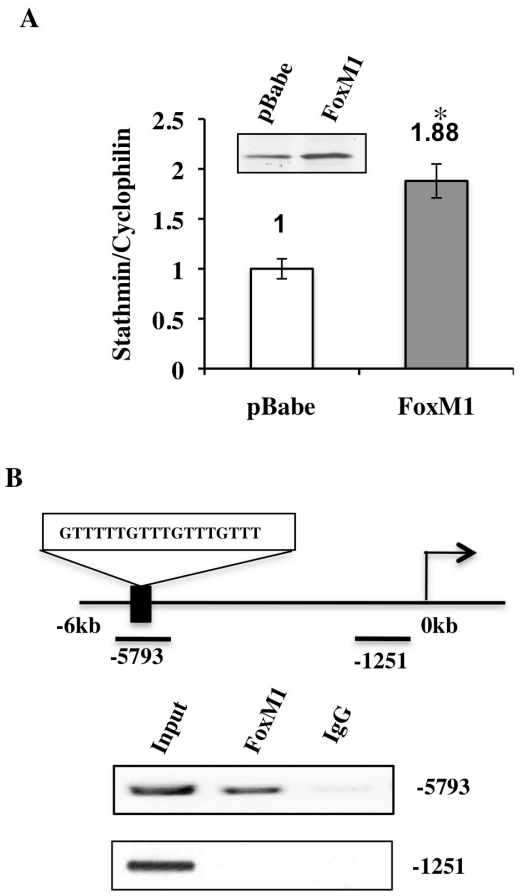

Figure 3.8. Stathmin is a transcriptional target of FoxM1. (A) RNA from SKBR3 pBabe and FoxM1 lines were collected and RT-PCR was used to measure stathmin. Values were normalized against cyclophilin. Inset shows relative protein expression by western blot *p<0.05. (B) Chromatin immunoprecipitation assay (ChIP) was performed in SKBR3 cells using an antibody specific to FoxM1 or IgG as a control. PCR was used to amplify the region surrounding the putative FoxM1 binding site at -5793 upstream of the transcriptional start site and the region surrounding –1371 as a non-specific control. Representative PCR results are shown.

Figure 3.9

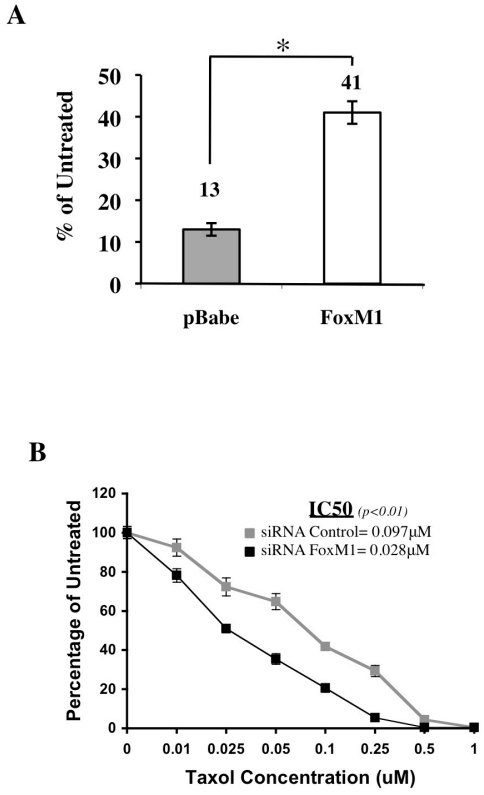

Figure 3.9. FoxM1 protects cells from combination therapy. (A) RNA from SKBR3 pBabe and FoxM1 lines were collected and RT-PCR was used to measure stathmin. Values were normalized against cyclophilin. Inset shows relative protein expression by western blot *p<0.05. (B) Chromatin immunoprecipitation assay (ChIP) was performed in SKBR3 cells using an antibody specific to FoxM1 or IgG as a control. PCR was used to amplify the region surrounding the putative FoxM1 binding site at -5793 upstream of the transcriptional start site and the region surrounding –1371 as a non-specific control. Representative PCR results are shown.

Figure 3.10

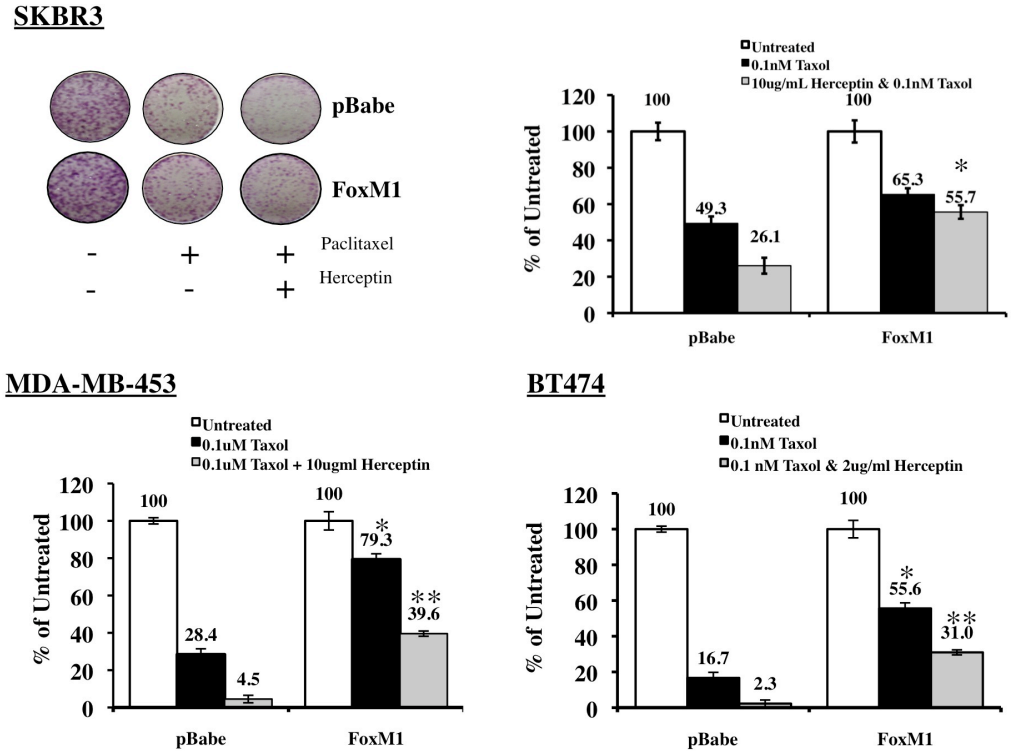

Figure 3.10. FoxM1 is protective during long term combination treatment. 3-5 x103 SKBR3, MDA-MB-453, or BT474 cells were seeded in each well in triplicate. Cells were either left untreated or pre-treated in 10ug/ml Herceptin for 72 hours then pulsed in 0.1μM Taxol for 4 hours. Wells that received Herceptin were continuously cultured in 10ug/ml for the duration of the experiment. Media was changed every 3 days. Cells were stained after a total of 17 days in crystal violet and representative wells are shown in the left panel. Graph shows quantification of triplicates from three separate experiments. Representative wells of SKBR3-pBabe and FoxM1 cells are shown in upper left *p<0.05, **p<0.001.

G. An ARF-Derived Peptide Inhibitor of FoxM1 is Sufficient to Sensitize Mammary Tumor Cells

Studies in our lab have shown that FoxM1 is inhibited by a small peptide that contains an 18-AA region of the p19ARF protein (residues between 26 and 44). This peptide has been shown to reduce proliferation and induce apoptosis of hepatocellular carcinoma cells in vivo (Gusarova et al., 2007). Treatment with the ARF-derived peptide and Herceptin led to a staggering 90% reduction in both SKBR3 and MDA-MB-453 resistant cell number as measured by colony forming assay, similar to parental lines treated with both (Figure 3.11). As expected, treatment with a mutant peptide did not show a difference in colony number as compared to parental lines and therefore was used as a control.

We went on to test the ability of the ARF-peptide to sensitize the FoxM1 expressing cells to treatment. Addition of the ARF-peptide to Herceptin, Taxol, or combination treatment showed a dramatic reduction in cell number as compared to mutant peptide. In pBabe-expressing lines, the ARF peptide was able to sensitize cells to all treatments, resulting in a greater effect from the same dosage. Most notably, addition of ARF-peptide had a significant effect in FoxM1 lines with less than 3% of cells surviving combination treatment (Figure 3.12). This data reveals that the use of ARF peptide in chemotherapeutic regimens could have great clinical promise.

Figure 3.11

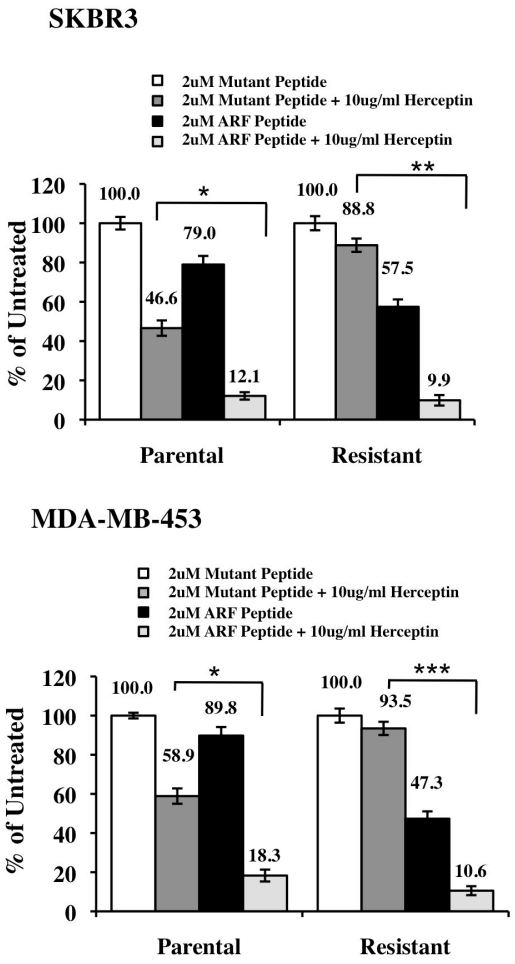

Figure 3.11. ARF-peptide sensitizes resistant lines to Herceptin. ARF-peptide or mutant peptide (2μM) was used to treat either parental or resistant SKBR3 and MDA-MB-453 cells. Cells were pretreated with peptide for 3 days then treated with both 10ug/ml Herceptin and peptide. Media was changed daily and cells were stained with crystal violet after 17 total days. Graph shows quantification of colony forming assay by Photoshop *$p<0.01$, **$p<10^{-4}$, ***$p<10^{-6}$.

Figure 3.12

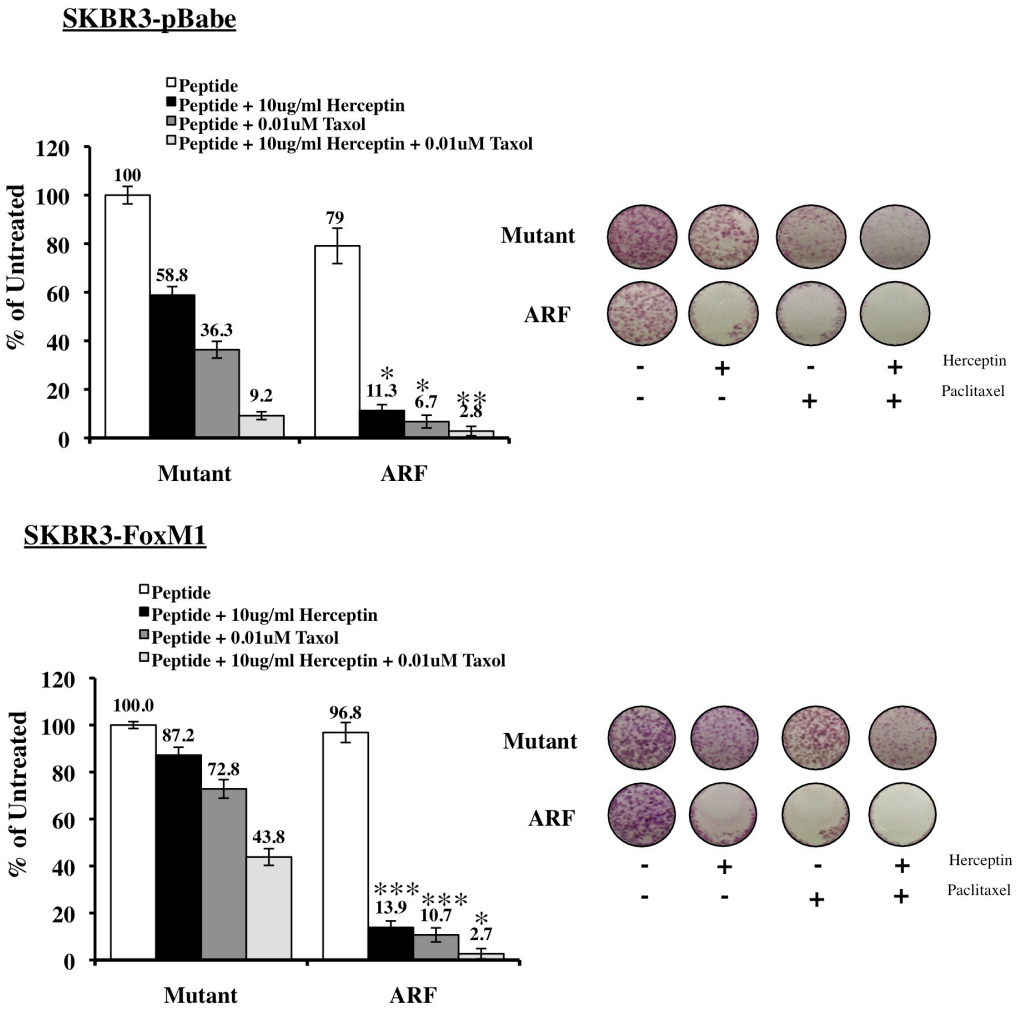

Figure 3.12. FoxM1 expressing cells can be sensitized to combination therapy by ARF-peptide treatment. SKBR3-pBabe and FoxM1 cell lines were treated with either mutant or ARF-peptide for three days. Wells receiving both Herceptin and Taxol were pre-treated for 72 hours with Herceptin before receiving indicated doses of Taxol. Quantification of triplicates is shown in the graph with representative images below $p<0.001$, $p<0.05$, $p<10^{-4}$.

4. DISCUSSION

A. Mechanisms of FoxM1 Upregulation in Tumor Cells

Previous studies identified several mechanisms for the elevation of *FoxM1* expression in tumors. Commonly activated oncogenic pathways, such as Ras signaling are upstream regulators of FoxM1 expression and activity (Behren et al., 2010; Park et al., 2009). Additionally, downregulation of p19ARF, a tumor suppressor and negative regulator of FoxM1, can result in increased FoxM1 activity (Kalinichenko et al., 2004). Several events that have been implicated in breast tumor development also are involved in the elevated expression of FoxM1. Recent studies indicate that FoxM1 expression is negatively regulated by p53, a frequently mutated gene in breast cancer (Barsotti et al., 2009; Pandit et al., 2009). In mammary tumors, Bektas and colleagues demonstrated that increased expression of FoxM1 is correlated with HER2/ErbB2 expression (Bektas et al., 2008). Subsequently, Francis et al showed that FoxM1 is a target of HER2 signaling, providing a mechanism for FoxM1 upregulation in HER2+ mammary tumors (Francis et al., 2009). The majority of mammary tumors are of luminal type that express estrogen and progesterone receptor without HER2 amplification (Dimri et al., 2005). *FoxM1* was recently validated as a transcriptional target of estrogen receptor signaling in mammary cell lines by ChIP and gel shift assays. RNA levels were elevated in response to estrogen and inhibited by estrogen antagonists (Millour et al., 2010). This indicates that increased expression of FoxM1 in mammary tumors could be a consequence of alterations in estrogen signaling.

B. Consequences of FoxM1 Overexpression

Tumor development and progression is a multi-step process. FoxM1 expression is elevated in all tumor types examined (Pilarsky et al., 2004). A considerable amount of work has gone into understanding the selective advantage FoxM1 provides tumor cells at the various steps of the cancer progression. FoxM1 stimulates expression of several cell cycle genes, and thus, supports the highly proliferative nature of tumor cells (Costa et al., 2005b). Recently, we showed that FoxM1 is a critical regulator of reactive oxygen species (ROS) in cancer cell lines (Park et al., 2009). Tumor cells expressing ROS-inducing

oncogenes, such as activated Ras or Akt, require FoxM1 for their survival. FoxM1 attenuates the levels of ROS by increasing expression of antioxidant genes. Additional studies have shown that elevated FoxM1 promotes tumor metastasis, cell survival, and a drug resistant phenotype (Kwok et al., 2008; Kwok et al., 2010; Carr et al., 2010; Park et al., 2011).

C. FoxM1 Promotes the Expansion of Undifferentiated Cells

As shown in Figure 4.1, we have created a model in which FoxM1 can function in a complex with the DNA methyltransferase, DNMT3b and in conjunction with Rb1 protein promote the promoter methylation and subsequent silencing of GATA-3 expression and the consequent inhibition of luminal differentiation. The observation that FoxM1 increases the pool of mammary luminal progenitors is of particular interest because the most common forms of breast cancers are of luminal origin (Sorlie et al., 2001). Additionally, recent work showed that deletion of tumor suppressor genes, specifically in luminal progenitors, led to the development of aggressive and poorly differentiated tumors (Jiang et al., 2010). It is possible that overexpression of FoxM1 in the luminal progenitors, in association with other changes, promotes the development of poorly differentiated mammary tumors.

Low-grade tumors that maintain markers of differentiation are associated with a positive patient outcome and are responsive to endocrine targeting therapies. Recently, one such marker, GATA-3 was shown to be a positive predictor of patient survival (Yoon et al., 2010). In a mouse model of luminal tumors, expression of GATA-3 is sufficient to promote tumor differentiation and inhibit metastasis (Kouros-Mehr et al., 2006). An understanding of the regulation of GATA-3 expression is key to understanding tumor progression, preventing metastasis, and improving patient survival. Our study indicates that FoxM1 inhibits differentiation through GATA-3 suppression, and as a result, promotes the expansion of tumor progenitor and stem cells. Breast cancers contain a small subset of cells that have tumorigenic potential (Al-Hajj et al., 2003). These cells have a stem like gene profile and increased numbers of these cells in tumors is associated with an aggressive tumor phenotype and high rates of relapse (Sorlie et al., 2001). Our data indicates that FoxM1 overexpression, a common event in breast

Figure 4.1

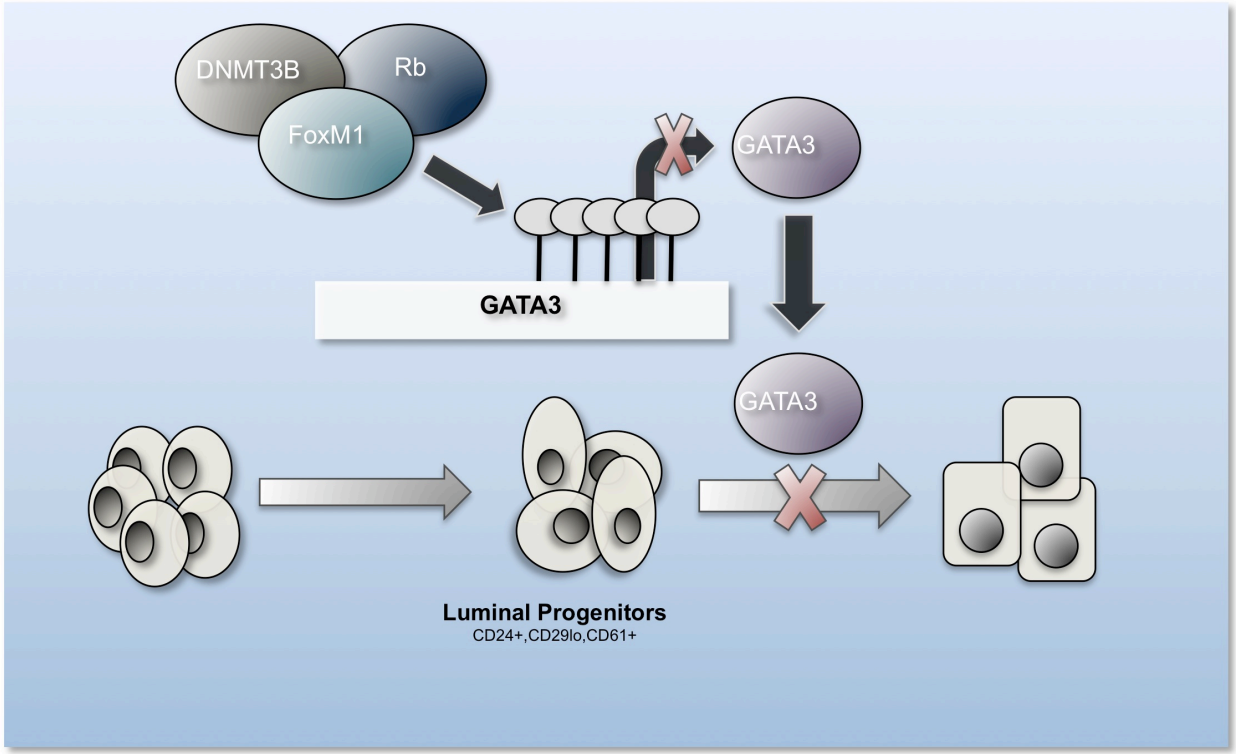
DNMT3B
Rb
FoxM1
GATA3
GATA3
GATA3
Luminal Progenitors
CD24+,CD29lo,CD61+

tumors, functions as a catalyst for aggressive tumor growth and points to FoxM1 as a potential target in differentiation therapy.

In this study, we observe that FoxM1 can regulate the expression of estrogen receptor alpha. The relationship between FoxM1 and the estrogen receptor is not straightforward. An early report by Madureira and colleagues demonstrated that FoxM1 and ERα were correlated in breast cancer cell lines. They went on to demonstrate that either overexpression or knockdown of FoxM1 led to the increased or decreased expression of ERα respectively. Also, that FoxM1 was bound to the estrogen recpetor promoter by ChIP (Madureira et al., 2006). More recently, it was shown that the regulation was reciprocal, that in fact, FoxM1 was a transcriptional target of ERα (Millour et al., 2010). It is possible that FoxM1 and ERα exist in a positive feedback loop, yet, both of these studies were independent and the reciprocal regulation and the existence of a loop is only implied and not rigorously tested. We have seen that FoxM1 functions as a negative regulator of ERα but it is likely that this is an indirect effect of GATA-3. The FoxM1 induced mammary defect does not phenocopy that of estrogen receptor deletion, supporting the idea that the regulation between FoxM1 and estrogen in this system may not be direct.

An additional and unexpected finding in this study is that the repression of GATA-3 transcription by FoxM1 relies on the retinoblastoma (Rb) protein. While previous reports showed that Rb and FoxM1 are interacting partners (Major et al., 2005; Wierstra and Alves 2006), a functional effect of this binding has not been reported. Here, we show that this interaction is required for the repression of GATA-3 in the mammary gland. The involvement of Rb in this process is of particular interest because Rb is generally thought to promote tissue differentiation (Sherr and McCormick 2002). Here, we show that the converse is true with regard to mammary luminal differentiation. Inhibition of differentiation by Rb is not unfounded. Previous studies indicate a repressive role of Rb in adipogenic differentiation (Fajas et al., 2002a). The inhibition of adipogenesis by Rb was further confirmed by in vivo experiments with mice harboring conditional knockout alleles of Rb (Calo et al., 2010). Authors of that study also showed that shRNA-mediated depletion of Rb relieved a block in differentiation in p53-/- osteosarcoma cells. Rb

binds to E2F4 to inhibit expression of PPAR-γ, a master regulator of adipogenic differentiation (Fajas et al., 2002a; Fajas et al., 2002b). This is similar to our observation in that Rb binds to FoxM1 to inhibit expression of GATA-3, a master regulator of mammary luminal differentiation. At this time, we cannot exclude the possibility that repression of GATA-3 by Rb may promote differentiation of another cell type. In that regard, it is noteworthy that mice expressing a constitutively active form of Rb in the mammary gland undergo premature differentiation. Virgin mice show positive staining for pregnancy markers indicating the cells had undergone alveolar differentiation (Jiang et al., 2002). Elf-5 has been identified as a key regulator of alveologenesis and increased expression of Elf-5 results in precocious differentiation. While pregnancy specific deletion of GATA-3 shows a defect in milk production, the expression patterns of Elf-5 and GATA-3 are distinct (Oakes et al., 2008; Siegel et al., 2010). One intriguing possibility is that Rb may promote alveolar differentiation through repression of GATA-3, yet this remains to be shown.

Deletion or mutation of Rb is a common event in basal-like subtypes of mammary tumors (Herschkowitz et al., 2008). There is evidence that basal type tumors overexpress FoxM1 and under express GATA-3 (Oncomine). We speculate that the Rb-related proteins p107 or p130 participate in GATA-3 repression in tumors harboring mutations in the Rb gene. Deletion of Rb using MMTV-Cre in p107 -/- mice resulted in development of basal mammary tumors (Jiang et al., 2010). Yet, Jiang and colleagues paradoxically observed tumors in mice by expressing constitutively active Rb. During involution, mice with active Rb show a deficiency in apoptosis, suggesting that Rb promotes cell survival (Jiang et al., 2002). The ability of Rb to protect cells from apoptosis provides a potential mechanism for tumor development in these mice. Therefore, it remains possible that the FoxM1/DNMT3b/Rb complex promotes the maintenance and survival of the progenitor pool through repression of GATA-3, and the reduced level of GATA-3, consequently, delays differentiation.

D. FoxM1 Confers a Drug Resistant Phenotype

Drug resistance, either inherent or acquired poses significant clinical challenges. The mechanisms by which cells acquire resistance are multiple and complex and our understanding will be important in order to create better therapeutic options. FoxM1 expression is elevated in a variety of tumors and several studies have pointed to the possibility that FoxM1 can promote a drug resistant phenotype. Gefitinib is an antibody inhibitor of epidermal growth factor receptor (EGFR) signaling. In a comparison of sensitive and resistant lines, after treatment, it was observed that FoxM1 was specifically repressed in cell lines that are sensitive to Gefitinib. From this observation, it was determined that FoxM1 is a downstream target of Gefitinib treatment. Importantly, when sensitive cell lines were transfected with a wildtype or constitutively active form of FoxM1, they became resistant to treatment indicating that FoxM1 can confer a resistant phenotype to Gefitinib treatment (McGovern et al., 2009).

Similar observations were made with Cisplatin treatment. Cisplatin is a platinum based chemotherapy that functions by inducing formation of DNA adducts that results in cell cycle arrest or apoptosis. Kwok and colleagues made a cisplatin resistant line by continuous exposure of MCF-7 cells to increasing concentrations of the drug. They noted that levels of FoxM1 mRNA and protein were considerably higher in resistant lines as compared to parental lines. Additionally, overexpression of FoxM1 in parental lines led to an upregulation of DNA repair pathways and protected cells from drug treatment. Also, a potential FoxM1 targeting therapeutic, Thiostrepton, was able to sensitize resistant lines to treatment (Kwok et al., 2010).

Given that the majority of breast cancers are estrogen and progesterone receptor positive, endocrine therapies are a cornerstone of breast cancer treatment. FoxM1 is a transcriptional target of estrogen receptor alpha and is responsive to both estrogen agonist or antagonist treatment, including tamoxifen. Knockdown of FoxM1 by siRNA sensitized cells to tamoxifen treatment and abrogated the mitogenic effects of estrogen on MCF-7 cells (Millour et al., 2010). Our studies have indicated that FoxM1 expression leads to an expansion of undifferentiated mammary cells. Given the strong

relationship between drug resistance and stem cells, our data suggests that in breast tumors FoxM1 may be an important target in the breast cancer stem cell pool.

The work presented here is the first report that high levels of FoxM1, commonly seen in tumors, offer mammary tumor cells an additional growth advantage, protection against Herceptin and Paclitaxel both alone and in combination by mechanisms illustrated in Figure 4.2. Previous reports from our lab have shown that FoxM1 can regulate p27 degradation and localization to allow cell cycle progression (Wang et al., 2002; Petrovic et al., 2008). The work presented here shows that this ability of FoxM1 to keep basal levels of p27 low and prevent p27 accumulation in response to Herceptin treatment is mediating a resistant phenotype in FoxM1 overexpressing cell lines. Yet, it is likely that FoxM1 can mediate resistance by other mechanisms. This is evident in cells harboring inherent resistance to Herceptin. The basal levels of p27 in BT474 and MDA-MB-453 are higher in resistant lines than in parental (data not shown), indicating dysregulation. In a pooled resistant cell line, it is feasible that the mechanisms by which cells evade therapy are heterogeneous yet, the result, as we observed, is increased FoxM1 expression and activity. These findings are significant because, regardless of p27 or p-Akt status, inhibition of FoxM1 induces resensitization. This data indicates that FoxM1 is likely a downstream mediator of resistance caused by multiple mechanisms and therefore a valuable therapeutic target.

Several studies have reported alterations in microtubules as a source of resistance to Taxol and some have implicated increased expression of Stathmin (Alli et al, 2002; Balachandran et al., 2003). Yet, upstream transcriptional regulators of Stathmin have not been reported. Not only do we demonstrate that FoxM1 directly increases expression of stathmin, but that microtubules in FoxM1 overexpressing lines fail to polymerize in response to Taxol treatment, an indicator that the Stathmin activity is high in these cells. The implications of this finding spread past breast cancer. As mentioned, FoxM1 expression is elevated in all tumor types examined to date and paclitaxel is a commonly used chemotherapeutic agent. It is likely that FoxM1 inhibition could be a successful tool to sensitize various tumor types to treatment. Therapeutically, Taxol has significant and limiting side effects including a decrease in blood cells (neutropenia, anemia, leukopenia) and chemotherapy-induced neuropathy (Lee et al., 2006). The addition

Figure 4.2

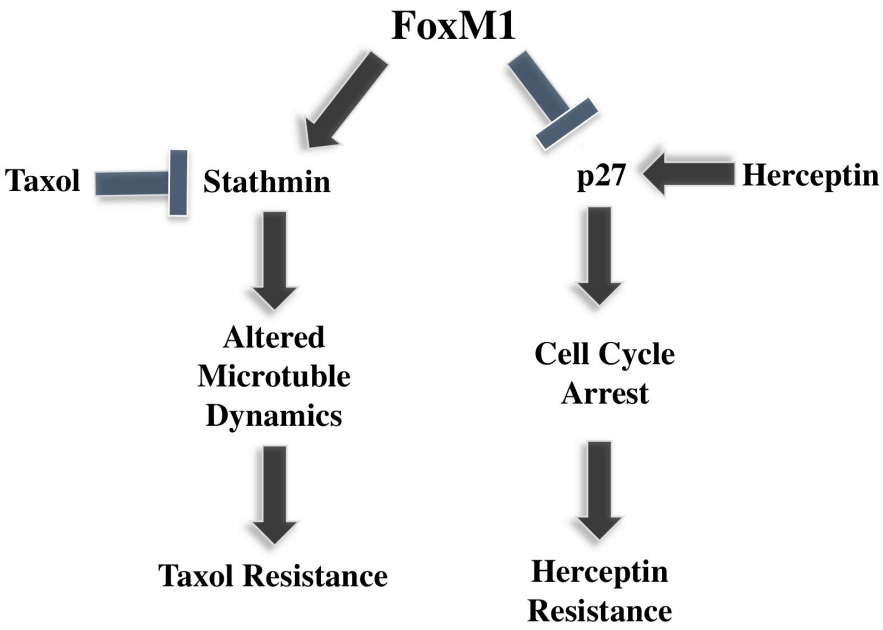
FoxM1
Taxol
Stathmin
p27
Herceptin
Altered Microtuble Dynamics
Cell Cycle Arrest
Taxol Resistance
Herceptin Resistance

of a FoxM1 inhibitor to a chemotherapeutic regimen could result in lower effective doses and a potential reduction in side effects for patients.

In the past several years, the ability of FoxM1 to promote tumorigenesis and tumor growth has become apparent. As a result, several groups have been working to develop FoxM1 inhibitors. In addition to the ARF-derived peptide inhibitor of FoxM1, it has been shown that the antibiotics Siomycin A and Thiostrepton could inhibit FoxM1 (Gusarova et al., 2007; Bhat et al., 2009a). In addition, proteasome inhibitors, a number of which are in use clinically can downregulate FoxM1 levels (Bhat et al., 2009b). Several studies have shown that FoxM1 functions to promote proliferation, inhibit apoptosis, evade senescence and promote angiogenesis (Park et al., 2009; Zhang et al., 2008; Myatt et al., 2007). Our studies also implicate that FoxM1 can promote a drug resistant phenotype in breast tumors and could be targeted, perhaps by the ARF-peptide, in sensitization therapy. Notably, previous in vivo studies using ARF peptide did not show toxicity in other organ systems, one important factor in choosing therapies (Gusarova et al., 2007).

Interestingly, several FoxM1 target genes have been implicated in resistance including Survivin, Polo Like Kinase 1 (PLK1), and Cks1. Survivin was shown to induce resistance to Taxol, VEGF inhibitors, and radiation therapy (Zaffaroni et al., 2002). Knockdown of PLK1 could sensitize cells to Cisplatin, Herceptin, and Taxol while Cks1 is implicated in Taxol resistance as well (Krishnan et al., 2008; Spankuch et al., 2006). As these factors are downstream targets of FoxM1 it is likely that therapies aimed at reducing FoxM1 also will serve as a method of sensitizing tumor cells to other therapies. The ability of FoxM1 to induce resensitization could be applicable in a variety of tumor types and therapies. Our study shows that FoxM1 is a valid target in drug resistant tumors and inhibitors of FoxM1 should be considered in future therapeutic trials.

5. Materials and Methods

A. Animal Studies

All animal experiments were preapproved by the UIC institutional animal care and use committee. WAP-rtTA-Cre mice were obtained from the Mouse Repository, NCI-Frederick. FoxM1 FL/FL mice have been previously characterized (Wang et al., 2005). C57BL/6 mice were purchased from Charles River laboratories. For deletion studies, mice were given 2mg/mL of doxycyline (Sigma) dissolved in 5% sucrose (Sigma) solution in water bottles. A detailed description of the *in vivo* overexpression system and flow cytometry analysis is provided in supplemental methods.

B. Bioinformatics and Statistical Analysis

Oncomine™ (Compendia Bioscience, Ann Arbor, MI) was used for analysis and visualization. To analyze the expression of FoxM1 and GATA-3 in human tumor arrays, breast cancer datasets were exported from Oncomine. Box plots are used to show fold-change of FoxM1 expression in each tumor grade subset. Human tissue arrays were scored by two independent pathologists. All p-values were calculated using the student's T-test. Standard deviation of each experiment is shown using error bars in column graphs.

C. Cell Culture, Constructs and Chemotherapeutic Agents

MDA-MB-453, SKBR3, BT474 and MCF-7 cell lines were obtained from American Type Culture Collection (ATCC). Cells were cultured in RPMI 1640 (Invitrogen) with 10% fetal bovine serum (Hyclone) and penicillin/streptomycin (Cellgro). Stable cell lines were generated by transfection of pBabe or pBabe-FoxM1 retroviral constructs followed by selection in puromycin. FoxM1-pcDNA3.1 was generated by PCR amplification and cloned into pcDNA3.1 followed by sequencing. Myc tagged DNMT3a and 3b were a kind gift of Frederic Chedin. Retroviral scrambled shRNA and Rb shRNA constructs were purchased from Origene. Plasmid transfection was done using Fugene 6 (Roche). Control siRNA as well as siRNA specific to FoxM1 (Dharmacon) was transfected using Lipofectamine

(Invitrogen). For Rb knockdown studies, a doxycycline inducible shRNA system in MCF-7 cells was used and described in detail below. Cell synchronization of MDA-MB-453 for cell cycle analysis was done using serum starvation (0.2%FBS) for 24 hours, followed by 10% FBS for 6 hours, and addition of 5ug/ml of aphidicolin (Calbiochem) for 16 hours. Mutant and ARF peptide have been described previously (Gusarova et al., 2007). Paclitaxel (Sigma) was dissolved in DMSO. Herceptin, a gift from Genentech (San Francisco, CA) was dissolved in sterile water.

D. Production of Inducible Knockdown MCF-7 Cell Lines (Benevolenskya Lab)

To produce an inducible knockdown system in MCF-7 cell lines, cells were first infected with viral particles carrying the pRetroX-Tet-off Advanced vector (Clontech), for constitutive expression of the tetracycline-controlled transactivator, tTa-Advanced. Cells with integrated constructs were selected for using G418 sulfate for two weeks. Isogenic clones were then isolated by plating cells in limiting dilutions on 10 cm plates, and validated by measuring tTA-Advanced expression by RT-qPCR. Inducibility was assessed by performing induction assays of cells further infected with pRetroX-Tight-Pur-Luc, a tTA-inducible luciferase reporter, for three days and performing a luciferase assay (Promega). Clones showing the highest tTA-Advanced expression and luciferase inducibility were used to produce second stable lines. In all, ~10 clones were isolated per line, which all showed at least some expression of tTA-Advanced. The clone showing greater than 20 fold inducibility by luciferase assays was used to produce second stable lines.

Second stable cell lines carrying vector for expression of miR-30-based shRNA to *Rb* or the empty control vector TGM, were made by infecting tTA-Advanced expressing clones with TMP-RB.670 (Dickins et al., 2005) retroviral particles (referred to as RB670 here within) and selecting for integrated constructs using puromycin dihydrochloride for several days. Individual clones were generated by limiting dilutions on 10 cm plates and validated by performing induction assays for 6 days. In particular, clones were evaluated for inducible GFP expression via fluorescent microscopy as well as protein lysates were prepared for Western blot analysis of pRB protein level.

E. Tubulin Assay

Separation of polymerized and soluble fractions was done in accordance with previously published assays (Giannakakou et al., 1997). Cells were seeded at 80% confluency in 24-well plates. The following day they were treated with 0 or 1nM Taxol for 24 hours. Cells were collected in hypotonic buffer (1mM $MgCl_2$, 2mM EGTA, 0.5% Nonidet P-40, 20mM Tris-HCl pH 6.8) and centrifuged for 10 minutes at room temperature (14,000 rpm). The supernatant was used as the soluble fraction while the pellet made up the polymerized fraction. Samples were analyzed by western blot.

F. Flow Cytometry (Cell Cycle), Proliferation Measurements and Colony Forming Assay

For cell cycle analysis by flow cytometry, cells were trypsinized, pelleted, and then resuspended in propidium iodide (PI) solution (50ug/ml PI, 0.1mg/ml RNaseA, 0.05% Triton-X). All reagents were purchased from Sigma. After 40 minutes of incubation at 37^0 cells were analyzed using a flow cytometer. 10μM of 5-Bromo-2-Deoxyuridine (BrDU) from Sigma was added to culture media. Cells were fixed and stained with anti-BrdU antibody (1:250, Dako) followed by anti-mouse FITC (Dako) and DAPI (Molecular Probes). Cell viability was measured using CellTiter-Glo Luminescent assay (Promega), which measures the amount of oxygenated oxyluciferin that has a direct correlation to ATP present. For colony forming assay, 3-5 x 10^3 cells were plated in triplicate in a 24-well plate. 24 hours later, treatment was initiated. After 14-17 days cells were fixed and stained with crystal violet. Quantification was done using Adobe Photoshop, a method described elsewhere (Lehr et al., 1997). All p-values were calculated using the student's t-test.

G. Semi-Quantitative RT-PCR

RNA was extracted using Trizol (Invitrogen) and cDNA was synthesized using reverse transcriptase (Bio-Rad). Equal amounts of cDNA were used for all PCR reactions (Promega). PCR products were analyzed over a series of cycle numbers in order to ensure that data was produced during

the PCR log-scale amplification. Samples were run on agarose gels, photographed, and quantified using Image J. Primers are listed in Table 1.

H. RT-PCR and Western Blot

RNA was Trizol extracted (Invitrogen) and cDNA was synthesized by reverse transcriptase (Bio-Rad). cDNA was amplified using SYBR Green mastermix (Bio-Rad) and analyzed via iCycler software and the delta-delta C_t method. Data from mouse studies was normalized to 18s RNA and human products to GAPDH. All primer sequences are shown in Table 1. Protein extracts from tissue were homogenized in lysis buffer containing: 50mM Hepes-KOH, 300mM NaCl, 1mM EDTA, 1mM EGTA, 1mM DTT, 0.1% Tween 20, and 10% glycerol. Extracts from cell lines were prepared in lysis buffer containing: 1mM EDTA, 0.15M NaCl, 0.05M Tris-HCl pH 7.5, and 0.5% Triton-X. Phosphate inhibitor cocktail set II (Calbiochem) and protease inhibitor (Roche) were added to lysis buffers before each experiment. All reagents are from Sigma-Aldrich unless otherwise noted. The rabbit polyclonal antibody against FoxM1 has been previously described (Major 2004). Anti kip1/p27 (1:10,000, BD Biosciences), GATA-3 (1:200, Santa Cruz), Stathmin (1:1000, Cell Signaling) and Cdk2 (1:200, Santa Cruz) were also used. For tubulin fractionation, α-tubulin antibody (1:10,000, Sigma) and β-tubulin (1:10,000, Neomarkers) were used for analysis.

I. Chromatin Immunoprecipitation (ChIP)

Cells were fixed in 1% formaldehyde for 10 minutes to allow crosslinking and then quenched with 125nM glycine. For in vivo ChIP single cell suspensions were generated using collagenase/hyaluronidase and then fixed. Cells were collected and lysed in SDS lysis buffer (1% SDS, 10mM EDTA, 50mM Tris pH8, protease and phosphate inhibitors). Lysate was sonicated, pre-cleared, and incubated with GFP (Clontech, JL-8), GATA-3 (Santa Cruz HG3-31), FoxM1 (developed by our lab), DNMT3b (Imgenex 52A1018), or Rb (Cell Signaling, 4H1) antibody as indicated followed by collection with Protein-A and Protein-G sepharose beads with salmon sperm (Upstate). Beads were

washed and DNA was extracted using a PCR purification kit (Qiagen). PCR products were visualized on a gel or analyzed using SYBR Green (Bio-Rad) and normalized to the IgG control (Santa Cruz) as indicated. PCR sequences are provided in Table 1.

J. Immunohistochemistry and In Situ Hybridization

For immunohistochemistry, glands were fixed in modified Davidson's fixative (30% of 37% formaldehyde-15% ethanol-5% acetic acid) for 48 hours, rinsed in PBS, left in 10% PBS buffered formalin overnight and embedded in paraffin. For staining, antigen retrieval was done using sodium citrate buffer (10mM sodium citrate pH 6.0 and 0.05% Tween) and antibodies were incubated overnight at the following dilutions: FoxM1 (Santa Cruz, K-19) 1:500, GATA-3 (Santa Cruz, HG3-31) 1:100, estrogen receptor alpha (Abcam 6F11) 1:40, cytokeratin 18 (Novus E431-1) 1:200, smooth muscle actin (Sigma, 1A4) 1:50,000, CD61 (Millipore, 04-1060) 1:50, p63 (Millipore, MAB1435) 1:200. Visualization was done using ABC and DAB and counterstained using Hematoxylin (Polyscientific). For antibodies of mouse origin, mouse on mouse (MOM) kit was used. All reagents are from Vector Labs unless otherwise indicated. For in situ hybridization, 322bp mouse FoxM1 probes were amplified from cDNA using the following primers: 5'-GCTATCCAACTCCTGGGAAGATTC-3' sense and 5'-CAATGTCTCCTTGATGGGGGTC-3' antisense. T7 polymerase (Ambion) and DIG labeled nucleotides (Roche) were used to make labeled RNA probes. Labeling of paraffin embedded sections was performed using IsHyb in situ hybridization kit (Biochain). Sections were counterstained in nuclear fast red (Vector Labs) or fixed briefly in paraformaldehyde and stained using antibodies to smooth muscle actin or cytokeratin 18 as indicated.

K. Whole Mount Imaging

For carmine alum whole mount staining, glands were removed, spread on glass slides and placed in Carnoy's fixative overnight. Glands were hydrated in an alcohol gradient and left in carmine alum (Sigma) overnight then cleared in xylene. For GFP imaging, glands were removed, spread on a glass

slide, fixed in 4% paraformaldehyde overnight, cleared in 50% glycerol in PBS for 4 hours, 75% glycerol for 4 hours, and 100% glycerol overnight. Glands were imaged using a fluorescent dissecting scope.

L. Methylation Analysis

Genomic DNA was isolated using Perfect Pure DNA isolation kit (5 Prime). Bisulfite conversion was done using EZ DNA Methylation kit (Zymo Research). Conversion efficiency was determined to be greater than 95% by using primers to converted and unconverted beta actin. Bisulfite converted DNA was amplified using methylation specific PCR as described (Herman et al., 1996, Liu et al., 2009). Primers did not amplify non-converted DNA but did amplify SssI methylase treated, bisulfite converted DNA.

M. Mammosphere Culture, Retroviral Infection, Cleared Mammary Fat Pad Transplant

Primary mammary epithelial cells were used to generate mammosphere cultures as previously described (Dontu et al., 2003). Specifically, #4 inguinal mammary glands were removed from 6-8 week old C57BL/6 mice. Glands were digested for 6 hours in collagenase/hyaluronidase. Cells were collected by centrifugation, red blood cells were lysed using ammonium chloride solution, and glands were further digested using 0.25% Trypsin (Cellgro) and Dispase. DNaseI (sigma) was used to remove DNA from dead cells. Cells were suspended in Hanks' balanced salt solution and 2%FBS and filtered through 0.4uM strainer (BD Biosciences). Cells were counted and incubated in retrovirus as described below. All reagents are from Stem Cell Technologies unless otherwise noted.

pMigR-FoxM1-EGFP was generated by cloning FoxM1 cDNA into pMigR-EGFP. pMigR-dsRed was made by exchanging dsRed express (Clontech) for EGFP in pMigR and GATA-3-dsRed was made by PCR amplification of GATA-3 cDNA and cloning into pMigR-dsRed (Refaeli et al., 2002). Scrambled and shRNA constructs against Rb1 and GATA-3 were purchased from Origene. Retrovirus was generated using 293 Ampho packaging cell line. Cells were plated at 40% confluency and infected with retroviral constructs using lipofectamine2000 (Invitrogen). After 24 hours, media was changed to 3% FBS and DMEM and fresh virus was used to infect mammospheres. Low DMEM was used to minimize the FBS

that stem cells are exposed to. 2ml of fresh virus was added to mammosphere cells from above along with polybrene. Cells were incubated with virus at 37^{o} for 120 minutes and gently mixed every 20 minutes. After 2 hours, cells were centrifuged, supernatant was removed, and cells were resuspended in media containing DMEM/F12 (Invitrogen/Gibco), serum-free B27 (Gibco), 20ng/mL EGF (Peprotech), 20ng/ml FGF (Peprotech), 4μg/mL Heparin (Sigma), and Penicillin/Streptamycin (Cellgro). Cells were plated at a density of 5 x 10^5/75cm^2 flask. Spheres were allowed to form for 7 days.

At the end of 7 days spheres were collected, digested in 0.05% trypsin for 10 minutes at 37^{o}, resuspended in Hanks' balanced salt solution and 2%FBS, centrifuged, and suspended in fresh media at a concentration of 1 x 10^6/ml. GFP, dsRed, or double positive cells were sorted using Beckman Coulter MoFlo sorter and Summit software. One thousand sorted cells were resuspended in matrigel (BD Biosciences) and were implanted into the cleared mammary fat pad of 3-4 week old C57BL/6 mice as previously described (DeOme et al., 1959). All data is shown normalized to the control gland from the same animal. All analysis was performed after 7-8 weeks of regrowth.

Flow Cytometry. For cell cycle analysis by flow cytometry, cells were trypsinized, pelleted, and then resuspended in propidium iodide (PI) solution (50ug/ml PI, 0.1mg/ml RNaseA, 0.05% Triton-X). All reagents were purchased from Sigma. After 40 minutes of incubation at 37 degrees Celsius, cells were analyzed using a flow cytometer. Analysis of primary mammary glands was done as previously described (Stingl et al., 2006). Briefly, glands were processed using sequential enzyme digestion (described in detail in supplemental methods), blocked using an antibody to CD16/CD32 and hematopoietic stem cells were removed using the epithelial cell enrichment kit (stem cell technologies). Cells were stained using CD24-PE (BD Biosciences), CD29-APC (e-Biosciences), CD61-biotin and streptavidin PE-Cy7 (BD Biosciences). Later studies in mammary gland involving two retroviruses (GFP and dsRed expressing) were stained using CD24-PE-Cy7 (BD Biosciences), CD29-APC, and CD61-biotin and streptavidin pacific blue (BD Biosciences). Analysis was done using a Beckman-Coulter flow cytometer and Summit software.

Table 1: Primer/Probe Information		
RT-PCR		
Gene Name	**Sense (5'→3')**	**Antisense (5'→3')**
FoxM1	GAGGAAAGAGCACCTTCAGC	AGGCAATGTCTCCTTGATGG
GATA-3	CCGAAACCGGAAGATGTCTA	AGATGTGGCTCAGGGATGAC
18s RNA	ACATCGACCTCACCAAGAGG	TCCCATCCTTCACATCCTTC
Rb1	TGATAACCTTGAACCTGCTTGTCC	GGCTGCTTGTGTCTCTGTATTTGC
Estrogen Receptor α	AAGGCGGCATACGGAAAGAC	ATCCAACAAGGCACTGACCATC
Amphiregulin	ACTCACAGCGAGGATGACAAGG	TAACGATGCCGATGCCAATAG
Cytokeratin 18	TTCAGTCTCAACGATGCCCTGG	ATTAGTCTCGGACACCACTCTGCC
Smooth Muscle Actin	ATCATTGCCCCTCCAGAACG	GCTTCGTCGTATTCCTGTTTGC
Cadherin 11	AATGTGCCTGAGAGGTCCAATG	CGAGAAATAGGGTTGTCCTTCAAG
Human FoxM1	GCAGGCTGCACTATCAACAA	TCGAAGGCTCCTCAACCTTA
Human GATA-3	TGTCAGACCACCACAACCAGAC	TGGATGCCTTCCTTCTTCATAGTC
Human GAPDH	ACACCCACTCCTCCACCTTT	TTCCTCTTGTGCTCTTGCTG
In Situ Hybridization Probes		
FoxM1	GCTATCCAACTCCTGGGAAGATTC	CAATGTCTCCTTGATGGGGGTC
Human GATA-3 Methylation Specific PCR		
Set 1 (Site -1431)	TTATCGGTGGGATAGTTTGC	AACCGCTAACCCGAAAATAC
Set 2 (Site -747)	CTTGTAATAGTTGAAGCGTGTTT	ATACCTTTAACTAAAACGTC
Beta-Actin	TGGTGATGGACGAGGTTTAGTAAGT	AACCAATAAAACCTACTCCTCCCTTA
Mouse GATA-3 ChIP		
Site -1686	CTGACGCTGTTCGTTCTGGAGA	AAGATTTGCCTCCGAACC
Site -721	ACGCCTCCTCCTCCTCCTCTAC	AGCACACCTCCGACAGCCAG
Site -291	GTCACACTCGGATTCCTCTCTCC	CCCCAAAAAAAAGCAGCAGACAC
Human GATA-3 ChIP		
Site -1730	CAAGTGGGCTCAGGAGAAA	GTGTGAGGGTCGTCGTGTT
Site -1431	TTCAGAACTTACTTTCAGGGACGG	AATGCTGCCAGGAGAGGGAGTG
Site -747	TCTCATCCCTCACTGTTGCCAC	TGTCATTGTCACCTCTTTCCCG
Non-Specific	TTTTACGGGGCAACTACGGC	CAGTGGCATCCATTAGCAGGTC

Table 2: Antibody Information		
Immunohistochemistry		
Protein	**Company/Catalog Number**	**Dilution**
FoxM1	Santa Cruz/K-19	1:500
GATA-3	Santa Cruz/HG3-31	1:100
Estrogen Receptor α	Abcam/6F11	1:40
Cytokeratin 18	Novus/E431-1	1:200
Smooth Muscle Actin	Sigma/IA4	1:50,000
CD61	Millipore/04-1060	1:50
p63	Millipore/MAB1435	1:200
Milk	Accurate Scientific/YNRMTM	1:10,000
PCNA	Calbiochem/414R	1:250
ChIP		
Protein	**Company/Catalog Number**	**Dilution**
FoxM1	Santa Cruz/K-19	1:1,000
GATA-3	Santa Cruz/HG3-31	1:500
DNMT3b	Imgenex/52A1018	1:500
Rb	Cell Signaling/4H1	1:250

6. References

1. Al-Hajj, M., Wicha, M.S., Benito-Hernandez, A., Morrison, S.J. and Clarke, M.F. (2003). Prospective identification of tumorigenic breast cancer cells. Proc Natl Acad Sci U S A 100, 3983-8.

2. Albergaria, A., et al. (2009). Expression of FOXA1 and GATA-3 in breast cancer: the prognostic significance in hormone receptor-negative tumours. Breast Cancer Res 11, R40.

3. Alli, E., Bash-Babula, J., Yang, J.M. and Hait, W.N. (2002). Effect of stathmin on the sensitivity to antimicrotubule drugs in human breast cancer. Cancer Res 62, 6864-9.

4. Asselin-Labat, M.L., et al. (2007). Gata-3 is an essential regulator of mammary-gland morphogenesis and luminal-cell differentiation. Nat Cell Biol 9, 201-9.

5. Asselin-Labat, M.L., et al. (2010). Control of mammary stem cell function by steroid hormone signalling. Nature 465, 798-802.

6. Azambuja, E., Durbecq, V., Rosa, D.D., Colozza, M., Larsimont, D., Piccart-Gebhart, M. and Cardoso, F. (2008). HER-2 overexpression/amplification and its interaction with taxane-based therapy in breast cancer. Ann Oncol 19, 223-32.

7. Balachandran, R., Welsh, M.J. and Day, B.W. (2003). Altered levels and regulation of stathmin in paclitaxel-resistant ovarian cancer cells. Oncogene 22, 8924-30.

8. Barsotti, A.M. and Prives, C. (2009). Pro-proliferative FoxM1 is a target of p53-mediated repression. Oncogene 28, 4295-305.

9. Baxter, F.O., Neoh, K. and Tevendale, M.C. (2007). The beginning of the end: death signaling in early involution. J Mammary Gland Biol Neoplasia 12, 3-13.

10. Behren, A., Muhlen, S., Acuna Sanhueza, G.A., Schwager, C., Plinkert, P.K., Huber, P.E., Abdollahi, A. and Simon, C. (2009). Phenotype-assisted transcriptome analysis identifies FOXM1 downstream from Ras-MKK3-p38 to regulate in vitro cellular invasion. Oncogene 29, 1519-30.

11. Bektas, N., Haaf, A., Veeck, J., Wild, P.J., Luscher-Firzlaff, J., Hartmann, A., Knuchel, R. and Dahl, E. (2008). Tight correlation between expression of the Forkhead transcription factor FOXM1 and HER2 in human breast cancer. BMC Cancer 8, 42.

12. Bhat, U.G., Halasi, M. and Gartel, A.L. (2009). FoxM1 is a general target for proteasome inhibitors. PLoS One 4, e6593.

13. Bhat, U.G., Halasi, M. and Gartel, A.L. (2009). Thiazole antibiotics target FoxM1 and induce apoptosis in human cancer cells. PLoS One 4, e5592.

14. Bocchinfuso, W.P., Lindzey, J.K., Hewitt, S.C., Clark, J.A., Myers, P.H., Cooper, R. and Korach, K.S. (2000). Induction of mammary gland development in estrogen receptor-alpha knockout mice. Endocrinology 141, 2982-94.

15. Bouras, T., Pal, B., Vaillant, F., Harburg, G., Asselin-Labat, M.L., Oakes, S.R., Lindeman, G.J. and Visvader, J.E. (2008). Notch signaling regulates mammary stem cell function and luminal cell-fate commitment. Cell Stem Cell 3, 429-41.

16. Buono, K.D., Robinson, G.W., Martin, C., Shi, S., Stanley, P., Tanigaki, K., Honjo, T. and Hennighausen, L. (2006). The canonical Notch/RBP-J signaling pathway controls the balance of cell lineages in mammary epithelium during pregnancy. Dev Biol 293, 565-80.

17. Burris, H.A., 3rd. (2000). Docetaxel (Taxotere) in HER-2-positive patients and in combination with trastuzumab (Herceptin). Semin Oncol 27, 19-23.

18. Calo, E., Quintero-Estades, J.A., Danielian, P.S., Nedelcu, S., Berman, S.D. and Lees, J.A. (2010). Rb regulates fate choice and lineage commitment in vivo. Nature 466, 1110-4.

19. Carr, J.R., Park, H.J., Wang, Z., Kiefer, M.M. and Raychaudhuri, P. (2010). FoxM1 mediates resistance to herceptin and paclitaxel. Cancer Res 70, 5054-63.

20. Chen, Y.J., Dominguez-Brauer, C., Wang, Z., Asara, J.M., Costa, R.H., Tyner, A.L., Lau, L.F. and Raychaudhuri, P. (2009). A conserved phosphorylation site within the forkhead domain of FoxM1B is required for its activation by cyclin-CDK1. J Biol Chem 284, 30695-707.

21. Cicalese, A., et al. (2009). The tumor suppressor p53 regulates polarity of self-renewing divisions in mammary stem cells. Cell 138, 1083-95.

22. Classon, M. and Harlow, E. (2002). The retinoblastoma tumour suppressor in development and cancer. Nat Rev Cancer 2, 910-7.

23. Costa, R.H., Kalinichenko, V.V., Holterman, A.X. and Wang, X. (2003). Transcription factors in liver development, differentiation, and regeneration. Hepatology 38, 1331-47.

24. Costa, R.H. (2005). FoxM1 dances with mitosis. Nat Cell Biol 7, 108-10.

25. Costa, R.H., Kalinichenko, V.V., Major, M.L. and Raychaudhuri, P. (2005). New and unexpected: forkhead meets ARF. Curr Opin Genet Dev 15, 42-8.

26. Creighton, C.J., et al. (2009). Residual breast cancers after conventional therapy display mesenchymal as well as tumor-initiating features. Proc Natl Acad Sci U S A 106, 13820-5.

27. Dave, B. and Chang, J. (2009). Treatment resistance in stem cells and breast cancer. J Mammary Gland Biol Neoplasia 14, 79-82.

28. Dean, M., Fojo, T. and Bates, S. (2005). Tumour stem cells and drug resistance. Nat Rev Cancer 5, 275-84.

29. Deome, K.B., Faulkin, L.J., Jr., Bern, H.A. and Blair, P.B. (1959). Development of mammary tumors from hyperplastic alveolar nodules transplanted into gland-free mammary fat pads of female C3H mice. Cancer Res 19, 515-20.

30. Dickins R., Hemann M., Zilfou J., Simpson D., Ibarra I., Hannon G., Lowe S. (2005) Probing tumor phenotypes using stable and regulated synthetic microRNA precursors. Nat Genet 37, 1289-95.

31. Dimri, G., Band, H. and Band, V. (2005). Mammary epithelial cell transformation: insights from cell culture and mouse models. Breast Cancer Res 7, 171-9.

32. Dontu, G., Jackson, K.W., McNicholas, E., Kawamura, M.J., Abdallah, W.M. and Wicha, M.S. (2004). Role of Notch signaling in cell-fate determination of human mammary stem/progenitor cells. Breast Cancer Res 6, R605-15.

33. Dunbar, M.E. and Wysolmerski, J.J. (1999). Parathyroid hormone-related protein: a developmental regulatory molecule necessary for mammary gland development. J Mammary Gland Biol Neoplasia 4, 21-34.

34. Dydensborg, A., Rose, A., Wilson, B., Grote, D., Paquet, M., Giguere, V., Siegel, P. and Bouchard, M. (2009). GATA3 inhibits breast cancer growth and pulmonary breast cancer metastasis. Oncogene 28, 2634-42.

35. Elston, C.W. and Ellis, I.O. (1991). Pathological prognostic factors in breast cancer. I. The value of histological grade in breast cancer: experience from a large study with long-term follow-up. Histopathology 19, 403-10.

36. Fajas, L., Egler, V., Reiter, R., Hansen, J., Kristiansen, K., Debril, M.B., Miard, S. and Auwerx, J. (2002). The retinoblastoma-histone deacetylase 3 complex inhibits PPARgamma and adipocyte differentiation. Dev Cell 3, 903-10.

37. Fajas, L., Landsberg, R.L., Huss-Garcia, Y., Sardet, C., Lees, J.A. and Auwerx, J. (2002). E2Fs regulate adipocyte differentiation. Dev Cell 3, 39-49.

38. Farnie, G. and Clarke, R.B. (2007). Mammary stem cells and breast cancer--role of Notch signalling. Stem Cell Rev 3, 169-75.

39. Fidler, I.J. and Kripke, M.L. (1977). Metastasis results from preexisting variant cells within a malignant tumor. Science 197, 893-895.

40. Fidler, I.J. and Hart, I.R. (1982). Biological diversity in metastatic neoplasms: origins and implications. Science 217, 998-1003.

40. Francis, R.E., et al. (2009). FoxM1 is a downstream target and marker of HER2 overexpression in breast cancer. Int J Oncol 35, 57-68.

41. Fu, Z., Malureanu, L., Huang, J., Wang, W., Li, H., van Deursen, J.M., Tindall, D.J. and Chen, J. (2008). Plk1-dependent phosphorylation of FoxM1 regulates a transcriptional programme required for mitotic progression. Nat Cell Biol 10, 1076-82.

42. Giannakakou, P., Sackett, D.L., Kang, Y.K., Zhan, Z., Buters, J.T., Fojo, T. and Poruchynsky, M.S. (1997). Paclitaxel-resistant human ovarian cancer cells have mutant beta-tubulins that exhibit impaired paclitaxel-driven polymerization. J Biol Chem 272, 17118-25.

43. Ginestier, C., et al. (2007). ALDH1 is a marker of normal and malignant human mammary stem cells and a predictor of poor clinical outcome. Cell Stem Cell 1, 555-67.

44. Girault, I., Tozlu, S., Lidereau, R. and Bieche, I. (2003). Expression analysis of DNA methyltransferases 1, 3A, and 3B in sporadic breast carcinomas. Clin Cancer Res 9, 4415-22.

45. Grimshaw, M.J., Cooper, L., Papazisis, K., Coleman, J.A., Bohnenkamp, H.R., Chiapero-Stanke, L., Taylor-Papadimitriou, J. and Burchell, J.M. (2008). Mammosphere culture of metastatic breast cancer cells enriches for tumorigenic breast cancer cells. Breast Cancer Res 10, R52.

46. Gusarova, G.A., Wang, I.C., Major, M.L., Kalinichenko, V.V., Ackerson, T., Petrovic, V. and Costa, R.H. (2007). A cell-penetrating ARF peptide inhibitor of FoxM1 in mouse hepatocellular carcinoma treatment. J Clin Invest 117, 99-111.

47. Hanahan, D. and Weinberg, R.A. (2011). Hallmarks of cancer: the next generation. Cell 144, 646-74.

48. Hennighausen, L. and Robinson, G.W. (2005). Information networks in the mammary gland. Nat Rev Mol Cell Biol 6, 715-25.

49. Heppner, G.H. (1984). Tumor heterogeneity. Cancer Res 44, 2259-65.

50. Herman, J.G., Merlo, A., Mao, L., Lapidus, R.G., Issa, J.P., Davidson, N.E., Sidransky, D. and Baylin, S.B. (1995). Inactivation of the CDKN2/p16/MTS1 gene is frequently associated with aberrant DNA methylation in all common human cancers. Cancer Res 55, 4525-30.

51. Herman, J.G., Graff, J.R., Myohanen, S., Nelkin, B.D. and Baylin, S.B. (1996). Methylation-specific PCR: a novel PCR assay for methylation status of CpG islands. Proc Natl Acad Sci U S A 93, 9821-6.

52. Herschkowitz, J.I., He, X., Fan, C., Perou, C.M. (2008). The functional loss of the retinoblastoma tumour suppressor is a common even in basal-like and luminal B breast carcinomas. Breast Cancer Res 10, 5.

53. Hoch, R.V., Thompson, D.A., Baker, R.J. and Weigel, R.J. (1999). GATA-3 is expressed in association with estrogen receptor in breast cancer. Int J Cancer 84, 122-8.

54. Huang, T.H. and Esteller, M. (2010). Chromatin remodeling in mammary gland differentiation and breast tumorigenesis. Cold Spring Harb Perspect Biol 2, a004515.

55. Jemal, A., Siegel, R., Xu, J. and Ward, E. (2010). Cancer statistics, 2010. CA Cancer J Clin 60, 277-300.

56. Jiang, Z. and Zacksenhaus, E. (2002). Activation of retinoblastoma protein in mammary gland leads to ductal growth suppression, precocious differentiation, and adenocarcinoma. J Cell Biol 156, 185-98.

57. Jiang, Z., et al. (2010). Rb deletion in mouse mammary progenitors induces luminal-B or basal-like/EMT tumor subtypes depending on p53 status. J Clin Invest 120, 3296-309.

58. Jones, P.A. and Baylin, S.B. (2002). The fundamental role of epigenetic events in cancer. Nat Rev Genet 3, 415-28.

59. Jones, P.A. and Baylin, S.B. (2007). The epigenomics of cancer. Cell 128, 683-92.

60. Joshi, P.A., Jackson, H.W., Beristain, A.G., Di Grappa, M.A., Mote, P.A., Clarke, C.L., Stingl, J., Waterhouse, P.D. and Khokha, R. (2010). Progesterone induces adult mammary stem cell expansion. Nature 465, 803-7.

61. Junttila, T.T., Akita, R.W., Parsons, K., Fields, C., Lewis Phillips, G.D., Friedman, L.S., Sampath, D. and Sliwkowski, M.X. (2009). Ligand-independent HER2/HER3/PI3K complex is disrupted by trastuzumab and is effectively inhibited by the PI3K inhibitor GDC-0941. Cancer Cell 15, 429-40.

62. Kakarala, M. and Wicha, M.S. (2008). Implications of the cancer stem-cell hypothesis for breast cancer prevention and therapy. J Clin Oncol 26, 2813-20.

63. Kalin, T.V., Wang, I.C., Ackerson, T.J., Major, M.L., Detrisac, C.J., Kalinichenko, V.V., Lyubimov, A. and Costa, R.H. (2006). Increased levels of the FoxM1 transcription factor accelerate development and progression of prostate carcinomas in both TRAMP and LADY transgenic mice. Cancer Res 66, 1712-20.

64. Kalinichenko, V.V., et al. (2004). Foxm1b transcription factor is essential for development of hepatocellular carcinomas and is negatively regulated by the p19ARF tumor suppressor. Genes Dev 18, 830-50.

65. Kim, I.M., Ramakrishna, S., Gusarova, G.A., Yoder, H.M., Costa, R.H. and Kalinichenko, V.V. (2005). The forkhead box m1 transcription factor is essential for embryonic development of pulmonary vasculature. J Biol Chem 280, 22278-86.

66. Kim, I.M., et al. (2006). The Forkhead Box m1 transcription factor stimulates the proliferation of tumor cells during development of lung cancer. Cancer Res 66, 2153-61.

67. Kordon, E.C. and Smith, G.H. (1998). An entire functional mammary gland may comprise the progeny from a single cell. Development 125, 1921-30.

68. Korkaya, H., Paulson, A., Iovino, F. and Wicha, M.S. (2008). HER2 regulates the mammary stem/progenitor cell population driving tumorigenesis and invasion. Oncogene 27, 6120-30.

69. Korver, W., Roose, J., Heinen, K., Weghuis, D.O., de Bruijn, D., van Kessel, A.G. and Clevers, H. (1997). The human TRIDENT/HFH-11/FKHL16 gene: structure, localization, and promoter characterization. Genomics 46, 435-42.

70. Korver, W., Roose, J., Wilson, A. and Clevers, H. (1997). The winged-helix transcription factor Trident is expressed in actively dividing lymphocytes. Immunobiology 198, 157-61.

71. Korver, W., Schilham, M.W., Moerer, P., van den Hoff, M.J., Dam, K., Lamers, W.H., Medema, R.H. and Clevers, H. (1998). Uncoupling of S phase and mitosis in cardiomyocytes and hepatocytes lacking the winged-helix transcription factor Trident. Curr Biol 8, 1327-30.

72. Kouros-Mehr, H., Slorach, E.M., Sternlicht, M.D. and Werb, Z. (2006). GATA-3 maintains the differentiation of the luminal cell fate in the mammary gland. Cell 127, 1041-55.

73. Kouros-Mehr, H., Bechis, S.K., Slorach, E.M., Littlepage, L.E., Egeblad, M., Ewald, A.J., Pai, S.Y., Ho, I.C. and Werb, Z. (2008). GATA-3 links tumor differentiation and dissemination in a luminal breast cancer model. Cancer Cell 13, 141-52.

74. Kretschmer, C., Sterner-Kock, A., Siedentopf, F., Schoenegg, W., Schlag, P.M. and Kemmner, W. (2011). Identification of early molecular markers for breast cancer. Mol Cancer 10, 15.

75. Krishnan, A., Hariharan, R., Nair, S.A. and Pillai, M.R. (2008). Fluoxetine mediates G0/G1 arrest by inducing functional inhibition of cyclin dependent kinase subunit (CKS)1. Biochem Pharmacol 75, 1924-34.

76. Krupczak-Hollis, K., et al. (2004). The mouse Forkhead Box m1 transcription factor is essential for hepatoblast mitosis and development of intrahepatic bile ducts and vessels during liver morphogenesis. Dev Biol 276, 74-88.

77. Kwok, J.M., Myatt, S.S., Marson, C.M., Coombes, R.C., Constantinidou, D. and Lam, E.W. (2008). Thiostrepton selectively targets breast cancer cells through inhibition of forkhead box M1 expression. Mol Cancer Ther 7, 2022-32.

78. Kwok, J.M., Peck, B., Monteiro, L.J., Schwenen, H.D., Millour, J., Coombes, R.C., Myatt, S.S. and Lam, E.W. (2010). FOXM1 confers acquired cisplatin resistance in breast cancer cells. Mol Cancer Res 8, 24-34.

79. LaMarca, H.L. and Rosen, J.M. (2007). Estrogen regulation of mammary gland development and breast cancer: amphiregulin takes center stage. Breast Cancer Res 9, 304.

80. Laoukili, J., Kooistra, M.R., Bras, A., Kauw, J., Kerkhoven, R.M., Morrison, A., Clevers, H. and Medema, R.H. (2005). FoxM1 is required for execution of the mitotic programme and chromosome stability. Nat Cell Biol 7, 126-36.

81. Le, X.F., Lammayot, A., Gold, D., Lu, Y., Mao, W., Chang, T., Patel, A., Mills, G.B. and Bast, R.C., Jr. (2005). Genes affecting the cell cycle, growth, maintenance, and drug sensitivity are preferentially regulated by anti-HER2 antibody through phosphatidylinositol 3-kinase-AKT signaling. J Biol Chem 280, 2092-104.

82. Lee, J.J. and Swain, S.M. (2006). Peripheral neuropathy induced by microtubule-stabilizing agents. J Clin Oncol 24, 1633-42.

83. Lehr, H.A., Mankoff, D.A., Corwin, D., Santeusanio, G., Gown, A.M. (1997) Application of photoshop-based image analysis to quantification of hormone receptor expression in breast cancer. J Histochem Cytochem 45, 1559-65.

84. Li, Y., et al. (2003). Evidence that transgenes encoding components of the Wnt signaling pathway preferentially induce mammary cancers from progenitor cells. Proc Natl Acad Sci U S A 100, 15853-8.

85. Li, X., et al. (2008). Intrinsic resistance of tumorigenic breast cancer cells to chemotherapy. J Natl Cancer Inst 100, 672-9.

86. Liao, M.J., et al. (2007). Enrichment of a population of mammary gland cells that form mammospheres and have in vivo repopulating activity. Cancer Res 67, 8131-8.

87. Lim, E., Vaillant, F., Wu, D., Forrest, N., Pal, B., Hart, A., Asselin-Labat, M., Gyorki, D., Ward, T., Partanen, A., et al. (2009). Aberrant luminal progenitors as the candidate target population for basal tumor development in BRCA1 mutation carriers. Nature Medicine 15, 907-913.

88. Lin, E.Y., Jones, J.G., Li, P., Zhu, L., Whitney, K.D., Muller, W.J. and Pollard, J.W. (2003). Progression to malignancy in the polyoma middle T oncoprotein mouse breast cancer model provides a reliable model for human diseases. Am J Pathol 163, 2113-26.

89. Lindvall, C., Evans, N.C., Zylstra, C.R., Li, Y., Alexander, C.M. and Williams, B.O. (2006). The Wnt signaling receptor Lrp5 is required for mammary ductal stem cell activity and Wnt1-induced tumorigenesis. J Biol Chem 281, 35081-7.

90. Liu, M., et al. (2006). FoxM1B is overexpressed in human glioblastomas and critically regulates the tumorigenicity of glioma cells. Cancer Res 66, 3593-602.

91. Liu, S., Howell, P., Ren, S., Fodstad, O. and Riker, A.I. (2009). The 14-3-3sigma gene promoter is methylated in both human melanocytes and melanoma. BMC Cancer 9, 162.

92. Lujambio, A. and Esteller, M. (2007). CpG island hypermethylation of tumor suppressor microRNAs in human cancer. Cell Cycle 6, 1455-9.

93. Madureira, P.A., Varshochi, R., Constantinidou, D., Francis, R.E., Coombes, R.C., Yao, K.M. and Lam, E.W. (2006). The Forkhead box M1 protein regulates the transcription of the estrogen receptor alpha in breast cancer cells. J Biol Chem 281, 25167-76.

94. Mailleux, A.A., et al. (2002). Role of FGF10/FGFR2b signaling during mammary gland development in the mouse embryo. Development 129, 53-60.

95. Major, M.L., Lepe, R. and Costa, R.H. (2004). Forkhead box M1B transcriptional activity requires binding of Cdk-cyclin complexes for phosphorylation-dependent recruitment of p300/CBP coactivators. Mol Cell Biol 24, 2649-61.

96. Mallepell, S., Krust, A., Chambon, P. and Brisken, C. (2006). Paracrine signaling through the epithelial estrogen receptor alpha is required for proliferation and morphogenesis in the mammary gland. Proc Natl Acad Sci U S A 103, 2196-201.

97. Mani, S.A., et al. (2008). The epithelial-mesenchymal transition generates cells with properties of stem cells. Cell 133, 704-15.

98. McGovern, U.B., et al. (2009). Gefitinib (Iressa) represses FOXM1 expression via FOXO3a in breast cancer. Mol Cancer Ther 8, 582-91.

99. Millour, J., et al. (2010). FOXM1 is a transcriptional target of ERalpha and has a critical role in breast cancer endocrine sensitivity and resistance. Oncogene 29, 2983-95.

100. Mueller, S.O., Clark, J.A., Myers, P.H. and Korach, K.S. (2002). Mammary gland development in adult mice requires epithelial and stromal estrogen receptor alpha. Endocrinology 143, 2357-65.

101. Myatt, S.S. and Lam, E.W. (2007). The emerging roles of forkhead box (Fox) proteins in cancer. Nat Rev Cancer 7, 847-59.

102. Nagata, Y., et al. (2004). PTEN activation contributes to tumor inhibition by trastuzumab, and loss of PTEN predicts trastuzumab resistance in patients. Cancer Cell 6, 117-27.

103. Nahta, R., Takahashi, T., Ueno, N.T., Hung, M.C. and Esteva, F.J. (2004). P27(kip1) down-regulation is associated with trastuzumab resistance in breast cancer cells. Cancer Res 64, 3981-6.

104. Nguyen, D.X., Bos, P.D. and Massague, J. (2009). Metastasis: from dissemination to organ-specific colonization. Nat Rev Cancer 9, 274-84.

105. O'Brien, C.S., Farnie, G., Howell, S.J. and Clarke, R.B. (2008). Are stem-like cells responsible for resistance to therapy in breast cancer? Breast Dis 29, 83-9.

106. Oakes, S.R., et al. (2008). The Ets transcription factor Elf5 specifies mammary alveolar cell fate. Genes Dev 22, 581-6.

107. Orr, G.A., Verdier-Pinard, P., McDaid, H. and Horwitz, S.B. (2003). Mechanisms of Taxol resistance related to microtubules. Oncogene 22, 7280-95.

108. Pandit, B., Halasi, M. and Gartel, A.L. (2009). p53 negatively regulates expression of FoxM1. Cell Cycle 8, 3425-7.

109. Park, C.H., Bergsagel, D.E. and McCulloch, E.A. (1971). Mouse myeloma tumor stem cells: a primary cell culture assay. J. Natl Cancer Inst. 46, 411-422.

110. Park, H.J., Costa, R.H., Lau, L.F., Tyner, A.L. and Raychaudhuri, P. (2008). Anaphase-promoting complex/cyclosome-CDH1-mediated proteolysis of the forkhead box M1 transcription factor is critical for regulated entry into S phase. Mol Cell Biol 28, 5162-71.

111. Park, H.J., Carr, J.R., Wang, Z., Nogueira, V., Hay, N., Tyner, A.L., Lau, L.F., Costa, R.H. and Raychaudhuri, P. (2009). FoxM1, a critical regulator of oxidative stress during oncogenesis. Embo J 28, 2908-18.

112. Park, H.J.G., G., Wang, Z., Carr, J.R., Li, J., Raychaudhuri, P. (2011). Deregulation of FoxM1 promotes tumor metastasis. EMBO Molecular Medicine 3, 21-34.

113. Perou, C.M., et al. (2000). Molecular portraits of human breast tumours. Nature 406, 747-52.

114. Petrovic, V., Costa, R.H., Lau, L.F., Raychaudhuri, P. and Tyner, A.L. (2008). FoxM1 regulates growth factor-induced expression of kinase-interacting stathmin (KIS) to promote cell cycle progression. J Biol Chem 283, 453-60.

115. Pilarsky, C., Wenzig, M., Specht, T., Saeger, H.D. and Grutzmann, R. (2004). Identification and validation of commonly overexpressed genes in solid tumors by comparison of microarray data. Neoplasia 6, 744-50.

116. Pohlmann, P.R., Mayer, I.A. and Mernaugh, R. (2009). Resistance to Trastuzumab in Breast Cancer. Clin Cancer Res 15, 7479-7491.

117. Psaila, B. and Lyden, D. (2009). The metastatic niche: adapting the foreign soil. Nat Rev Cancer 9, 285-93.

118. Rakha, E.A., et al. (2010). Breast cancer prognostic classification in the molecular era: the role of histological grade. Breast Cancer Res 12, 207.

119. Refaeli Y., Van Parijs L., Alexander S., Abbas A. (2002). Interferon gamma is required for activation-induced death of T lymphocytes. J Exp Med, 196, 999-1005.

120. Reya, T., Morrison, S.J., Clarke, M.F. and Weissman, I.L. (2001). Stem cells, cancer, and cancer stem cells. Nature 414, 105-11.

121. Reya, T. and Clevers, H. (2005). Wnt signalling in stem cells and cancer. Nature 434, 843-50.

122. Reynolds, B.A. and Weiss, S. (1996). Clonal and population analyses demonstrate that an EGF-responsive mammalian embryonic CNS precursor is a stem cell. Dev Biol 175, 1-13.

123. Robinson, G.W., Wagner, K.U. and Hennighausen, L. (2001). Functional mammary gland development and oncogene-induced tumor formation are not affected by the absence of the retinoblastoma gene. Oncogene 20, 7115-9.

124. Roll, J.D., Rivenbark, A.G., Jones, W.D. and Coleman, W.B. (2008). DNMT3b overexpression contributes to a hypermethylator phenotype in human breast cancer cell lines. Mol Cancer 7, 15.

125. Romanov, S.R., Kozakiewicz, B.Z., Hoist, C.R., Stampfer, M.R., Haupt, L.M. and Tisty, T.D. (2001). Normal human mammary epithelial cells spontaneously escape senescence and acquire genomic changes. Nature 409, 633-637.

126. Shackleton, M., Vaillant, F., Simpson, K.J., Stingl, J., Smyth, G.K., Asselin-Labat, M.L., Wu, L., Lindeman, G.J. and Visvader, J.E. (2006). Generation of a functional mammary gland from a single stem cell. Nature 439, 84-8.

127. Sherr, C.J. and McCormick, F. (2002). The RB and p53 pathways in cancer. Cancer Cell 2, 103-12.

128. Siegel, P.M. and Muller, W.J. (2010). Transcription factor regulatory networks in mammary epithelial development and tumorigenesis. Oncogene 29, 2753-9.

129. Smalley, M. and Ashworth, A. (2003). Stem cells and breast cancer: A field in transit. Nat Rev Cancer 3, 832-44.

130. Sorlie, T., et al. (2001). Gene expression patterns of breast carcinomas distinguish tumor subclasses with clinical implications. Proc Natl Acad Sci U S A 98, 10869-74.

131. Spankuch, B., Heim, S., Kurunci-Csacsko, E., Lindenau, C., Yuan, J., Kaufmann, M. and Strebhardt, K. (2006). Down-regulation of Polo-like kinase 1 elevates drug sensitivity of breast cancer cells in vitro and in vivo. Cancer Res 66, 5836-46.

132. Stingl, J., Eirew, P., Ricketson, I., Shackleton, M., Vaillant, F., Choi, D., Li, H.I. and Eaves, C.J. (2006). Purification and unique properties of mammary epithelial stem cells. Nature 439, 993-7.

133. Sutherland, K.D., Lindeman, G.J. and Visvader, J.E. (2007). The molecular culprits underlying precocious mammary gland involution. J Mammary Gland Biol Neoplasia 12, 15-23.

134. Uddin, S., et al. (2011). Genome-wide expression analysis of Middle Eastern colorectal cancer reveals FOXM1 as a novel target for cancer therapy. Am J Pathol 178, 537-47.

135. Vaillant, F., Asselin-Labat, M.L., Shackleton, M., Forrest, N.C., Lindeman, G.J. and Visvader, J.E. (2008). The mammary progenitor marker CD61/beta3 integrin identifies cancer stem cells in mouse models of mammary tumorigenesis. Cancer Res 68, 7711-7.

136. Visvader, J.E. (2009). Keeping abreast of the mammary epithelial hierarchy and breast tumorigenesis. Genes Dev 23, 2563-77.

137. Wagner, K.U. and Rui, H. (2008). Jak2/Stat5 signaling in mammogenesis, breast cancer initiation and progression. J Mammary Gland Biol Neoplasia 13, 93-103.

138. Wang, X., Kiyokawa, H., Dennewitz, M.B. and Costa, R.H. (2002). The Forkhead Box m1b transcription factor is essential for hepatocyte DNA replication and mitosis during mouse liver regeneration. Proc Natl Acad Sci U S A 99, 16881-6.

139. Wang, I.C., Chen, Y.J., Hughes, D., Petrovic, V., Major, M.L., Park, H.J., Tan, Y., Ackerson, T. and Costa, R.H. (2005). Forkhead box M1 regulates the transcriptional network of genes essential for mitotic progression and genes encoding the SCF (Skp2-Cks1) ubiquitin ligase. Mol Cell Biol 25, 10875-94.

140. Wang, Z., Banerjee, S., Kong, D., Li, Y. and Sarkar, F.H. (2007). Down-regulation of Forkhead Box M1 transcription factor leads to the inhibition of invasion and angiogenesis of pancreatic cancer cells. Cancer Res 67, 8293-300.

141. Wang, I.C., Meliton, L., Ren, X., Zhang, Y., Balli, D., Snyder, J., Whitsett, J.A., Kalinichenko, V.V. and Kalin, T.V. (2009). Deletion of Forkhead Box M1 transcription factor from respiratory epithelial cells inhibits pulmonary tumorigenesis. PLoS One 4, e6609.

142. Wang, Z., Park, H.J., Carr, J.R., Chen, Y., Li, J., Tyner, A.L., Costa, R.H., Bagchi, S., Raychaudhuri, P. (2011). FoxM1 in tumorigenicity of the neuroblastoma cells and renewal of the neural progenitors. Cancer Res 71, 4292-4302.

143. Weiss, M.J. and Orkin, S.H. (1995). GATA transcription factors: key regulators of hematopoiesis. Exp Hematol 23, 99-107.

144. Westendorf, J.M., Rao, P.N. and Gerace, L. (1994). Cloning of cDNAs for M-phase phosphoproteins recognized by the MPM2 monoclonal antibody and determination of the phosphorylated epitope. Proc Natl Acad Sci U S A 91, 714-8.

145. Wierstra, I. and Alves, J. (2006). Transcription factor FOXM1c is repressed by RB and activated by cyclin D1/Cdk4. Biol Chem 387, 949-62.

146. Wierstra, I. and Alves, J. (2007). FOXM1, a typical proliferation-associated transcription factor. Biol Chem 388, 1257-74.

147. Williams, J.M. and Daniel, C.W. (1983). Mammary ductal elongation: differentiation of myoepithelium and basal lamina during branching morphogenesis. Dev Biol 97, 274-90.

148. Wonsey, D.R. and Follettie, M.T. (2005). Loss of the forkhead transcription factor FoxM1 causes centrosome amplification and mitotic catastrophe. Cancer Res 65, 5181-9.

149. Woodward, W.A., Chen, M.S., Behbod, F., Alfaro, M.P., Buchholz, T.A. and Rosen, J.M. (2007). WNT/beta-catenin mediates radiation resistance of mouse mammary progenitor cells. Proc Natl Acad Sci U S A 104, 618-23.

150. Wysolmerski, J.J., Philbrick, W.M., Dunbar, M.E., Lanske, B., Kronenberg, H. and Broadus, A.E. (1998). Rescue of the parathyroid hormone-related protein knockout mouse demonstrates that parathyroid hormone-related protein is essential for mammary gland development. Development 125, 1285-94.

151. Xiao, H., Verdier-Pinard, P., Fernandez-Fuentes, N., Burd, B., Angeletti, R., Fiser, A., Horwitz, S.B. and Orr, G.A. (2006). Insights into the mechanism of microtubule stabilization by Taxol. Proc Natl Acad Sci U S A 103, 10166-73.

152. Yan, P.S., Rodriguez, F.J., Laux, D.E., Perry, M.R., Standiford, S.B. and Huang, T.H. (2000). Hypermethylation of ribosomal DNA in human breast carcinoma. Br J Cancer 82, 514-7.

153. Yan, W., Cao, Q.J., Arenas, R.B., Bentley, B. and Shao, R. (2010). GATA3 inhibits breast cancer metastasis through the reversal of epithelial-mesenchymal transition. J Biol Chem 285, 14042-51.

154. Yang, D.K., Son, C.H., Lee, S.K., Choi, P.J., Lee, K.E. and Roh, M.S. (2009). Forkhead box M1 expression in pulmonary squamous cell carcinoma: correlation with clinicopathologic features and its prognostic significance. Hum Pathol 40, 464-70.

155. Yao, K.M., Sha, M., Lu, Z. and Wong, G.G. (1997). Molecular analysis of a novel winged helix protein, WIN. Expression pattern, DNA binding property, and alternative splicing within the DNA binding domain. J Biol Chem 272, 19827-36.

156. Yarden, Y. (2001). The EGFR family and its ligands in human cancer. signalling mechanisms and therapeutic opportunities. Eur J Cancer 37 Suppl 4, S3-8.

157. Yau, C., Wang, Y., Zhang, Y., Foekens, J.A. and Benz, C.C. (2011). Young age, increased tumor proliferation and FOXM1 expression predict early metastatic relapse only for endocrine-dependent breast cancers. Breast Cancer Res Treat 126, 803-10.

158. Ye, H., Kelly, T.F., Samadani, U., Lim, L., Rubio, S., Overdier, D.G., Roebuck, K.A. and Costa, R.H. (1997). Hepatocyte nuclear factor 3/fork head homolog 11 is expressed in proliferating epithelial and mesenchymal cells of embryonic and adult tissues. Mol Cell Biol 17, 1626-41.

159. Yoon, N.K., et al. (2010). Higher levels of GATA3 predict better survival in women with breast cancer. Hum Pathol 41, 1794-801.

160. Yu, D., Jing, T., Liu, B., Yao, J., Tan, M., McDonnell, T.J. and Hung, M.C. (1998). Overexpression of ErbB2 blocks Taxol-induced apoptosis by upregulation of p21Cip1, which inhibits p34Cdc2 kinase. Mol Cell 2, 581-91.

161. Yu, J., et al. (2011). Array-Based Comparative Genomic Hybridization Identifies CDK4 and FOXM1 Alterations as Independent Predictors of Survival in Malignant Peripheral Nerve Sheath Tumor. Clin Cancer Res

162. Zaffaroni, N., Pennati, M., Colella, G., Perego, P., Supino, R., Gatti, L., Pilotti, S., Zunino, F. and Daidone, M.G. (2002). Expression of the anti-apoptotic gene survivin correlates with taxol resistance in human ovarian cancer. Cell Mol Life Sci 59, 1406-12.

163. Zhang, Y., Zhang, N., Dai, B., Liu, M., Sawaya, R., Xie, K. and Huang, S. (2008). FoxM1B transcriptionally regulates vascular endothelial growth factor expression and promotes the angiogenesis and growth of glioma cells. Cancer Res 68, 8733-42.

7. VITA

Janai RyanMarie Carr

EDUCATION

University of Illinois College of Medicine, Chicago IL **June 2005-Current**
Medical Scientist Training Program (MD/PhD) – Expected Completion: May 2013
Thesis Advisor: Pradip Raychaudhuri PhD, Department of Biochemistry and Molecular Genetics
University of California, San Diego **June 1998-2002**
B.S. Biology

HONORS and AWARDS

National Research Service Award (NRSA), National Cancer Institute, Fellowship, 2008-2011
Keystone Symposium Travel Award, Stem Cells and Cancer Meeting, March 2011
College of Medicine Research Forum, Poster Presentation Award -2nd place, 2010
Gordon Research Conference, Carl Storm Fellowship Award, Mammary Gland Biology Meeting June 2010
Keystone Symposium Travel Award, New Paradigms in Cancer Therapeutics Meeting, March 2010
National Academy of Science Bridge to the Doctorate Fellow, 2005-2007

PUBLICATIONS

1. **Carr JR**, Kiefer M, Park H, Li J, Wang Z, Fontanarosa J, DeWaal D, Kopanja D, Benevolenskya E, Guzman G, Raychaudhuri P. *FoxM1 Regulates Mammary Luminal Cell Fate*. **Cell Reports.** June 1(6): 715-729. 2012.

2. Park HJ, Gusarova G, Wang Z, **Carr JR**, Li J, Kim K, Park Y, Williamson P, Hay N, Tyner A, Lau L, Costa R, Raychaudhuri P. *Deregulation of FoxM1b leads to tumour metastasis*. **EMBO Molecular Medicine**. Jan; 3(1): 21-34. 2011.

3. **Carr JR**, Park HJ, Wang Z, Kiefer M, Raychaudhuri P. *FoxM1 Mediates Resistance to Herceptin and Paclitaxel*. **Cancer Research.** Jun 15; 70(12):5054-63. 2010.

4. Oppegard SC, Nam KH, **Carr JR**, Skaalure SC, Eddington DT. *Modulating temporal and spatial oxygenation over adherent cellular cultures*. **PLoS One.** Sep 3;4(9):e6891. 2009.

5. Park HJ, **Carr JR**, Wang Z, Nogueira V, Hay N, Tyner AL, Lau LF, Costa RH, Raychauhduri P. *FoxM1, a critical regulator of oxicdative stress during oncogenesis*. **EMBO Journal.** Oct 7; 28(19):2908-18. 2009.

6. O-Sullivan I, Chopra A, **Carr J**, Kim TA, Cohen EP. *Immunity to Grb10, a signal transduction molecule, inhibits the growth of breast cancer in mice*. **Cancer Research**. Apr; 68(7):2463-70. 2008.

7. Chopra A, O-Sullivan I, **Carr J**, Kim TS, Cohen EP. *T-regulatory cells are relatively deficient in squamous carcinomas undergoing regression in mice immunized with a squamous carcinoma vaccine enriched for immunotherapeutic cells*. **Cancer Gene Therapy**. Jun; 14(6):573-82. 2007.

8. Wan J, **Carr JR**, Baloh RW, Jen JC. *Nonconcensus Intronic Mutations Cause Episodic Ataxia*. **Annals of Neurology**. Jan; 57:131-135. 2005.

9. Jen JC, Chan WM, Bosley TM, Wan J, **Carr JR**, Rub U, Shattuck D, et al. *Mutations in a human ROBO gene disrupt hindbrain axon pathway crossing and morphogenesis*. **Science**. June 4; 304(5676):1509-13. 2004.

10. Sanchez-Alavez M, Gombart LM, Huitron-Resendiz S, **Carr JR**, Wills DN, Berg G, Campbell IL, Gauvin DV, Henriksen SJ, Criado JR. *Physiological and behavioral effects of methamphetamine in a mouse model of endotoxemia: a preliminary study*. **Pharmacology, Biochemistry, and Behavior**. Feb;77(2):365-70. 2004.

ABSTRACTS

1. **Carr, J.** and Raychaudhuri, P. FoxM1 is an Inhibitor of Mammary Luminal Differentiation Stem Cells, Cancer, and Metastasis. Keystone Symposia, March 2011, Keystone, Colorado.

2. **Carr, J**. and Raychaurdhuri, P. FoxM1 Disrupts Mammary Luminal Differentiation by Transcriptional Repression of GATA3. Mammary Gland Biology, Gordon Research Conference, June 2010, Lucca, Italy.

3. **Carr, J.** and Raychaudhuri, P. Targeting FoxM1 in Parental and Resistant Breast Cancer Cells Sensitizes to Chemotherapeutic Regimens. New Paradigms in Cancer Therapeutics, Keystone Symposia, March 2010, Victoria Canada.

4. **Carr, J.** and Raychaudhuri, P. FoxM1 Represses GATA3, a Factor Required for Luminal Differentiation. Days in Molecular Medicine, Harvard Medical School 2009 .

5. Jen, J., **Carr, J**., Sharpe, J., Jollands, A., Goudie, D., Mamsa, H., Wan, J., Baloh, R. Compound heterozygous ROBO3 mutations cause horizontal gaze palsy with progressive scoliosis in non-consanguineous individuals. American Academy of Neurology April 2005. Miami, Florida.

6. Gallegos, R., Lee, R., Crawford, E., Wills, D., **Carr, J**., Zhukov, V., Slaght, K., Huitrón-Reséndiz, S., Criado, J., Henriksen, S. Selective lesion of ventral tegmental area neurons expressing mu-opiod receptors alters EEG power spectrum across sleep/wake cycle. No. 276.14. Society for Neuroscience 2002.

7. Huitrón-Reséndiz, S., Sánchez-Alavez, M., Gallegos, R., **Carr, J**., Zhukov, V., Criado, J., Landreth, G., Feinstein, D., Henriksen, S. Effects of a peroxisome proliferator-activated gamma receptor agonist in LPS treated mice. No. 193.13. Society for Neuroscience 2002.

8. Huitrón-Reséndiz, S., Sánchez-Alavez, M., Guitierrez, T., Stobbs, S. McClellan, K., **Carr, J**., Gallegos, R., Games, D., Henriksen, S., Criado, J. Effect of total sleep deprivation on amyloid precursor protein transgenic mice. Society for Neuroscience Meeting Abstract, 2001.

9.Huitrón-Reséndiz, S., Sánchez-Alavez, M., Criado, J., Gutierrez, T., Stobbs, S., **Carr, J**., Gallegos, R., Wills, D., Games, D., Henriksen, S. Alterations in the homeostatic mechanisms of sleep in b-amyloid precursor protein transgenic mice. Associated Professional Sleep Societies Meeting Abstract, Chicago, Illinois, June 2001.

10.Huitrón-Reséndiz, S., Sánchez-Alavez, M., Gombart, L., **Carr, J.,** Steffensen, S., Gallegos, R., Games, D., Criado, J., Henriksen, S. Sleep patterns in b-amyloid precursor protein transgenic mice. Society for Neuroscience Abstract, 26: 738, 2000.

11.Sánchez-Alavez, M., Huitrón-Reséndiz, S., Gallegos, R., Gombart, L., **Carr, J.**, Steffensen, S., Chesebro, B., Oldstone, M., Criado, J., Henriksen, S. Role of Neuronal PrP in the sleep/wake cycle. Society for Neuroscience Abstract, 26: 739, 2000.